

Copyright
by
Cem Topkaya
2002

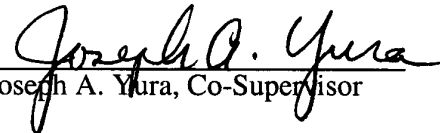
The Dissertation Committee for Cem Topkaya Certifies that this is the approved version
of the following dissertation:

**BEHAVIOR OF CURVED STEEL TRAPEZOIDAL BOX
GIRDERS DURING CONSTRUCTION**

COMMITTEE:



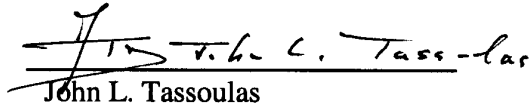
Eric B. Williamson, Supervisor



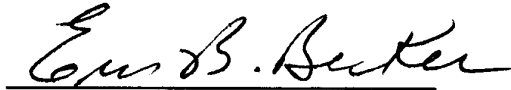
Joseph A. Yura, Co-Supervisor



Karl H. Frank



John L. Tassoulas



Eric B. Becker

BEHAVIOR OF CURVED STEEL TRAPEZOIDAL BOX
GIRDERS DURING CONSTRUCTION

by

Cem Topkaya, B.S., M.S.E.

DISSERTATION

Presented to the Faculty of the Graduate School
of The University of Texas at Austin
in Partial Fulfillment
of the Requirements
for the Degree of

DOCTOR OF PHILOSOPHY

The University of Texas at Austin

August 2002

To My Family

ACKNOWLEDGMENTS

The study presented herein was made possible through the funds from the Texas Department of Transportation. Their support is greatly appreciated.

Further thanks go to Dr. Eric B. Williamson and Dr. Joseph A. Yura for their supervision and to other committee members for their guidance.

BEHAVIOR OF CURVED STEEL TRAPEZOIDAL BOX GIRDERS DURING CONSTRUCTION

Publication No. _____

Cem Topkaya, Ph.D.
The University of Texas at Austin, 2002

Supervisors: Eric B. Williamson and Joseph A. Yura

Due to advances in fabrication technology, the use of steel trapezoidal box girders for curved interchange structures has become popular. The rapid erection, long span capability, economics, and aesthetics of these girders make them more favorable than other structural systems. Composite box girders with live loading, and quasi-closed box girders during construction, have to be evaluated during the design of these bridges. Considering both cases, the design for construction loading is the least understood and is the most important. Stresses due to construction loading can reach up to 60-70 percent of the total design stress for a given cross section.

A three-phase study has been undertaken to investigate the behavior of curved trapezoidal box girders during construction. In the first phase, laboratory tests have been performed to investigate the shear transfer between the concrete deck and steel girder at early concrete ages. In the second phase, an easy-to-use finite element program has been developed for the analysis of these systems under construction loads. The program has the capability of modeling the effects of semi-cured concrete. The third phase focused on the monitoring of two curved trapezoidal box bridges during construction. The measured forces and stresses in the field were compared with the analyses using the developed software. Findings from laboratory and field tests revealed that composite action develops at very early concrete ages. The developed software provides good correlation between measured field data and computed results.

TABLE OF CONTENTS

CHAPTER 1: INTRODUCTION.....	1
1.1 Scope.....	1
1.2 Mechanical Properties of Mature Concrete.....	3
1.3 Mechanical Properties of Concrete at Early Ages.....	4
1.4 Behavior of Steel-Concrete Interface.....	6
1.4.1 Behavior of Shear Studs.....	6
1.4.2 Mechanics of Shear Transfer.....	9
1.4.3 Evaluation of the Push-out Test and Definition of Stud Strength.....	10
1.5 Problem Statement.....	10
 CHAPTER 2: EXPERIMENTAL INVESTIGATION OF THE STEEL- CONCRETE INTERFACE BEHAVIOR AT EARLY AGES.....	13
2.1 General.....	13
2.2 Push-out Test Setup.....	14
2.3 Test Program.....	16
2.4 Test Procedure.....	17
2.5 Test Results.....	18
2.5.1 Push-out Tests.....	18
2.5.2 Tests for Determining Concrete Properties.....	23
2.5.3 Development of Expressions for Maximum and Design Strength.....	26
2.5.4 Effects of Changing Concrete Properties on the Performance of Shear Studs Pre-loaded at Early Ages...	28
2.5.5 Effect of Surface Bond.....	29
2.6 Summary of Test Results.....	30

CHAPTER 3: DEVELOPMENT OF COMPUTATIONAL SOFTWARE FOR POUR SEQUENCE ANALYSIS.....	32
3.1 Analysis Module.....	32
3.2 Program Capabilities.....	32
3.3 Input Requirements.....	33
3.4 Algorithm of the Analysis Module.....	34
3.4.1 Node Locations and Element Connectivity.....	34
3.4.2 Modeling of the Physical System.....	35
3.4.3 Assembly of the Global Stiffness Matrix.....	38
3.4.4 Shell Element Formulation.....	38
3.4.5 Truss Element Formulation.....	41
3.4.6 Spring Element Formulation.....	41
3.4.7 Solution Capability.....	42
3.4.8 Post-Processing Capability.....	43
3.5 Graphical User Interface.....	44
3.6 Verification of the Computational Software.....	46
 CHAPTER 4: FIELD STUDIES.....	 49
4.1 Bridges Under Study.....	49
4.2 Monitoring of Connect Z.....	50
4.3 Concrete Deck Pour on Direct Connect Z.....	51
4.4 Top Lateral Results for Z-Connect.....	53
4.4.1 Pour 1.....	53
4.4.2 Pour 2.....	54
4.4.3 Pour 3.....	55
4.5 Discussion of Analysis Results.....	58
4.5.1 Finite Element Model Used in ABAQUS.....	58
4.5.2 Shortcomings of the UTrAp Model.....	58
4.5.3 Sensitivity Study.....	60
4.6 Monitoring of Connect K.....	62

4.7 Concrete Deck Pour on Direct Connect K.....	63
4.8 Top Lateral and Girder Stress Results for the K-Connect.....	64
4.8.1 Pour 1.....	64
4.8.2 Pour 2.....	66
4.8.3 Pour 3.....	67
4.9 Summary of Analytical Predictions.....	69
CHAPTER 5: SUMMARY AND CONCLUSIONS.....	70
APPENDIX A.....	73
APPENDIX B.....	100
APPENDIX C.....	101
APPENDIX D.....	102
BIBLIOGRAPHY.....	104
VITA.....	108

CHAPTER 1

INTRODUCTION

1.1 Scope

Due to advances in fabrication technology, the use of steel trapezoidal box girders for curved interchange structures has become popular. The rapid erection, long span capability, economics, and aesthetics of these girders make them more favorable than other structural systems. A typical box girder system consists of one or more U-shaped steel girders that act compositely with a cast-in-place concrete deck. The composite action between the steel girder and concrete deck is achieved through the use of shear studs welded to the top flanges of the girders.

The major structural advantage of the trapezoidal box is its large torsional stiffness. A closed box has a torsional stiffness 100 to 1000 times greater than a comparable I-section (Kollbrunner and Basler, 1969). However, before hardening of the concrete deck, the steel box is an open U-section with very low torsional stiffness and strength. A typical cross section of a trapezoidal box girder system is given in Figure 1.1. To stabilize the girders during construction and to increase the torsional stiffness prior to hardening of the deck, internal braces are provided. Internal braces are in the form of a permanent, top-lateral truss system used to provide a pseudo-closed section and K-braces that control stability and cross section distortion. In addition, external diaphragms which are typically in the form of temporary trusses are provided. External braces are usually removed after the concrete deck hardens to prevent fatigue problems.

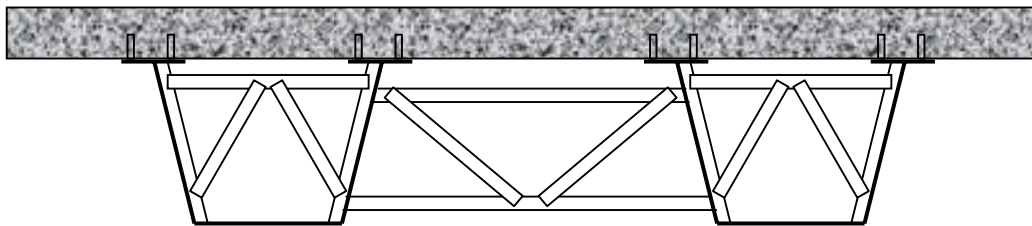


Figure 1.1: A Typical Cross Section of a Trapezoidal Box Girder System

Composite box girders with live loading and quasi-closed box girders during construction have to be considered during the design of these bridges. Considering both of these cases, the design for construction loading is the least understood (Sennah and Kennedy, 2001) and is the most important. Stresses coming from construction loading can reach up to 60-70 percent of the total stress on a cross section (Holt, 2001). In addition, the forces acting on the bracing members depend almost entirely on the construction loads. For all these reasons, great emphasis should be placed on this issue.

The design for construction loading requires the determination of correct cross sectional stresses and member forces. This determination could be achieved by making use of analytical techniques that are capable of capturing the response of a bridge with acceptable accuracy. Since curved, trapezoidal girder bridges have a very complex geometry, their analysis presents a great challenge. Several analytical methods exist for analyzing curved box girders including the following: approximate hand methods and computer methods of analysis such as the finite difference method, the finite strip method, the grid analysis and the finite element method. Among these, the Finite Element Method (FEM) is the most suitable for construction-load analysis. FEM is capable of modeling the structure in great detail and is more accurate than other methods of analysis. One limitation of this method, however, is that it requires knowledge of Finite Element Method on the designer's part. There are general-purpose, commercial Finite Element programs widely available, but their use is very limited in the design of curved trapezoidal box girders due designer's lack of knowledge on FEM. In addition, parameter studies can be difficult because changing structural layout requires generating a new mesh.

The Finite Element Method, just like all other analysis methods, requires the correct mathematical representation of the physical problem being considered. To be able to do accurate modeling, knowledge of curved box girder behavior during construction is essential. The majority of the loading during construction comes from the weight of wet concrete. The entire deck is usually not cast in one stage because of the large volume of concrete and to control shrinkage. As a result, parts of the girders may become partially composite in sequential stages. Analysis for construction loading

should take into account the partial composite action developing between the stages. In order to accurately model this phenomenon, a thorough understanding of the behavior of both the concrete deck and steel-concrete interface at early ages is essential.

1.2 Mechanical Properties of Mature Concrete

Knowledge of mechanical properties of mature concrete is well established. Among the properties, compressive strength (f'_c), stiffness (E_c), and stress-strain response are the ones that draw the most attention. The strength and stiffness varies according to the mix design used. In general, concrete exhibits a nonlinear compressive stress-strain response. (Fig 1.2) The stress-strain curve could be visualized as a rising portion followed by a descending branch. The rising portion resembles a parabola with its vertex at the maximum stress. The maximum stress is reached at a strain of between 0.0015 and 0.003.

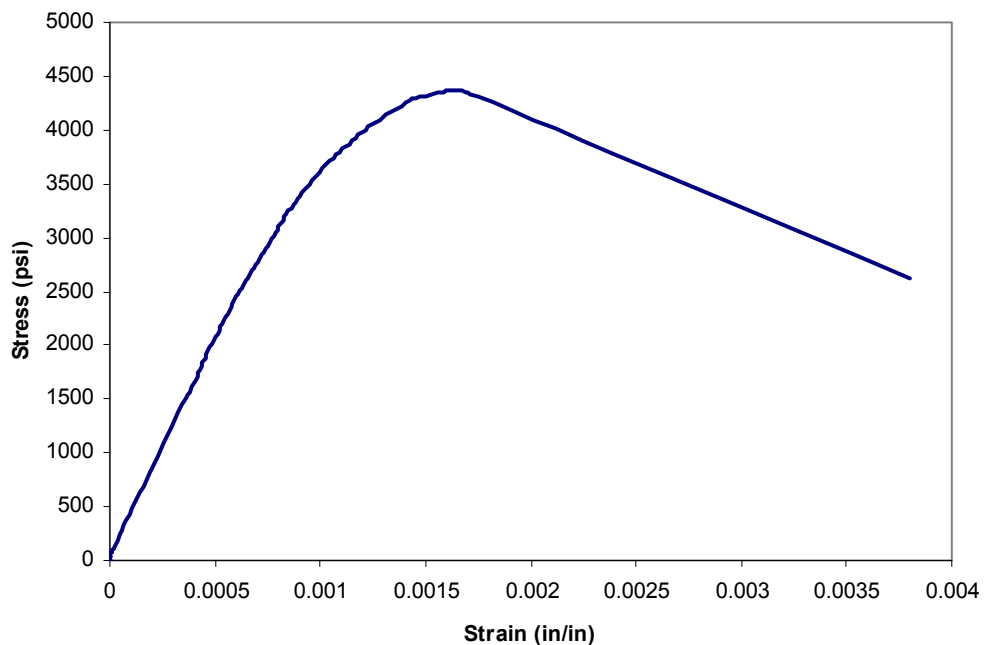


Figure 1.2: Stress-Strain Response of Mature Concrete

Initial tangent modulus of elasticity increases with an increase in compressive strength. The modulus of elasticity, E_c , is a function of the modulus of elasticity of the cement paste and that of the aggregate. Empirical relations had been developed to express E_c as a function of f'_c . For normal weight concrete with a density of 145 lb/ft³, ACI Sec 8.5.1 gives the modulus of elasticity as:

$$E_c = 57000\sqrt{f'_c} \quad \text{psi} \quad (1.1)$$

This equation was derived from short duration tests on concrete and corresponds to the secant modulus of elasticity at approximately 0.45-0.5 f'_c . Since this equation does not include the type of aggregate, there is wide scatter of the data. Measured values might range from 120 to 80 percent of the specified value. (ACI Commentary)

1.3 Mechanical Properties of Concrete at Early Ages

Concrete gains stiffness and strength with time. The rate of strength gain is dependent on the type of cement and admixtures used as well as the moisture and temperature conditions during curing. For any type of concrete, the rate of increase in strength is greatly affected by temperature of cure. The combined effect of time and temperature is expressed by an index called *maturity*. Maturity is defined as the summation of the product of curing temperature and the time the concrete has cured at that temperature. It has units of degree-day (or hour). The definition can be written as:

$$M = \sum (T - 10) \Delta t \quad (1.2)$$

where T is temperature of concrete at any time in degrees Fahrenheit, and Δt is the increment of time. Relationships between maturity and compressive strength of concrete can be found in the literature.(MacGregor,1997)

Apart from the strength gain, other mechanical properties at early ages have been investigated by several researchers. Below is a summary of the key work in this field.

H. S. Lew, and T. W. Reichard (1978) : These researchers have investigated the possibility of using maturity of concrete as a parameter to correlate with the rate of gain of the splitting tensile strength, pullout bond strength, and elastic modulus. Standard

cylinder compression tests, splitting tensile tests and pullout bond tests were performed on specimens cured at different temperatures. Tests were carried out at ages varying from 1 to 42 days. The study revealed that the maturity concept could be applied to the parameters mentioned above. It was determined that the rate of increase in the splitting tensile strength is approximately the same as that of compressive strength. In addition, the rate of increase in the pullout bond strength and modulus were found to be slightly greater than that of the compressive strength.

F. A. Oluokun, E. G. Burdette, and J. H. Deatherge (1991) : Oluokun et al. investigated the applicability of existing relations between the properties of concrete at early ages. The cylinder compressive strength, elastic modulus and Poisson's ratio were tested for four different concrete mixes at times ranging from 6 hours to 28 days. A significant finding of these researchers was that the ACI 318 relation for elastic modulus is valid at ages 12 hours and greater. Poisson's ratio was found to be insensitive to the age and concrete mix and could be taken as approximately 0.2.

A. A. Khan, W. D. Cook, and D. Mitchell (1995) : This work focused on the early age compressive stress-strain properties of low, medium, and high strength concretes. The specimens were subjected to three different curing conditions, namely, temperature-matched, sealed, and air-dry curing. Stress-strain behavior was monitored at times ranging from 8 hours to 91 days. Their study revealed that during the first few hours of hydration, the stress-strain response exhibited extremely low moduli, low compressive strength, and very high strains corresponding to peak compressive stress. After about 24 hours, the response for all of the concretes started to resemble the response at 28 days. During the first few hours, very high peak strains were observed. The elastic modulus was observed to grow very rapidly at early ages. In addition, it was concluded that the ACI expression for elastic modulus overestimates the stiffness for very early age concretes.

1.4 Behavior of Steel-Concrete Interface

Composite action between a steel girder and concrete deck is achieved by the horizontal transfer of shear at the steel-concrete interface. This transfer can be attributed to several mechanisms, including, adhesion, friction, and bearing. Adhesion and friction should not be considered during design due to their lack of reliability. Therefore, steel elements welded to the girder and embedded in the concrete are assumed to provide a reliable shear connection. Among the many type of connectors available, welded headed shear stud is the most widely used in both bridge and building construction (Viest et al, 1997). A knowledge of shear stud behavior is necessary to be able to understand the mechanism of shear transfer between steel and concrete.

1.4.1 Behavior of Shear Studs

An experimental investigation of shear stud behavior is carried out by performing push-out tests. Although there is not a standardized procedure for fabricating and testing push-out test specimens, other researchers have used similar, though slightly different, procedures (Viest et al, 1997) in the past. In a typical push-out test specimen, studs are welded to both flanges of a W-shape. Later, a slab is poured on each side of the W-shape so that the studs will be embedded in concrete. The specimens are tested by applying an axial force to the W-shape. A conventional push-out test specimen is shown in Figure 1.3. During the test, vertical slip between the slab and beam are measured. Specimens are generally loaded up to failure with or without unloading and reloading during the test. A load-slip response for a shear stud such as the one shown in Fig. 1.4 is obtained as a result of a push-out test. The load slip behavior is nonlinear. In general, the unloading of specimens does not affect the envelope of the curves. The reloading is linear until the maximum load prior to unloading is reached.

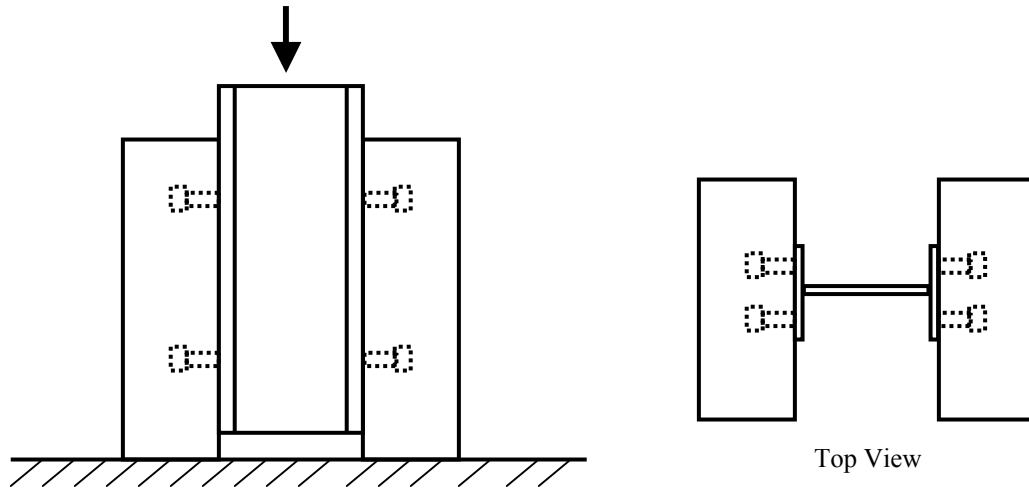


Figure 1.3: Conventional Push-out Test Setup

The ultimate strength of a shear stud and the mathematical representation of the load-slip relationship are the two most important results of a push-out test. A large body of knowledge exists for shear stud tests. Among all previous investigations, the study by Ollgaard et al (1971) is the most frequently cited and forms the basis of the AISC and AASHTO specifications.

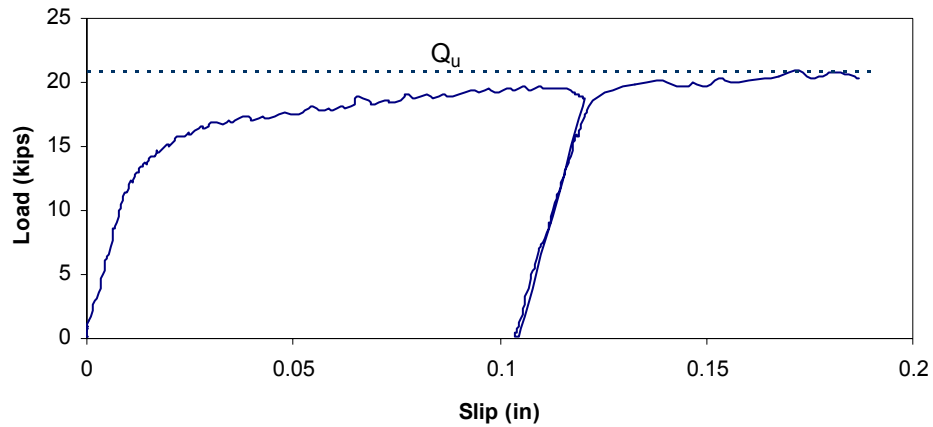


Figure 1.4: Typical Load-Slip Response for a Shear Stud

Ollgaard, Slutter, and Fisher (1971) studied the strength of shear connectors in lightweight and normal-weight concrete. Forty-eight push-out specimens were tested during their investigation. The variables considered were concrete compressive strength, split tensile strength, modulus of elasticity, density of concrete, stud diameter, type of aggregate, and number of connectors per slab. Based on regression analysis of the results of this and earlier studies, they proposed the following equation for ultimate connector strength, Q_u :

$$Q_u = 0.5A_{sc}\sqrt{f'_c E_c} \leq A_{sc}F_u \quad (1.3)$$

where, A_{sc} = cross-sectional area of shear stud (in²), F_u = minimum specified tensile strength of stud steel, and f'_c and E_c in ksi.

In addition to the connector strength formula, two different load-slip relationships were proposed. For continuously loaded specimens, an empirical formula was determined as:

$$Q = Q_u \left(1 - e^{-18\Delta}\right)^{2/5} \quad (1.4)$$

where, Δ = slip.

At zero load this function gives an initial tangent of infinity. This result is due to the initial bond between steel and concrete, and has been observed during the tests.

For the specimens that were loaded up to the working load level of connectors, then unloaded and reloaded to their ultimate load, a load-slip relationship for the reloading branch was proposed as:

$$Q = Q_u \frac{80\Delta}{1 + 80\Delta} \quad (1.5)$$

Contrary to having a vertical tangent, this equation gives a slope of $80 Q_u$ (kips/in) at zero load. Comparison of Equations 1.4 and 1.5 are given in Fig. 1.5.

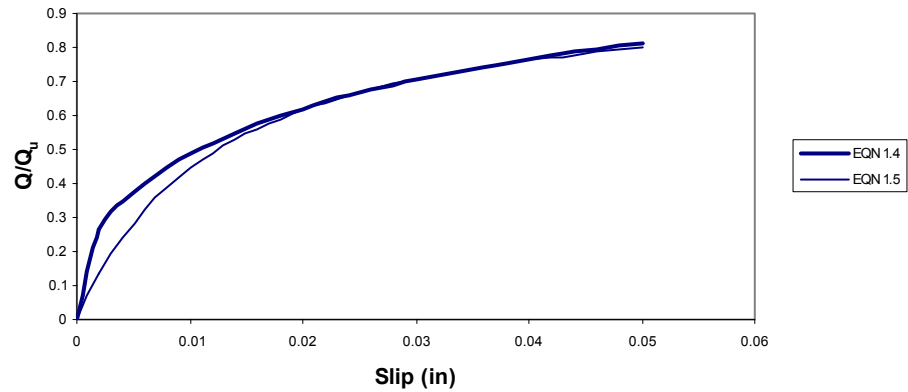


Figure 1.5: Load-Slip Relationships for Shear Studs

1.4.2 Mechanics of Shear Transfer

The mechanics of shear transfer is not yet fully understood. It requires micro-modeling of the shear connector. However, specimens cut into halves after testing give some insight into the deformation pattern (Ollgaard et al, 1971). An interesting observation is that shear studs exhibit ductile behavior. Formation of high local stresses result in the global ductility of the connection. Concrete, however, will experience inelastic, permanent deformations or local crushing around the welded part of the stud. The void that forms due to local crushing permits the stud to deform (Viest et al, 1997). Figure 1.6 shows the deformation pattern of the steel connector-concrete interface. Because of the deformations occurring in the stud, the overall behavior is ductile.

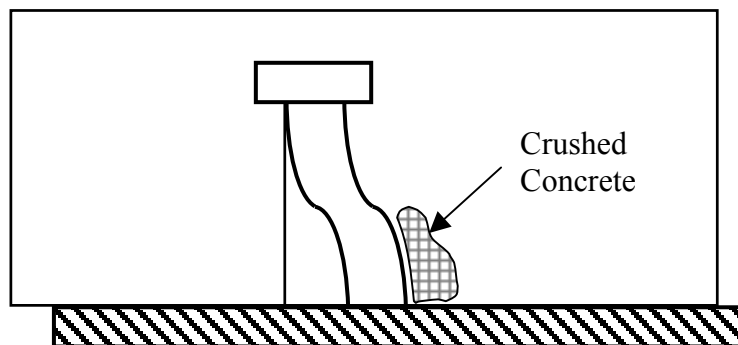


Figure 1.6: Deformation Pattern of Steel Connector-Concrete Interface

1.4.3 Evaluation of the Push-out Test and the Definition of Stud Strength

As mentioned earlier, there is no standard procedure for push-out tests. There is wide scatter in the results due to differences in test specimens, the methods of casting, and test procedure. This kind of test is prone to premature separation between the slab and the steel W-shape in the direction normal to the slab surface. In addition, results are affected by the frictional forces developing between the base of the test slabs and the reaction floor.

Another discrepancy arises during the interpretation of the test results. The ultimate strength of the shear connector is defined as the maximum load attained per stud during a test. However, this definition does not consider the serviceability limit state. In the study by Ollgaard et al., 1971, the maximum load was reached at slips varying from 0.23 to 0.42 in. In reality, these kind of deformations cause significant serviceability problems. Therefore, when defining the ultimate strength of the shear connectors, a criteria that satisfies both strength and serviceability should be selected. The investigation of this issue is still under scrutiny by AISC committees.

1.5 Problem Statement

As explained earlier, construction loading should be handled with great care during the design of curved trapezoidal steel box girders. Such design requires a thorough understanding of curved girder behavior during construction and the use of accurate analytical tools. Lack of knowledge of curved girder behavior and/or use of inadequate tools has resulted in catastrophic failures in the past. Figure 1.7 shows a trapezoidal box girder failure during construction.

Currently, the behavior of steel-concrete interface at early concrete ages is unknown. Recent field studies on curved trapezoidal box girders (Cheplak, 2001) revealed that the composite action develops at very early concrete ages. The development of early composite action has some beneficial effects. The use of early-age concrete deck to overcome construction loads might eliminate some of the bracing members and might also lead to the use of smaller plate members. In addition, the use of

early composite action might reduce construction times. Reduction in member sizes and construction time could lead to significant cost savings.



Figure 1.7: Trapezoidal Box Girder Failure During Construction

In order to use the idea of the early composite action, analysis tools capable of accurately modeling this phenomenon are essential. Current computer programs available to designers do not permit the definition of a semi cured concrete deck in the model. Only general-purpose finite element packages are capable of solving this kind of a problem but they require the knowledge of finite element method. Therefore, the general purpose finite element programs are not widely used in the design of these bridges.

It is the focus of this research to investigate the steel-concrete interface behavior at early ages and provide for its implementation into an analysis package. An experimental program was designed to investigate the performance of shear connectors

on curved bridges during early concrete ages. The study was limited to one typical concrete mix design used in these types of bridges. In addition to laboratory experiments, a computer program was developed for the analysis of curved trapezoidal box girders under construction loads. The program was based on finite element analysis and requires minimal knowledge of the FEM on user's part. As a third task, two bridges were monitored in the field during construction. Successive chapters will include detailed explanations of the investigations and the development of an analysis package to be used for construction loading simulations. The comparisons of the analytical predictions with the field observations will be presented.

CHAPTER 2

EXPERIMENTAL INVESTIGATION OF THE STEEL-CONCRETE INTERFACE BEHAVIOR AT EARLY AGES

2.1 General

Current literature lacks experimental evidence of steel-concrete interface behavior at early concrete ages. This information is essential in understanding the shear transfer between concrete deck and top flange during construction of bridges. All push-out tests previously reported were performed on mature concrete. It is necessary to obtain load-slip curves for studs embedded in concrete and subjected to shear forces from 3 to 48 hours after concrete has been poured. Obtaining this information entails certain experimental challenges. Standard push-out tests were found not suitable for testing specimens at early ages. There are constraints on the test setup that need to be addressed in testing specimens with early-age concrete.

The testing should be completed in a very short time period. Otherwise, time elapsed during testing of replicate specimens would cause concrete to change properties that result in different load-displacement behavior. All replicate specimens should be tested within fifteen minutes.

Prior to testing, specimens should not be moved because unnecessary handling may damage the early-age concrete. Transportation of specimens may also expand the time interval between tests. This constraint limits the use of a test machine since specimens have to be cast and tested in place.

If possible, specimens should not be anchored to the floor or to another fixture. Application of loads to low strength concrete may cause damage to the specimen around anchorage regions, and local failures in these locations may result in an undesirable behavior.

2.2 Push-out Test Setup

A self-contained push-out test setup was developed for testing shear studs embedded in early-age concrete that meets all the above-mentioned constraints. The test setup consisted of a loading fixture (A), a test specimen (B) and a spreader beam (C). (Figures 2.1 and 2.2)

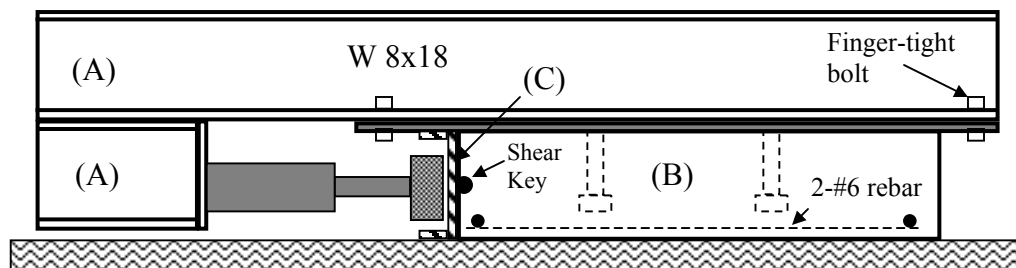


Figure 2.1: Schematic of the Push-out Test Setup



Figure 2.2: Side View of the Push-out Test Setup

For each specimen, a box-type formwork having dimensions of 36in. x 24in. x 8in. was prepared. Plywood was placed on three sides while a 24-in. long C8x11.5 channel section was placed on the remaining side. The channel section served as formwork as well as a spreader beam during the loading process. Two #6 reinforcing

bars in both directions were placed at the bottom. Reinforcing bars are located 2 inches from the edges of the formwork. Two 3/4 in. diameter, 5 in. tall shear studs were welded to a 5/8 in. x 10 in. x 48 in. flat bar using standard stud installation equipment. A plastic sheet was wrapped around the flat bar to prevent bonding between the steel plate and the concrete. The flat bar was placed on top of the formwork with the studs oriented downward. After completing all the forms for each test specimen, concrete was cast inside all the forms and vibrated according to standard specifications.

The specimens were tested by making use of a loading fixture. A loading fixture was constructed by welding a 12-in. and a 72-in. W8x18 wide flange steel section together. A 60-kip capacity hydraulic ram was bolted to a plate that was welded to the short section of the loading fixture. The loading fixture was lifted into position and was connected to the flat plate of the test specimen by four 3/4-in. diameter A325 bolts. Two holes with a diameter 11/16 in. were drilled into the flange of the channel section, while, two holes with a diameter 17/16 in. were drilled into the flat plate at coinciding locations. Two 5/8 in. diameter A325 bolts were used to connect the two parts. These bolts were necessary to counteract the tendency of the loading frame and the concrete slab to separate due to the eccentricity of the jack loading axis and the shear plane. A hydraulic ram was connected to a hand pump in order to apply the loading.

During a typical test the load-displacement behavior was documented by collecting data at every second with a data acquisition system. The load was monitored by making use of a 50-kip load cell that was attached to the loading ram. Displacements were measured with two linear potentiometers that have an accuracy of 0.0001 inches.

One minor detail about the setup is also worth mentioning. Although the spreader beam was not connected to the floor, it did not uplift together with the loading beam when both were tied together. The tendency to uplift was prevented by the formation of frictional resistance between the channel section and concrete block as a result of the applied load. In order to increase the resistance against uplift, a layer of #6 reinforcing bars was welded to the web of the channel section to act as a shear key.

2.3 Test Program

A test program was designed to obtain load-displacement behavior of shear studs embedded in early-age concrete. Eight testing times were chosen, 4 hours, 8 hours, 13 hours, 22 hours, 3 days, 7 days, 14 days, and 28 days after initial casting. At all of these times, concrete cylinders were also tested to obtain material properties. For each time period, three push-out tests, three cylinder compression tests, and three split cylinder tests were performed.

Class-S type concrete, which is used for bridge slabs in the state of Texas, was selected for use in the test specimens. According to the Texas Department of Transportation construction specifications (1993) Class-S type concrete should meet the following requirements:

Minimum Compressive Strength (f'_c) (28 day) : 4000 psi

Minimum Flexural Strength (7 day) : 570 psi (525 psi when Type II or Type I/II cement is used)

Maximum Water/Cement Ratio: 0.47

Desired Slump: 3 inches (4 inches maximum)

Concrete was ordered from a local ready-mix concrete supplier. Weights of the ingredients per cubic yard of delivered concrete are given in Table 2.1. The measured slump of the concrete was 3.5 inches, and the calculated water/cementitious ratio (including fly ash) of the above mix was 0.35.

A shear stud diameter of 3/4 inches was chosen for all specimens because this size is the most widely used in practice. All studs were 5 in. tall. The push-out specimens were prepared in two rows each consisting of 12 specimens. (Figure 2.3) The loading beam was hoisted from one specimen to another for testing.

Table 2.1: Weights per Cubic Yard of Concrete

Material	Source	Weight
Cement	TXI Type I/II	430 lbs
Fly Ash	JTM Industries Class C	150 lbs
Fine Aggregate	TXI Concrete Sand	1168 lbs
Coarse Aggregate	TXI 1" Washed Gravel	1952 lbs
Total Water	City of Austin	204 lbs
Water Reducer / Retarder	D-65	25 ozs
Water Reducer / Retarder	D-17	9 ozs
Air Entrainment	Daravair	3.6 ozs

2.4 Test Procedure

The same test procedure was followed for all push-out tests. The specimens were loaded until the load-displacement curve reached a horizontal asymptote. Then the specimens were unloaded to zero load and reloaded until the load-displacement curve indicated a maximum load had been reached or the shear displacement was excessive (approximately, one half of the stud diameter). Finally, the specimens were unloaded, and the loading beam was removed.

Concrete cylinders were tested under compression to determine the load-displacement curve. The loading procedure defined in ASTM C 469-94 was used. Specimens were tested using a 600-kip compression test machine. A compressometer with a linear potentiometer was placed around the concrete cylinders to monitor the displacement. Because the test machine was load-controlled, only the ascending branch of the load-displacement curve was obtained. In addition to compression tests, split cylinder tests were also performed in accordance with ASTM C 496-96 procedures.

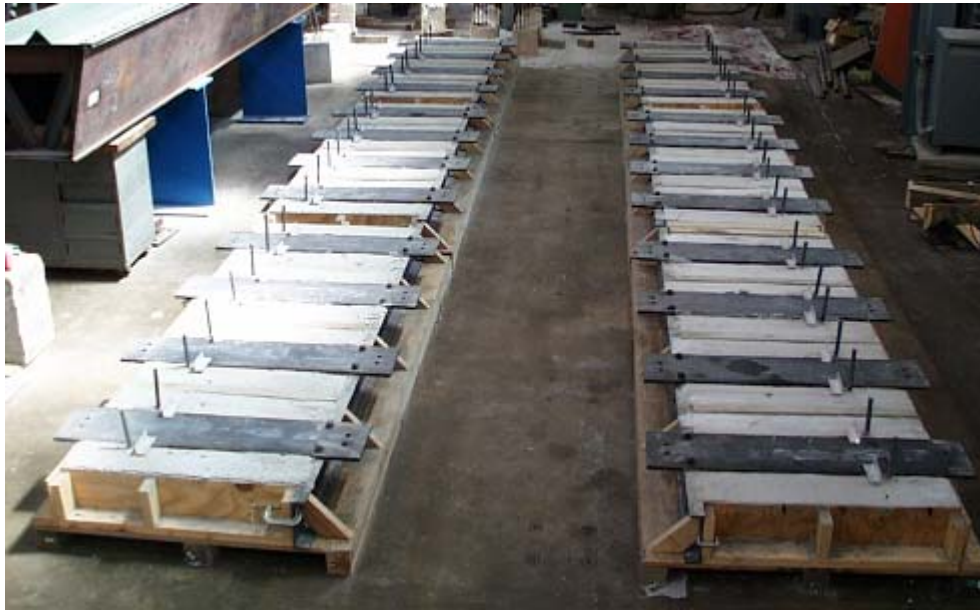


Figure 2.3: View of All Push-out Test Specimens

The approximate elapsed times for testing of the three push-out specimens, three compression specimens, and three split cylinder specimens were 30, 30, and 20 minutes respectively. Therefore, each testing cycle took about 80 minutes to complete. The specimens were cast and air cured inside the laboratory where the ambient temperature was between 85-95°F during the 28-day period.

2.5 Test Results

2.5.1 Push-out Tests

As mentioned earlier, three push-out tests were performed for each of the eight time periods. A typical load displacement response obtained from a push-out test is given in Fig. 2.4. In addition, the first loading cycle of all tests is presented in Fig. 2.5. In general the load-slip relationship of replicate specimens were similar except for the set of specimens that were tested at 8 hours and 13 hours where large scatter was observed.

4hr Push-out Test Specimen #1

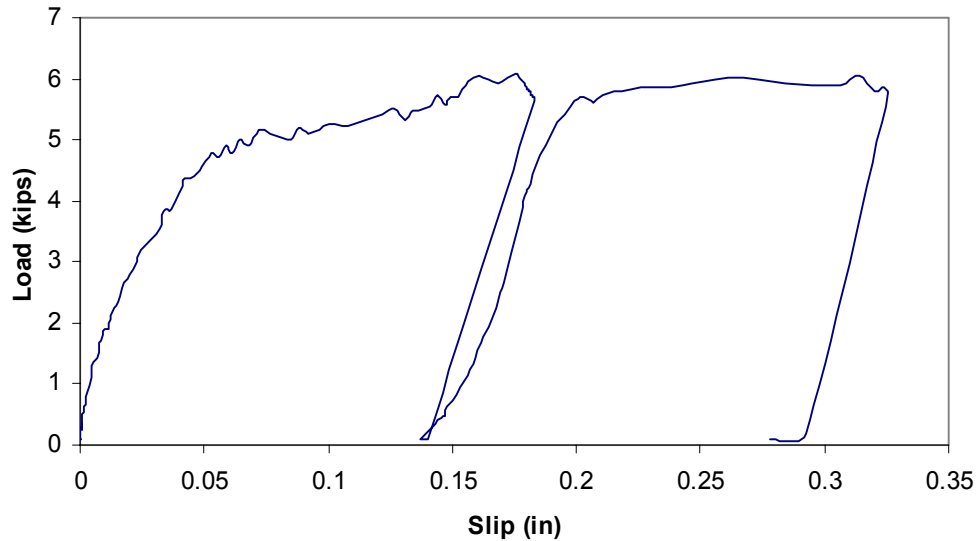


Figure 2.4: A Typical Push-out Test Result

It is evident from the results that even at very early ages, studs exhibit considerable stiffness and strength. In order to quantify the results, certain definitions are required. As explained in Chapter 1, the failure load obtained from a push-out test was considered as the ultimate capacity of the shear stud. However, this definition does not consider the serviceability limit state. Failure load is reached at very high displacement levels that a structure could not tolerate. Therefore, the concept of design strength (Q_d), which is based on a serviceability limit state, is proposed in this section. Similar yet different procedures were proposed by other researchers for the design shear connector resistance and stiffness. For example, in a study by Wang(1998), the design resistance is taken as 80% of the ultimate resistance, and the stiffness is conservatively estimated as the secant stiffness at design strength with an equivalent slip of 0.03 inches.

The proposed design strength (Q_d) is defined as the value of the load attained at a displacement value of 0.03 inches (Diameter/25). (Fig 2.6) This limit ensures that during the lifetime of the structure, the studs do not experience deformations in excess of 0.03

inches (D/25). Maximum strength (Q_{max}) is defined as the maximum load attained during the test regardless of a displacement limit state. (Fig 2.6) Because the specimens were not loaded up to failure, the maximum strength is expected to be slightly lower than the ultimate value predicted by current design equations.

The sensitivity in the definition of design strength was investigated by considering a range of serviceability limits in the vicinity of 0.03 inches of slip. Test results showed that defining the design strength based on displacement values of 0.025 inches and 0.035 inches gives on average 6.7% lower and 5.7% higher design strength values, respectively, when compared to the proposed definition. It could be concluded that design strength is not very sensitive to the slip level in the vicinity of 0.03 inches.

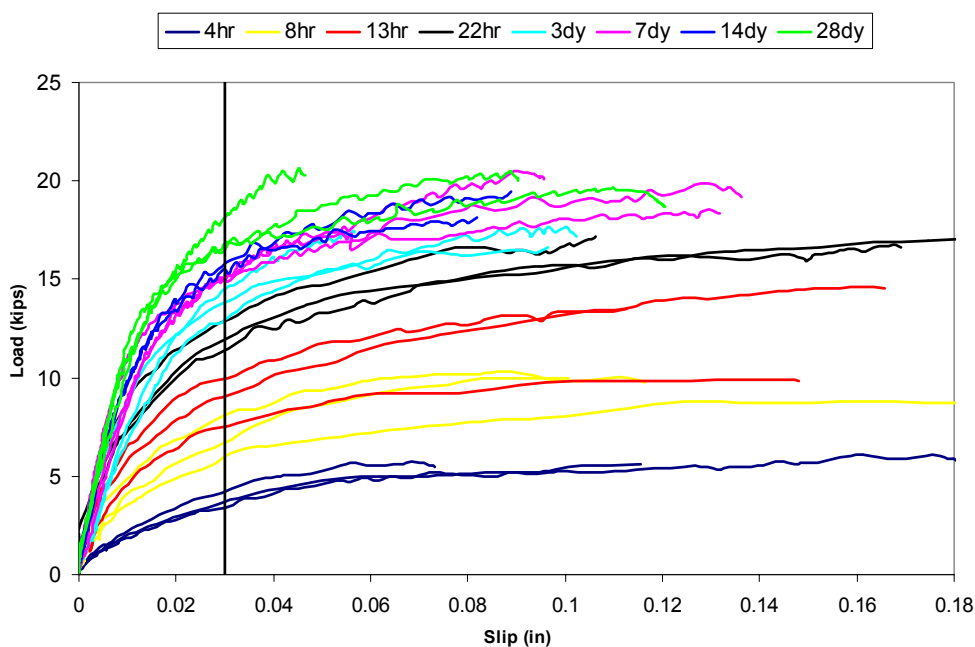


Figure 2.5: Load-Slip Relationship from Push-out Tests

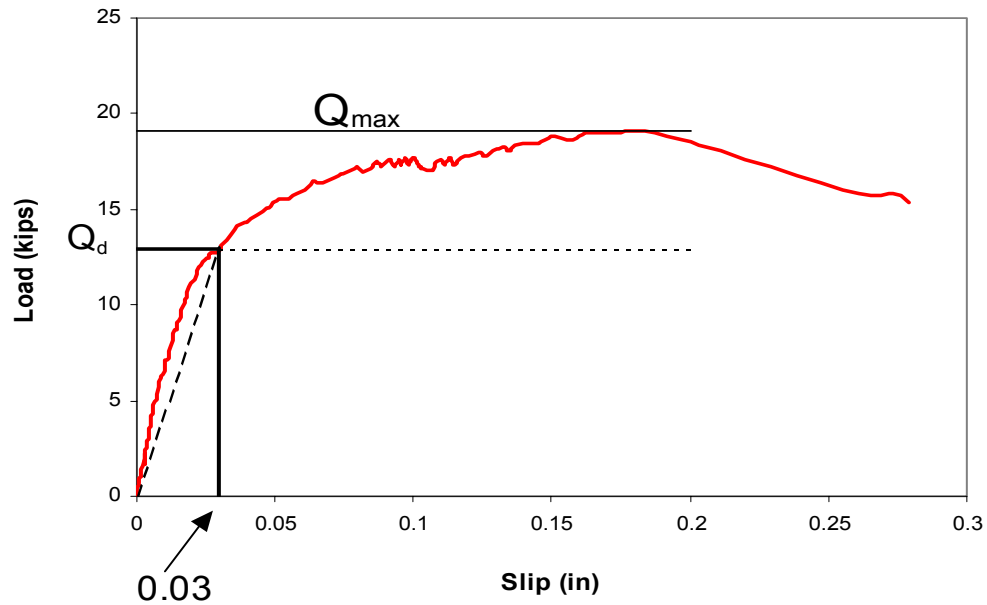


Figure 2.6: Definition of Design and Maximum Strength

Table 2.2 summarizes the design and maximum strength values obtained from the push-out tests.

Table 2.2: Push-out Test Results

Time	Stud Design Strength, Q_d (kips)				Stud Maximum Strength, Q_{max} (kips)			
	Specimen Number			Average	Specimen Number			Average
	1	2	3		1	2	3	
4 hr	3.6	4.4	3.7	3.9	6.0	6.2	6.1	6.1
8 hr	8.1	6.3	6.9	7.1	10.2	8.85	10.0	9.6
13 hr	10.1	7.7	9.00	8.9	13.5	10.1	14.7	12.7
22 hr	11.9	13.0	11.5	12.1	17.5	17.6	17.5	17.5
3 day	13.8	14.5	13.0	13.7	17.5	19.4	19.1	18.7
7 day	14.9	15.0	14.9	14.9	18.4	20.2	19.8	19.4
14 day	15.3	16.0	xxx	15.6	19.2	20.1	21.2	20.2
28 day	18.3	16.4	17.0	17.2	21.0	21.0	21.0	21.0

A mathematical representation of the load-slip behavior for shear studs is required for proper modeling of their behavior in analysis packages. For this purpose, a simple load-slip response curve was developed. All load-displacement curves obtained from push-out tests were normalized with respect to design strength and 0.03 inches of displacement. All data were plotted together (Fig. 2.7). A fifth degree polynomial with an R^2 value equal to 0.97 was fit to all the data shown in Fig. 2.7. Then a simplified equation was developed that represents the fifth degree curve. The proposed load slip relationship is given by equation 2.1. This equation gives an initial tangent stiffness of $100 Q_d$ and a secant stiffness at design load of $33.3 Q_d$.

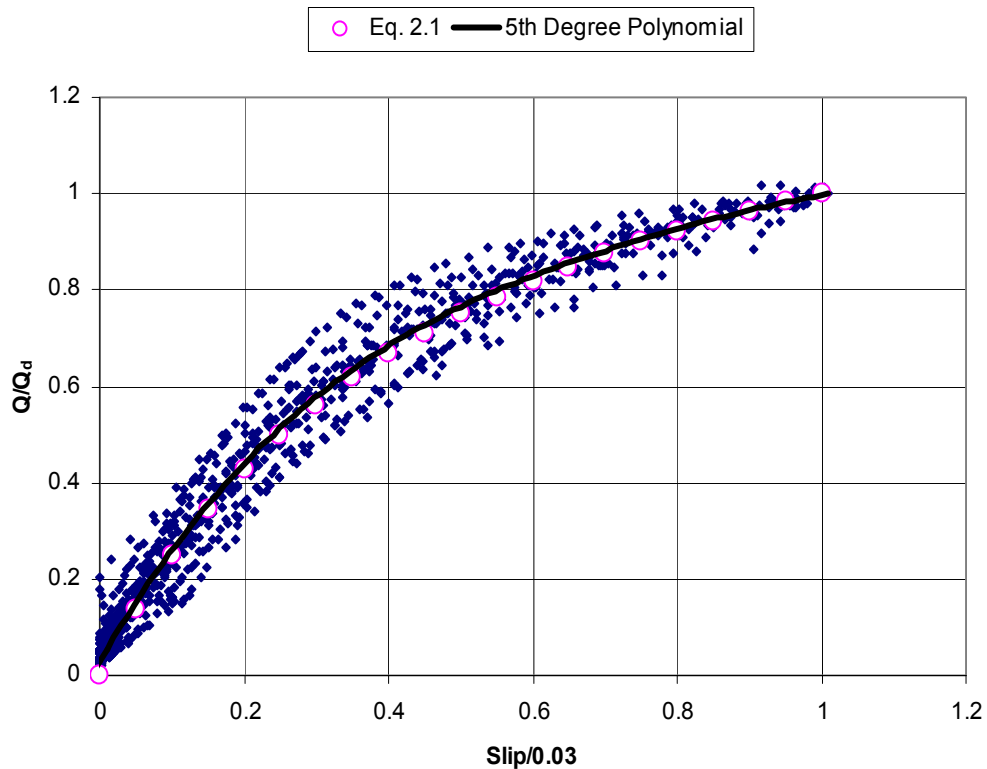


Figure 2.7: Load-Slip Relation for Shear Studs

$$\frac{Q}{Q_d} = \frac{3\left(\frac{\Delta}{0.03}\right)}{1 + 2\left(\frac{\Delta}{0.03}\right)} \quad (2.1)$$

2.5.2 Tests for Determining Concrete Properties

Three compressive and three split cylinder tests were performed on concrete specimens for each time period. During the compressive tests, the displacement was monitored to obtain the stress-strain response. Table 2.3 summarizes the ultimate compressive strength, secant stiffness at 40% of ultimate strength and split cylinder test results for concrete specimens. In addition, the stress-strain curves for compression are presented in Fig. 2.8.

Table 2.3: Concrete Properties at Different Times

			Time							
			4 hr	8 hr	13 hr	22 hr	3 dy	7 dy	14 dy	28 dy
Compressive Strength (psi)	Specimen Number	1	286	715	1230	1970	3530	3740	4530	4370
		2	304	832	1230	1830	3080	4420	4450	4370
		3	364	859	1250	1820	3060	4040	4380	4510
	Average		318	802	1237	1873	3223	4067	4453	4417
Compressive Stiffness (ksi)	Specimen Number	1	1220	2578	2900	3433	4408	4067	4316	xxx
		2	xxx	2802	3315	3868	4038	4552	4468	4148
		3	1280	3132	3204	3647	3923	4789	4341	4237
	Average		1250	2837	3140	3649	4123	4469	4375	4193
Tensile Strength (psi)	Specimen Number	1	38	105	119	278	328	374	340	375
		2	25	93	159	238	282	315	433	450
		3	32	98	141	250	293	318	450	442
	Average		32	99	139	255	301	335	408	422

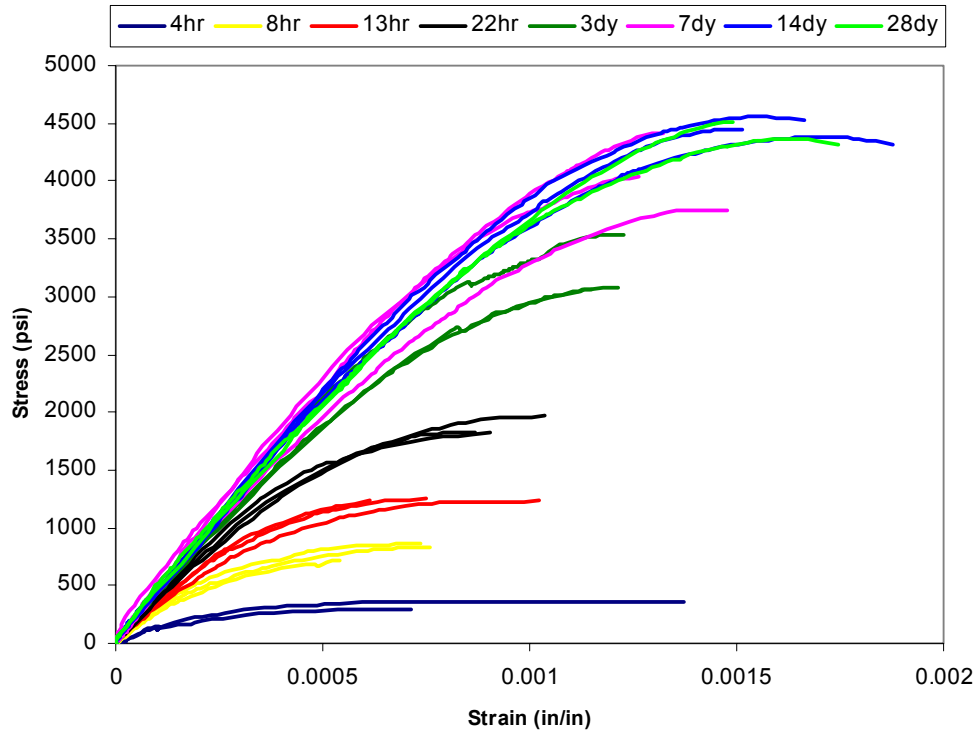


Figure 2.8: Compressive Stress-Strain Response of Concrete at Early Ages

Test results revealed that the rate of stiffness gain is much higher compared to the rate of strength gain. Specimens reached almost 90 percent of the 28-day stiffness after 22-hour cure. At very early ages, the stress-strain response mimics elastoplastic behavior. Concrete specimens tested after 22 hours exhibit a stress-strain response that is similar to the 28-day response. Figure 2.9 presents the time dependence of concrete properties together with the push-out test results. For concrete the rate of stiffness gain is much higher in comparison to the rate of strength gain. The stud maximum and design strength increases faster than concrete strength and slower than concrete stiffness.

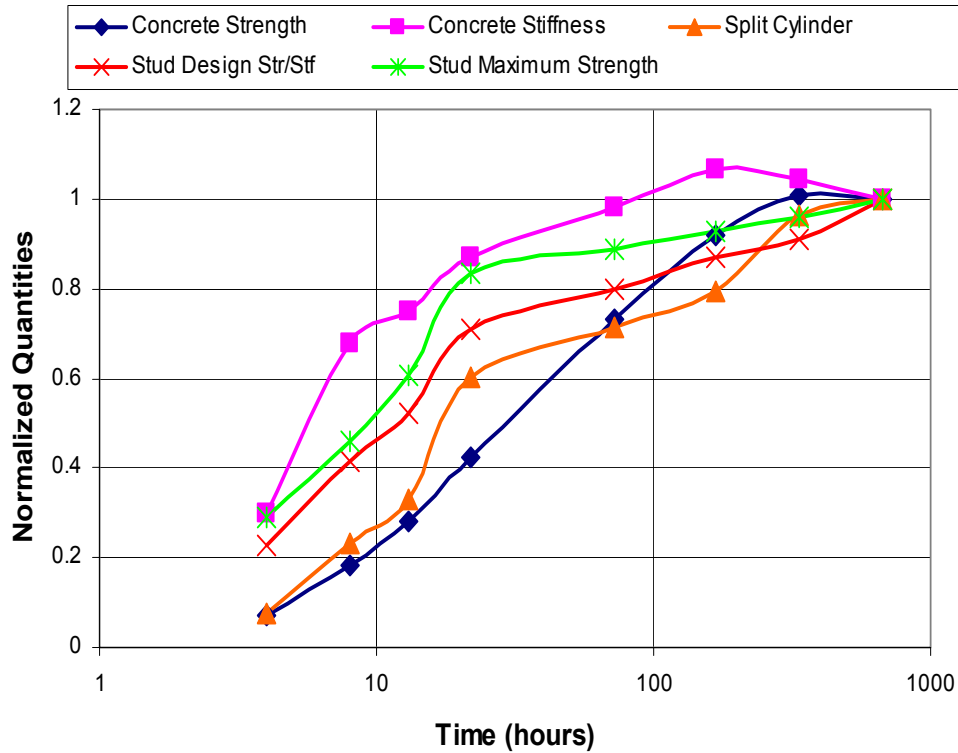


Figure 2.9: Time Dependence of Properties

Based on the concrete cylinder tests, the applicability of the existing ACI relation (Equation 1.1) in predicting the stiffness of early age concrete was investigated. Figure 2.10 shows the comparison of the test results from four different researchers compared with the ACI relation. Careful examination of the data reveals that each set of data is consistent in itself. Data from this study shows stiffer response while data from Mo exhibits more flexible behavior in comparison to ACI's relation. This result could be attributable to different curing conditions and mix designs used for concrete specimens. Also differences in the stiffness of the aggregates used by different researchers could cause scatter among test results. In general, the ACI relation is satisfactory and applicable in predicting the stiffness of concrete at early ages given its strength.

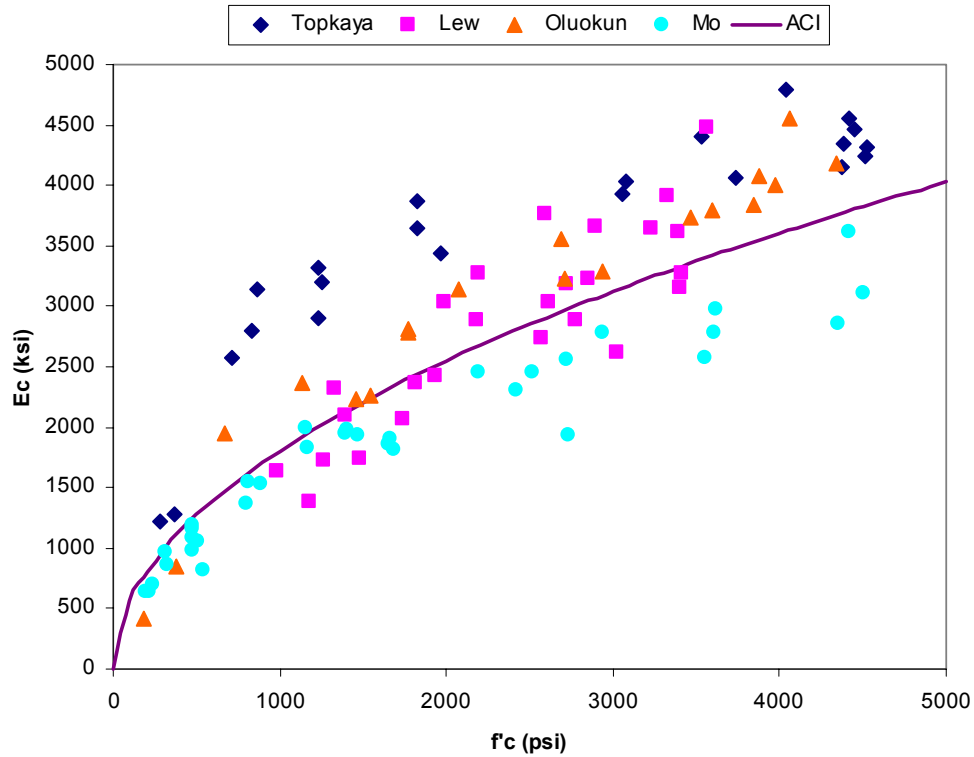


Figure 2.10: Concrete Stiffness Test Results

2.5.3 Development of Expressions for Maximum and Design Strength

Based on the experimental data gathered, expressions for estimating the design and maximum strength of shear studs were developed. These expressions are applicable to both mature and early-age concrete cases. Expressions were developed in such a way that they have a form similar to the one used in the current design specifications. Load on the stud is normalized by the cross-sectional area of the shear connector. Regression analyses were performed to find out the dependency of concrete parameters on the design and maximum connector strength. The coefficients obtained from regression analyses were rounded off to find out simpler equations for estimating quantities. Equations 2.2 and 2.3 were developed to estimate the design and maximum strength of shear connectors

based on concrete properties. Figure 2.11 shows how the developed equations represent the experimental findings.

$$\frac{Q_{\max}}{A_{sc}} = 2.5(f'_c E_c)^{0.3} \quad (2.2)$$

$$\frac{Q_d}{A_{sc}} = 1.75(f'_c E_c)^{0.3} \quad (2.3)$$

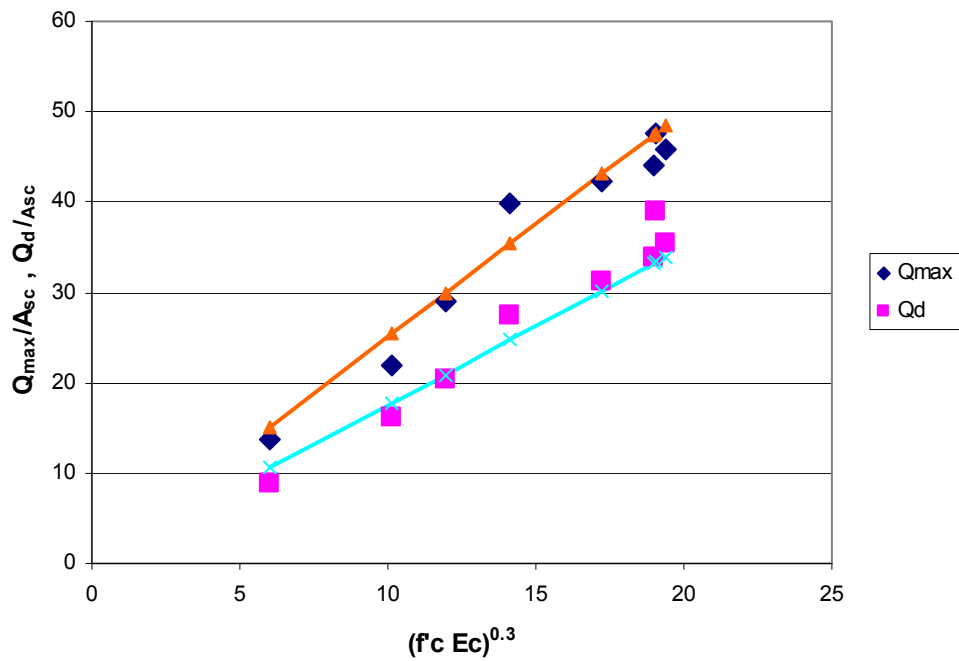


Figure 2.11: Stud Strength Results and Recommendations

2.5.4 Effects of Changing Concrete Properties on the Performance of Shear Studs Pre-loaded at Early Ages

The effect of loading studs in early-age concrete on the long-term performance is investigated. For this purpose, all specimens were retested after 28 days using the same testing procedure explained in section 2.4. During the original tests, specimens were loaded up to different displacement limits. The residual slip level attained in earlier tests is an indication of damage to the early-age concrete. Figure 2.12 was prepared to investigate the effect of the level of damage on the long-term ultimate performance of the shear stud. For each test specimen, the residual slip value from initial tests was plotted versus the maximum load reached during re-testing at 28 days. According to the trendline fitted to the data, the maximum capacity of the stud decreases as the level of damage increases. In addition the plot reveals that studs loaded up to the recommended design displacement value of 0.03 inches at early concrete ages could be able to develop their full strength after 28 days.

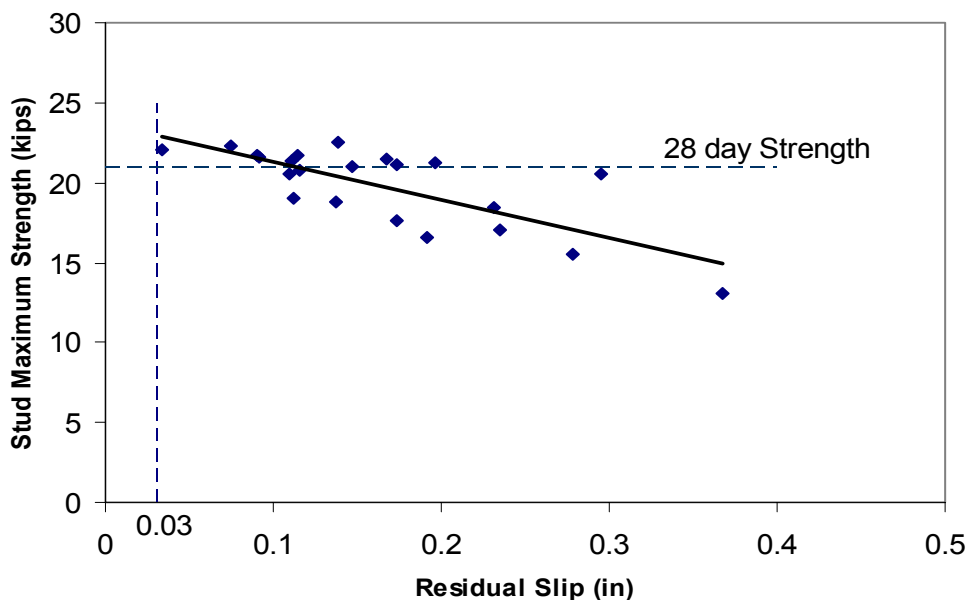


Figure 2.12: Residual Slip versus Maximum Strength for Retested Specimens

Another observation on the load-slip behavior of re-tested studs is worth mentioning. Although pre-tested studs may develop their full capacity at 28 days, there might be a change in their initial stiffness. Figure 2.13 qualitatively represents this phenomenon. Load-displacement curves for two specimens are presented. The first specimen is tested at 13 hours while the second one is tested at 14 days. Both specimens were re-tested at 28 days and they developed their full capacity. However, for the 13-hour specimen, the retesting curve has a very low initial stiffness compared to the 14-day specimen. This observation shows that for specimens tested at very early ages, localized concrete damage around the stud weld location causes a weak zone that results in further stiffness reduction of the overall system.

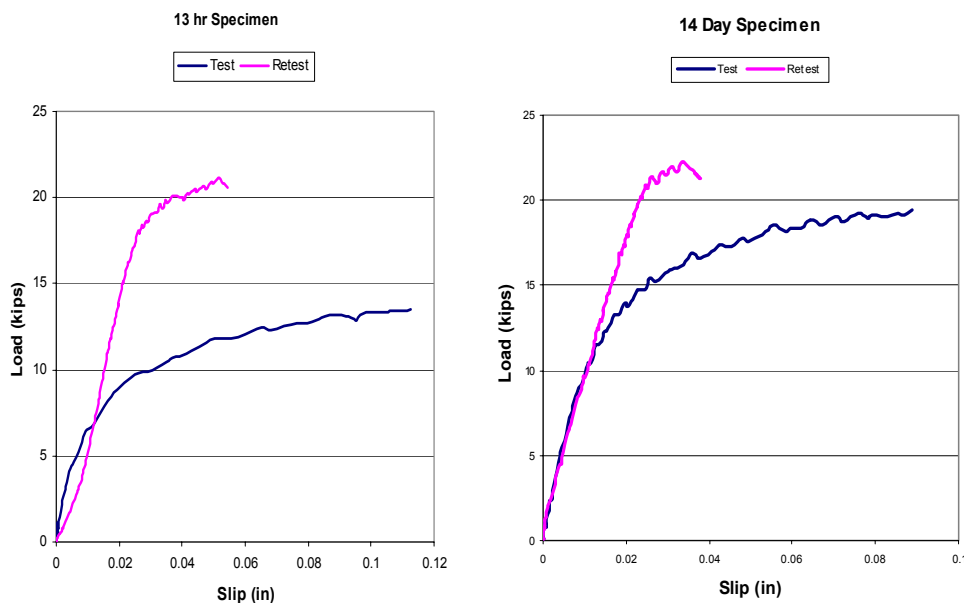


Figure 2.13: Load-slip Behavior of Retested Specimens

2.5.5 Effect of Surface Bond

The test setup was designed to obtain the load-slip relation for shear studs by minimizing the effects of bond occurring at the concrete-flat bar interface. This minimization was achieved by wrapping plastic sheets to steel flat plates. In order to investigate the necessity of these sheets for a standardized test, the plate of one specimen

was left unwrapped. This specimen belonged to the group of specimens that were tested at 14 days. Figure 2.14 presents the load-slip relationship for this set of specimens. It is clear from the curves that bond between steel and concrete has tremendous influence on the initial stiffness of studs. For a standardized test, bond should be minimized to obtain conservative initial stiffness values. The use of plastic sheets is one way to eliminate the bond.

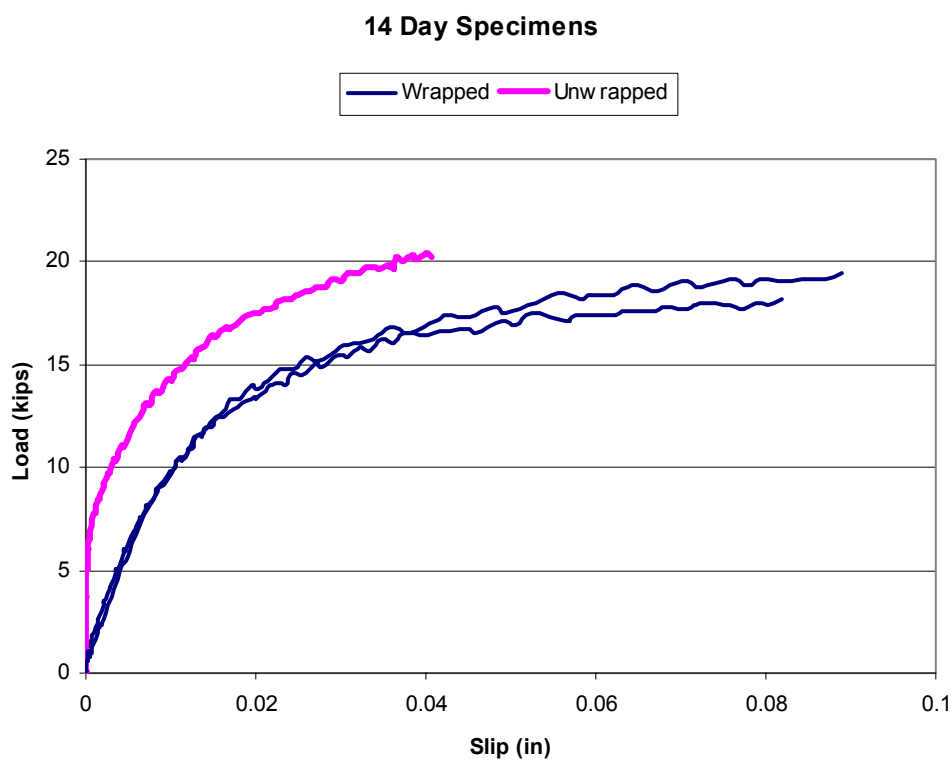


Figure 2.14: Effect of Steel Surface Treatment on Stud Behavior

2.6 Summary of Test Results

Tests on shear studs embedded in early-age concrete revealed that studs transfer shear as early as 4 hours. The concept of design strength was introduced. An equation for predicting design strength and load-slip behavior for shear studs was developed.

Mechanical properties of concrete were monitored for early concrete ages in addition to the stud tests. Tests on cylinders revealed that the stiffness of concrete increases much more rapidly compared to its strength. The existing ACI equation for predicting modulus was found to be applicable to early age concrete.

All push-out test specimens were tested at 28 days to investigate the effects of early age loading. Test results indicated that most specimens gained their full strength despite the fact that they were preloaded. The level of strength gain was found to be inversely proportional to the ultimate displacement level attained in the earlier tests. Significant local crushing may occur if studs are deformed to high displacement levels at early ages. Local crushing may reduce the initial stiffness of the studs.

CHAPTER 3

DEVELOPMENT OF COMPUTATIONAL SOFTWARE FOR POUR SEQUENCE ANALYSIS

A computer program (UTrAp) with a graphical user interface (GUI) was developed for pour sequence analysis. The package consists of an analysis module, which was written in FORTRAN, and a GUI, which was written in Visual Basic. The program was developed for use on personal computers. The following sections provide documentation of the program in detail.

3.1 Analysis Module

The analysis module consists of a three-dimensional finite element program with pre- and post-processing capabilities. Input for the analysis module is provided by a text file that is created through use of the GUI. The module itself is capable of generating a finite element mesh, element connectivity data and material properties based on the geometrical properties supplied through the GUI. The program also generates nodal loading based on the values given in the input file. After the pre-processing is completed, the program assembles the global stiffness matrix and solves the equilibrium equations to determine the displacements corresponding to a given analysis case. As a last step, the module post-processes the displacements in order to compute cross-sectional forces, stresses and brace member forces. The following sections document the formulation of the analysis module and discuss current capabilities and limitations.

3.2 Program Capabilities

The analysis module is capable of analyzing curved, trapezoidal, steel box girders under construction loads. This program can analyze only single and dual girder systems with a constant radius of curvature. The number of girders is limited to two because systems with more than two girders are very uncommon in practice, and the solution of such bridges with FEM will require computer resources that surpass the

capabilities of current personal computers. Nowadays, a typical PC used by an engineer has 256 MB memory and 1 GHz processor speed. Although not very widely used, personal computers with up to 2 GB memory and 1.7 GHz processor speed are available. A typical twin girder system with the mesh adopted by this program requires about 700 MB of physical memory for in-core solution.

The analysis module allows the thickness of the plates to vary while the centerline distance of all components (e.g., web, top flange) is held constant. Internal, external and top lateral braces can be specified in the program, and supports can be placed at any location along the bridge length. There is no internal constraint on the number of braces, length of the bridge or number of supports. The program is for linear analysis and is capable of handling multiple analysis cases.

3.3 Input Requirements

Geometric Properties: The number of girders, radius of curvature, length of the bridge and cross-sectional dimensions are required input. Cross-sectional dimensions include depth of the web, width of the bottom flange, top flange width, width of the concrete deck and thickness of the concrete deck. In addition, the program requires the thickness of the web, bottom flange and top flange along the bridge length. There is no restriction on the number of different plate properties that a user can specify.

Supports: Support locations must be specified by the user. Locations are defined by the distance relative to a coordinate along the arc length. Supports are assumed to be either pinned or a roller. Actual properties of the support bearings are currently not considered in the program.

Braces: Locations, types and areas of internal, external and top lateral braces must be specified.

Pour sequence: There can be several analyses performed that are independent of each other. The concrete deck can be divided into segments. The length of each segment must be provided as input. For each analysis, properties of the concrete deck can be varied. There are three properties associated with a deck segment. These properties are the concrete modulus, stud stiffness associated with particular segment and the distributed load on the segment.

3.4 Algorithm of the Analysis Module

Program UTrAp uses 9-node shell elements, truss and stud elements to construct a finite element mesh. Steel plates and the concrete deck are modeled with shell elements. Braces and studs are modeled with truss and stud elements, respectively. The following paragraphs present the details of the program algorithm.

3.4.1 Node Locations and Element Connectivity

The program automatically forms the node locations and element connectivity based upon the geometric properties of the bridge specified by the user through the GUI. A constant mesh density is used for all bridges. The webs and bottom flanges of the girders are modeled with 4 shell elements while 2 elements are used for top flanges. The concrete deck is modeled with 10 and 20 shell elements for single and dual girder systems, respectively. Previous work on curved trapezoidal girders (Fan, 1999) revealed that this mesh density is adequate for most of the typical cross-section dimensions. Along the length of the bridge, each element is two-feet long. This mesh density assures elements of aspect ratios less than two for most practical cases. According to the geometrical dimensions and radius of curvature, the program forms the locations of the nodes. For each node, three mutually orthogonal unit vectors (V_1 , V_2 , V_3) are formed. These unit vectors are used in defining the shell element geometry. Fig. 3.1 shows the nodes and unit vectors on a single girder system. Unit vectors are formed in such a way that V_3 points in the direction through the thickness of the shell element and V_2 is tangent to the arc along the bridge length. V_1 is formed such that it is orthogonal to both V_2 and V_3 .

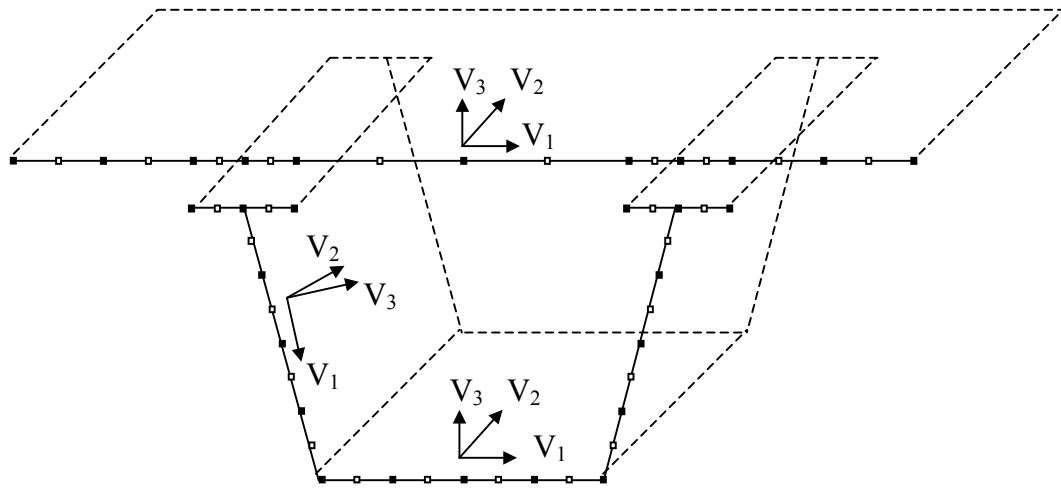


Figure 3.1: Node Locations and Unit Vectors

3.4.2 Modeling of the Physical System

There are several modeling techniques presented in the literature for analyzing the steel girder-concrete deck interaction. One proposed method is to model the steel section with shell elements and the concrete deck with brick elements (Tarhini and Frederick, 1992). (Fig. 3.2) Spring elements are placed at the interface to model the shear studs. This type of modeling produces a very large number of degrees of freedom, because, in order to capture the deck response with sufficient accuracy, a large number of brick elements must be used.

In another technique, both the steel cross section and the concrete deck are modeled with shell elements (Brockenbrough, 1986, and Tabsh and Sahajwani, 1997). The steel and concrete sections are connected together with connector (beam) elements. (Fig. 3.2) The length of the connector elements has to be chosen by the analyst to properly model the deck offset. This approach is the most favored technique presented in the literature despite the fact that there is no consensus on how to choose the connector length.

In the software developed for the current research, another approach is used to model the cross section which addresses both problems mentioned above. Two types of shell elements were used in modeling a given cross section. In shell element formulation,

the three-dimensional domain is represented by a surface. The selection of the representative surface depends on the particular formulation. Any surface along the thickness could be considered as a reference surface. Two types of shell elements used in the program are similar in formulation but differ in the reference surface definitions. For steel sections, the reference surface is considered to be the middle surface while for the concrete deck, the bottom surface is used as a reference. (Fig. 3.3) Steel sections and the concrete deck are connected together by spring elements that represent the stud connectors. This modeling technique reduces the degrees of freedom when compared with the brick model. In addition, it properly models the interface behavior by eliminating the beam elements and including the girder offset by using the bottom shell surface as the reference surface.

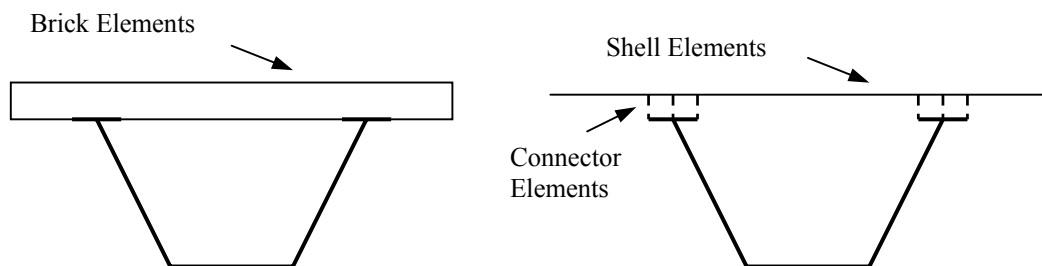


Figure 3.2: Different Modeling Techniques for Deck-Flange Interface

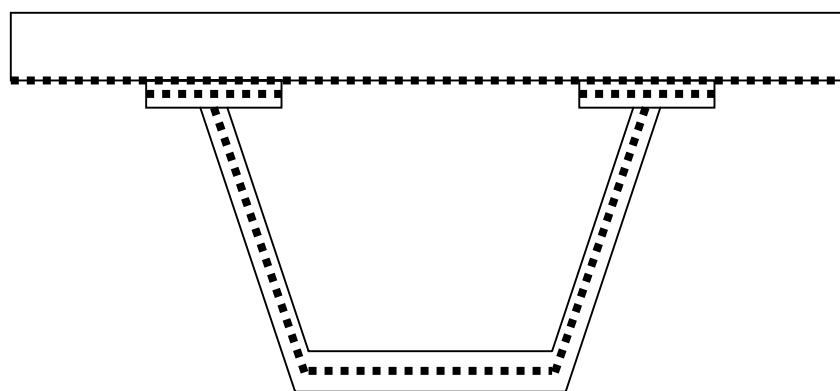


Figure 3.3: Reference Surfaces for Shell Elements

Internal, external and top lateral braces are modeled with truss elements. The program calculates the nodal connectivity of the brace elements from the supplied location values. Currently, only one type of internal brace and one type of external brace is handled in the program. (Fig. 3.4) The ones included are the typical types used in practice.

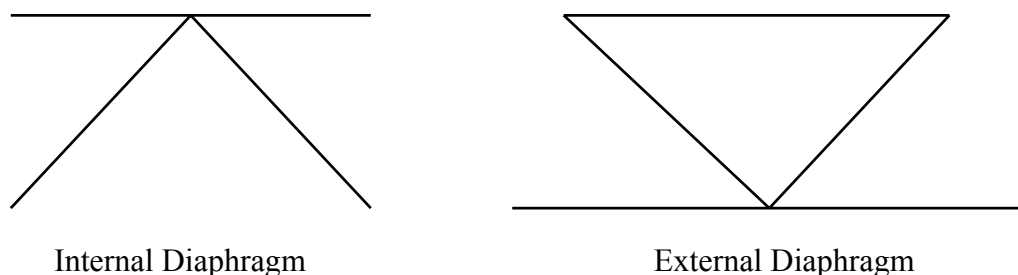


Figure 3.4: Internal and External Diaphragms Used in the Program

Spring elements are used to model the shear studs. For each top flange, three nodes are connected to the concrete deck. The connection is achieved by spring elements in all three global directions. Springs are placed every foot along the bridge length even if studs are not physically present. The stiffness properties of each spring element are modified by the analysis module according to the physical distribution of studs in a particular region. For each spring element there is a corresponding stiffness modification factor. The modification factor is calculated by dividing the stud spacing value by 12 inches. If there are less than three studs per flange, very low modification factors are assigned to the studs which are not present. In the case where the number of studs per flange is greater than three, the modification factor is further multiplied by the number of studs per flange and divided by three.

In practice, diaphragms in the form of thick plates are placed at the support locations to reduce stresses caused by high torsional forces. Diaphragms form a solid cross section with very high torsional and distortional stiffness. The program internally assembles a very stiff truss system (Fig. 3.5) at the support locations to simulate the effects of the steel diaphragm. These elements are placed at locations where a support is

specified. The stiff truss system prevents the distortion of the cross section by restraining the relative movements of the edges of the cross section.

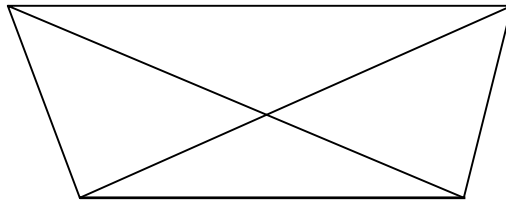


Figure 3.5: Truss System Used at Support Locations

3.4.3 Assembly of the Global Stiffness Matrix

Based on the element connectivity and boundary conditions, degrees of freedom are assigned to nodes throughout the structure. After the degrees of freedom have been determined, the global stiffness matrix is assembled. In order to assemble the internal and external braces, a condensation technique is used. First, the truss elements are assembled together to form a superelement. Second, the degrees of freedom, which are not shared with the steel girder, are condensed out. During the kinematic condensation, numerical singularities may occur due to round off errors. In order to alleviate this problem, very flexible springs in all three global directions were placed at the nodes where four truss members meet. After assembling the springs, the condensation is carried out. The following sections summarize the formulation of the element stiffness matrices used in the program.

3.4.4 Shell Element Formulation

A nine-node, isoparametric shell element (degenerated brick) originally developed by Ahmad, Irons and Zienkiewicz (1970) was implemented in the program. The formulation accounts for shear deformations. At each node, a unit vector V_3 extends through the thickness of the element. The unit vectors undergo rigid body motion during the deformation of the element. The element is mapped into material coordinates (ξ, η, ζ) where ξ, η are the two coordinates in the reference plane and the ζ coordinate is through

the thickness of the shell. The geometry \mathbf{x} throughout the element is interpolated as follows:

$$\mathbf{x}(\xi, \eta, \zeta) = \sum_{i=1}^9 \left[\left(\mathbf{x}_i + \zeta \frac{h}{2} \mathbf{V}_3 \right) N_i(\xi, \eta) \right] \quad (3.1)$$

where h is the thickness of the shell and $N_i(\xi, \eta)$ are the Lagrangian shape functions given explicitly in Appendix C.

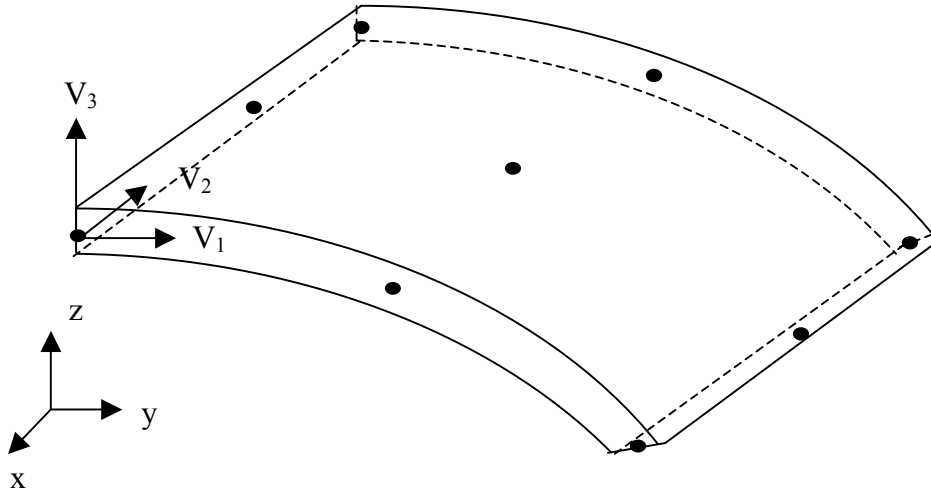


Figure 3.6: Nine-node Shell Element

The displacement field is defined by the three displacement (u, v, w) and two rotational (α, β) degrees of freedom. In order to define the rotation axes for α and β , a right-handed triplet of mutually orthogonal unit vectors (V_1, V_2, V_3) are specified as input. Rotations α and β are the rotations about V_1 and V_2 axes, respectively. The displacement field \mathbf{u} is interpolated as follows:

$$\mathbf{u}(\xi, \eta, \zeta) = \sum_{i=1}^9 \left[\left(\mathbf{u}_i + \zeta \frac{h}{2} (-\alpha_i \mathbf{V}_2 + \beta_i \mathbf{V}_1) \right) N_i(\xi, \eta) \right] \quad (3.2)$$

where u_i is the vector of Cartesian components of the reference surface displacement at node i .

The element formulation includes the basic shell assumption that the stress normal to any lamina ($\zeta=\text{constant}$) is zero. This assumption implies that at any point in the domain, a local rigidity matrix similar to the one used in two-dimensional plane stress analysis must be used. For analysis of an assemblage of shell elements, this local rigidity matrix has to be transformed into global coordinates. For transformation purposes, the local orthogonal coordinate axes consisting of unit vectors $\mathbf{t}_1, \mathbf{t}_2, \mathbf{t}_3$ should be formed where \mathbf{t}_3 is the vector normal to the shell surface at the point of consideration. The orthogonal local axes are formed according to Algorithm 1:

Algorithm 1

1. At the point of consideration:

$$\mathbf{t}_1 = \frac{\partial}{\partial \xi} \mathbf{x} \quad \mathbf{t}_2 = \frac{\partial}{\partial \eta} \mathbf{x}$$

2. Form unit vectors:

$$\mathbf{t}_1 = \frac{\mathbf{t}_1}{|\mathbf{t}_1|} \quad \mathbf{t}_2 = \frac{\mathbf{t}_2}{|\mathbf{t}_2|}$$

3. Calculate the normal vector \mathbf{t}_3 :

$$\mathbf{t}_3 = \mathbf{t}_1 \times \mathbf{t}_2$$

4. Re-orient the \mathbf{t}_2 vector:

$$\mathbf{t}_2 = \mathbf{t}_3 \times \mathbf{t}_1$$

By making use of the direction cosines of the orthonormal local axes, a transformation matrix $\tilde{\mathbf{R}}$ is formed. The global rigidity matrix is calculated as follows:

$$\mathbf{D} = \mathbf{R}^T \mathbf{D}^{local} \mathbf{R} \quad (3.3)$$

The stiffness matrix is calculated as:

$$\mathbf{K} = \int_{\Omega} \mathbf{B}^T \mathbf{D} \mathbf{B} \, d\Omega \quad (3.4)$$

where Ω is defined as the domain of the element.

The implementation uses regular integration: 3 Gauss integration points in ξ, η directions and 2 integration points in the ζ direction.

As it was explained in the previous sections, the concrete deck is much thicker than the steel plates that form the cross-section. Therefore, the middle surface of the concrete deck has an offset with the middle surface of top flange plates. In order to use the same reference surface for both the top flange elements and the concrete deck elements, the bottom surface is considered as the reference surface for concrete deck elements. For this purpose the shell element is modified so that the reference surface could be taken as the bottom surface of the element. Deck offset is properly taken into account when the reference surface is the bottom surface of the element.

3.4.5 Truss Element Formulation

A standard 3 dimensional, 2-node linear truss element is implemented into the program. The stiffness matrix formulation is provided in Appendix B.

3.4.6 Spring Element Formulation

A standard 2-node, three-dimensional spring element is implemented into the program. The stiffness matrix formulation appears in Appendix B.

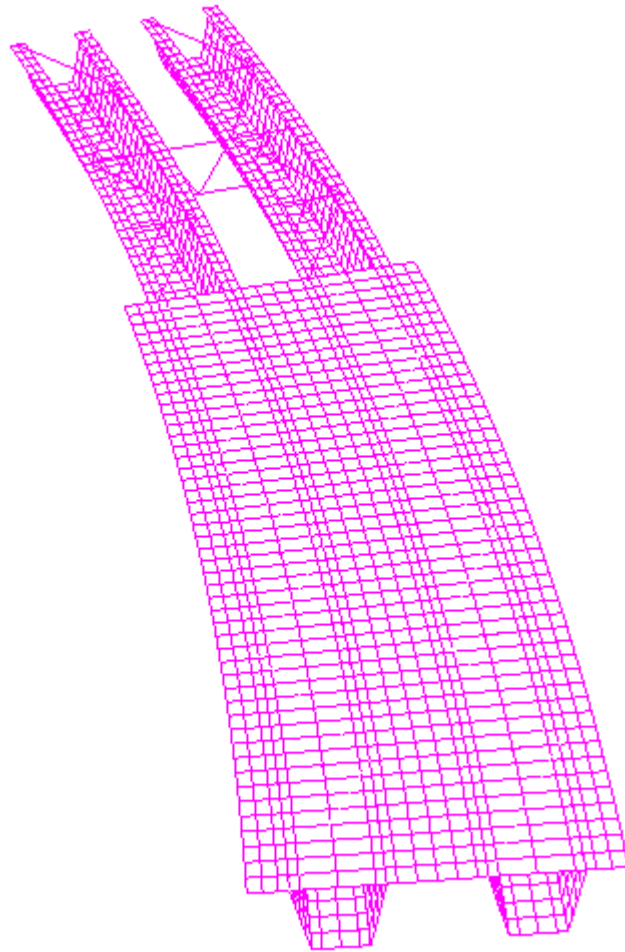


Figure 3.7: Portion of a Finite Element Model

3.4.7 Solution Capability

Large-scale, finite element analyses produce a system of linear equations which requires extensive computer resources to be solved. Until recently, most of these analyses were performed on UNIX workstations. With advances in computer technology, large-scale systems can be handled with personal computers. Since bridges are long and thin structures, the mesh adopted to represent the physical model produces a global stiffness matrix that is sparse in nature. In sparse systems most of the entries that form the stiffness matrix are zero. The solution could be achieved by using either direct

or iterative sparse solvers. Iterative solvers were found to create numerical problems in models involving shell elements. (Gullerud et al., 2001) Therefore, in this program a direct sparse solver was chosen for the solution of the system of linear equations. A sparse solver developed by Compaq, which is a part of the Compaq Extended Math Library (CXML), is adapted to the program. The solver is supplied as a library file by the Compaq Visual Fortran 6.5 compiler and can be compiled with the finite element program. Only the nonzero entries of the upper triangular half of the matrix need to be stored. In addition, two vectors which are used to define the locations of the nonzero entries are required by the solver. Based on the information of nonzero entries and their locations, the solver is capable of reordering and factoring the stiffness matrix and solving for displacements. The solver dynamically allocates all the arrays required during the solution process. It is capable of performing operations using the virtual memory whenever available physical memory is not enough.

The non-zero terms in the global stiffness matrix are located in rows and columns which correspond to the degrees of freedom that are connected to each other. Before the global stiffness matrix is assembled, the two position vectors that keep track of the locations of the non-zero terms have to be formed. A subroutine was developed for this purpose. The subroutine accepts the nodal connectivity information as input. For every degree of freedom, the associated degrees of freedom are found. This information is further used to form the position vectors.

At the initial stages of the program development, several solvers were tried for adoption to the analysis module. The NASA Vector Sparse Solver, Y12maf sparse solver, a frontal solver, and the CXML sparse solver were compared. The CXML solver was found to be the most efficient in terms of memory usage and the speed of solution.

3.4.8 Post-Processing Capability

The program is capable of generating output useful to designers based on the displacements obtained after the solution process. Output obtained from post processing is written to text files which are further read by making use of the GUI. The program outputs vertical deflection and cross-sectional rotation along the length of the bridge. In

addition, the program calculates axial forces for all top lateral, internal and external braces. Cross-sectional stresses and forces are calculated at every two feet along the bridge length since elements have a length of two feet. For each cross section, stresses at the center of the top surface for each element are calculated. Therefore, for each cross section shear and normal stresses are obtained at 26 and 52 locations for single and dual girder systems respectively. These stress components are in the local directions (ie. normal and perpendicular to the cross section). No further transformation of stresses is necessary. In addition to stresses, cross sectional shear, moment and torsion are calculated. For each element on the cross section, the nodal internal forces and moments are computed for three nodes that lie on that cross section. These forces and moments are transformed from global coordinates to local coordinates. Finally, the transformed forces and moments for all elements are summed up to find out the total tractions on the cross section.

3.5 Graphical User Interface

The Graphical User Interface was designed to provide an environment in which the user easily enters required input data. In addition, the GUI has the capability of displaying both the numerical and graphical output of the analysis results. Figure 3.8 shows the main form of the interface. The GUI is written in Visual Basic and has the following menus and graphics capabilities.

File Menu: This menu consists of submenus and is used for data management. User can either start a new project (a new project description) or continue with an existing project. Any changes made to a new or existing project could be saved with the Save Project option.

Geometry Menu: This menu brings the Geometric Properties form to the screen. Information on the number of girders, radius of curvature, length of bridge, girder offset and cross sectional dimensions should be supplied by making use of this form.

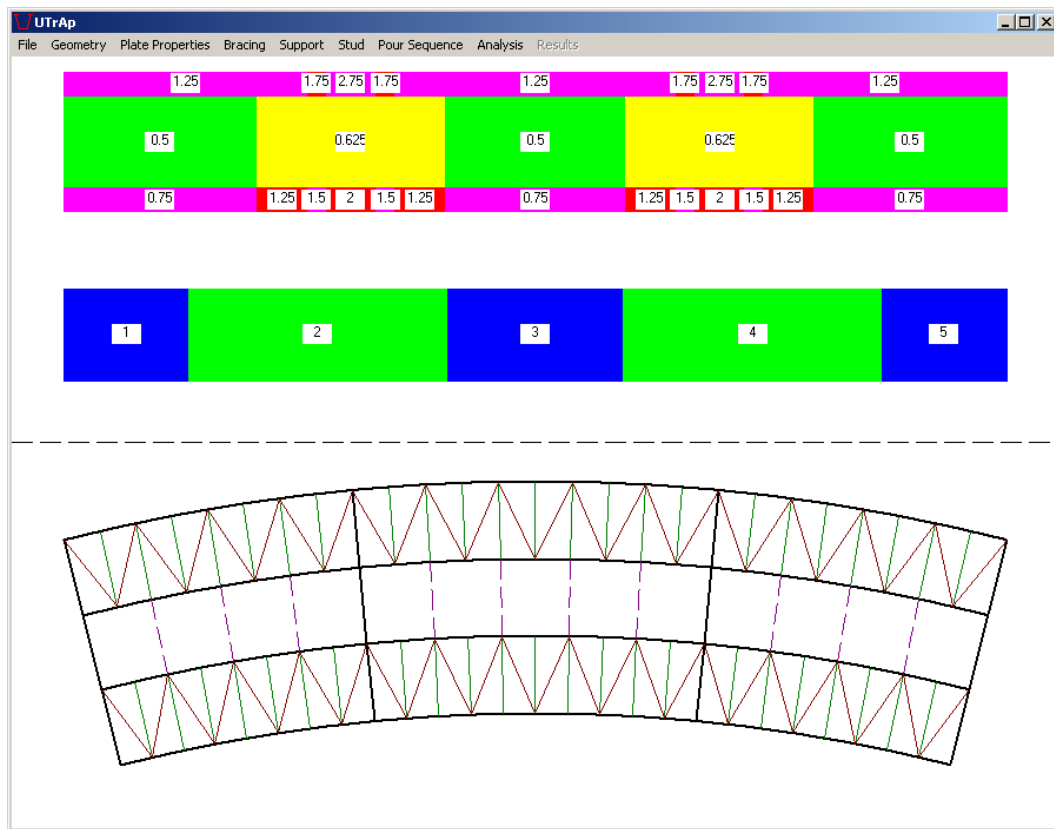


Figure 3.8: The Graphical User Interface

Plate Properties Menu: This menu brings the Plate Properties form to the screen. This form has three folders for entering web thickness, bottom flange thickness, and top flange thickness properties. In each of the folders, length of the plate and its thickness from start to the end of the bridge should be provided.

Bracing Menu: This menu brings the Bracing Properties form to the screen. This form has three folders for entering internal brace, external brace, and top lateral brace information. For internal and external braces, location of the brace, its type and cross sectional area of its members needs to be specified. For top lateral braces, start and end locations, type and cross sectional area information needs to be supplied. Each folder has buttons to assign the same type and cross sectional area to all the brace members. In addition, buttons are provided for entering equally spaced braces between two locations.

Support Menu: This menu brings the Support Locations form to the screen. In this form, the locations of the supports are entered by the user.

Stud Menu: This menu brings the Stud Properties form to the screen. In this form, spacing of studs and number of studs per flange along the length of the girder need to be supplied.

Pour Sequence Menu: This menu brings the Pour Sequence form to the screen. In this form, tabulated data related to the pour sequence need to be supplied. There can be several analyses cases and the concrete deck could be divided into segments. The length of each segment needs to be entered. For each analysis case, concrete modulus, concrete stiffness and loading information for every deck segment needs to be supplied.

Analysis Menu: This menu executes the analysis module. Before the execution, a text input file, which is read by the analysis module, is prepared based on the information supplied in the graphical user interface.

Results Menu: This menu has eight submenus. The submenus are used to visualize the analysis results. Vertical deflection and cross sectional rotation of the bridge, brace member forces, cross sectional stresses and forces could be tabulated or displayed graphically.

A more detailed explanation of the Graphical User Interface along with an example problem is given in Appendix A.

3.6 Verification of the Computational Software

Results from the developed software were compared with published solutions. Researchers Fan and Helwig (1999) had developed a hand method for predicting the top lateral brace member forces in curved box girders. The proposed method was compared against an independent finite element analysis performed using a commercially available general-purpose program. The predictions of the hand method were in excellent agreement with the finite element analysis. In this section, the published finite element analysis results are compared with the results obtained from UTrAp. The bridge analyzed by Fan and Helwig (1999) was a three-span single girder system having a radius of 954.9 feet and a length of 640 feet. The details of the bridge are given in Fig. 3.9.

Internal braces were located at every 10 feet and there was an X-type top lateral system between internal brace points. The top lateral brace members were WT 6x13 sections while the internal brace elements were L 4x4x5/16 sections. The bridge was analyzed under uniform load of 3.3 k/ft. A constant top flange width of 14 inches was assumed. The thickness of top flange plates in Section N was modified to 3.8 inches to give the same plate area.

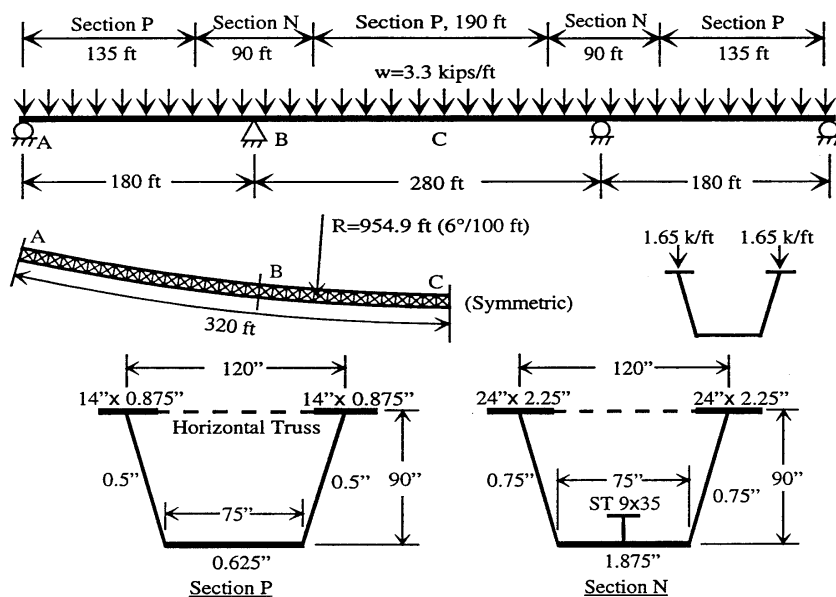


Figure 3.9: Layout and Cross-Sectional Dimensions of the Bridge (Fan (1999))

The top lateral members were grouped into two (X1 and X2) according to their orientation. Force levels for these two lateral members obtained from finite element analysis were presented by Fan and Helwig (1999). These force levels are compared with the predictions from UTrAp in Figs. 3.10 and 3.11. From the graphs, it could be concluded that the developed software is capable of producing results similar to the published solutions. The program will further be compared with the experimental findings in the next chapter.

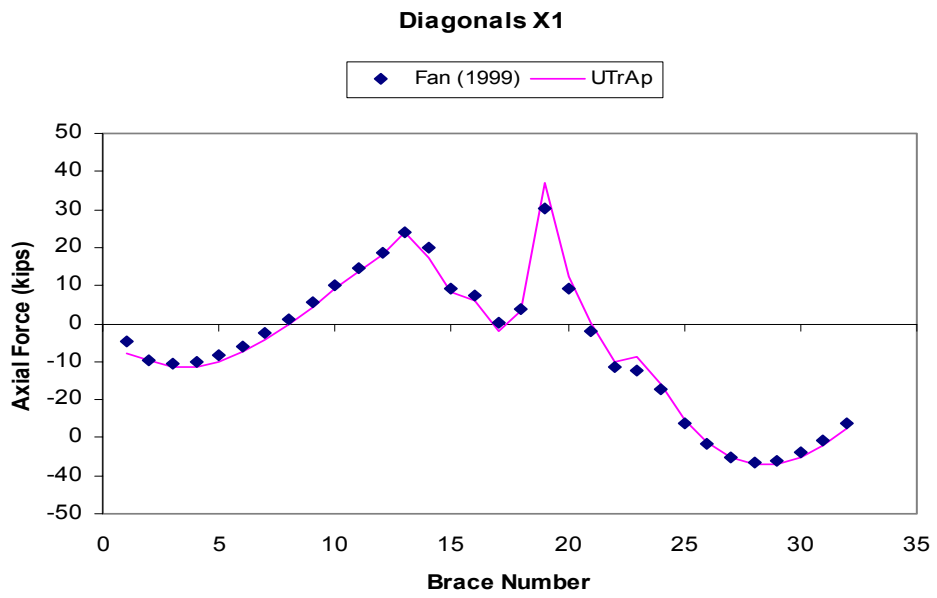


Figure 3.10: Comparison of Published and UTrAp Results for X1 Diagonals

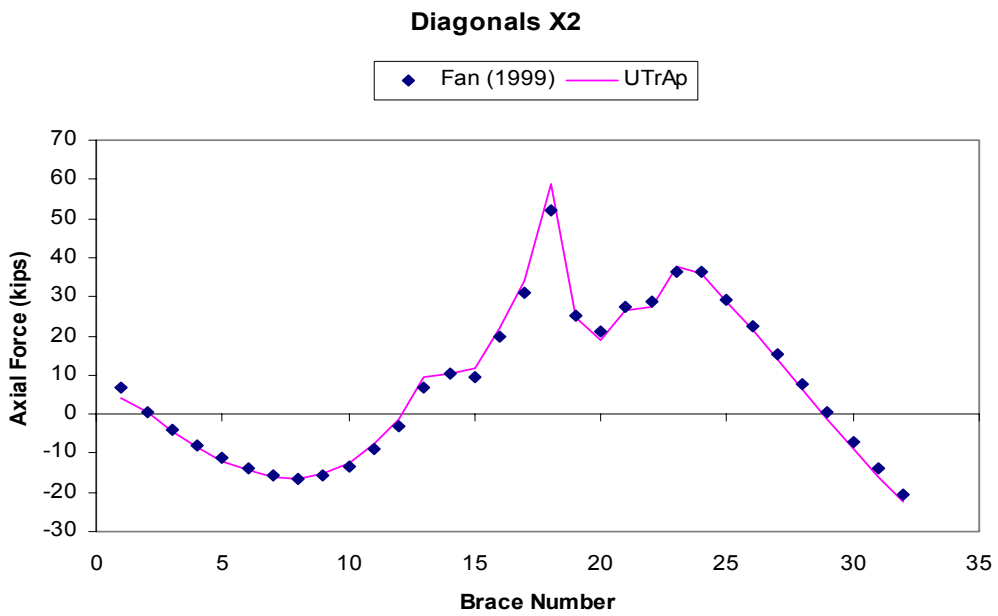


Figure 3.11: Comparison of Published and UTrAp Results for X2 Diagonals

CHAPTER 4

FIELD STUDIES

The study presented herein was a part of a larger research project that was sponsored by the Texas Department of Transportation. The aim of the project was to investigate the behavior of curved, steel, trapezoidal box girders during construction and under live loads. This chapter focuses on the field monitoring of two bridges that were investigated as a part of the research project.

4.1 Bridges Under Study

Four trapezoidal steel box girder bridges were constructed at the intersection of IH35 and US290 in Austin, TX. The construction took place between September 1999 and July 2001. Brace members and cross sectional locations were instrumented for two bridges. The instrumented bridges were called Z and K connects. Figure 4.1 shows the site location for these bridges.

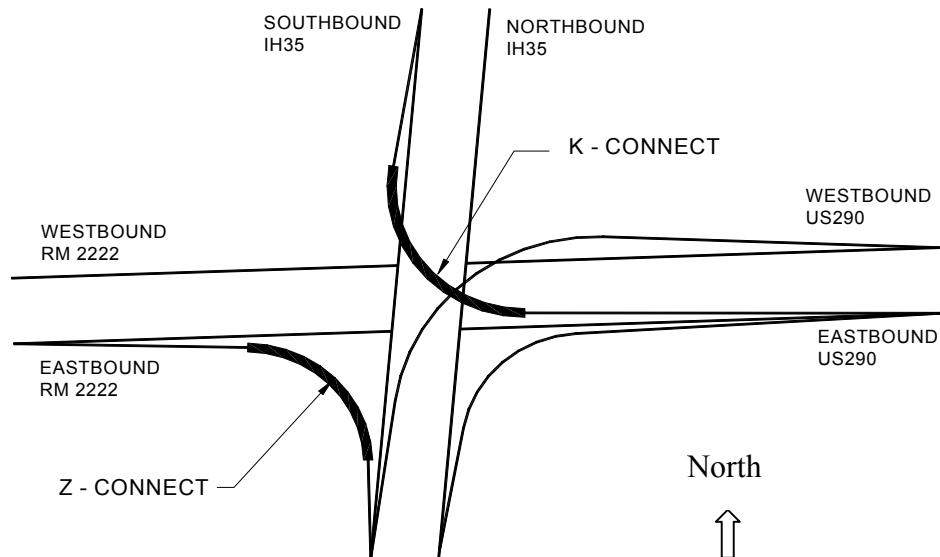


Figure 4.1: Site Location

4.2 Monitoring of Connect Z

Connect Z provides direct access from eastbound US290 to southbound IH35. The steel portion of the bridge consists of one three-span bridge adjacent to a two-span bridge. The three-span portion of the bridge was monitored. The twin-girder symmetrical bridge has two side spans of approximately 150 feet in length and a middle span of 190 feet. The centerline radius of the bridge is 450 feet. A plan view of the bridge is given in Fig. 4.2.

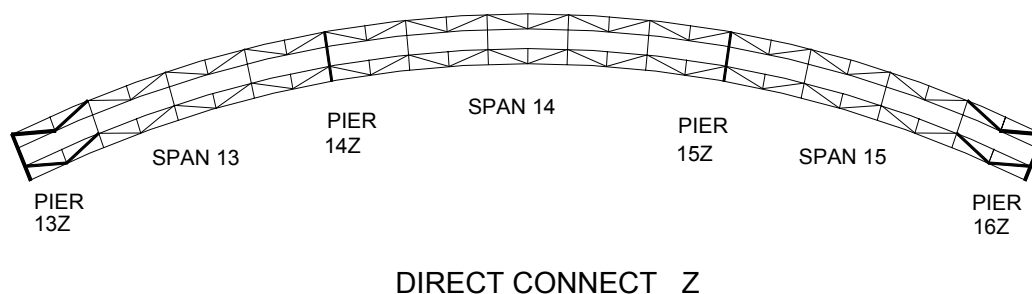


Figure 4.2: Plan View of the Direct Connect Z

The dimensions of the girder cross section are shown in Fig. 4.3. The top and bottom flanges and webs vary in thickness along the length of the bridge (Appendix D).

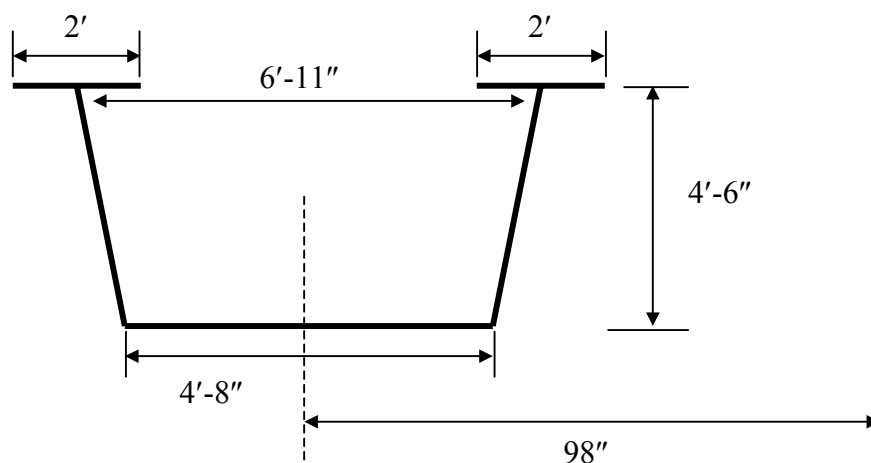


Figure 4.3: Dimensions of the Girder Cross Section

K-type internal diaphragms were spaced approximately every 20 feet to prevent distortion of the cross section. Details of internal and external braces are given in Appendix D. Solid plates were used at support locations to reduce torsional stresses. A top lateral truss system made of WT 7x21.5 sections was fastened near the top flanges to form a quasi-closed box section. Each girder centerline was offset by 98 inches from the bridge centerline. The concrete deck had a width of 360 inches. Studs having 7/8 inch diameter were spaced every 12 inches at both ends of the bridge for a distance of ten feet from the pier. For the remainder of the bridge, studs were spaced at every 24 inches. There were 3 studs per flange over the entire length of the bridge.

4.3 Concrete Deck Pour on Direct Connect Z

After the erection of the steel girders, permanent metal deck forms (PMDF) were installed between the top flanges of the girders. Longitudinal and transverse reinforcement were then placed on top of the PMDF. (Fig. 4.4) The 30-foot wide concrete deck was placed on the bridge by making use of a concrete screed. Class-S type concrete was used for the deck. A total of five pours were specified on the three-span bridge. The pour sequence and the length of pours is given in Fig. 4.5. The arrows indicate the direction of the screed movement during each pour segment.

Pours 1 through 3 took place in the early morning of September 1, 2000, while segments 4 and 5 were poured a week later on September 8, early in the morning. Four top lateral members, which were located near the ends of the girders, were instrumented during pours 1 through 3. (Fig. 4.2) The timing of the pour progress is given in Fig. 4.6. Timing is particularly important in analyzing the early composite action developing during concrete placement. The next section presents the changes in top lateral member forces due to pours 1 through 3 together with the predictions from the developed software.



Figure 4.4: Deck Forms and Reinforcement Installation

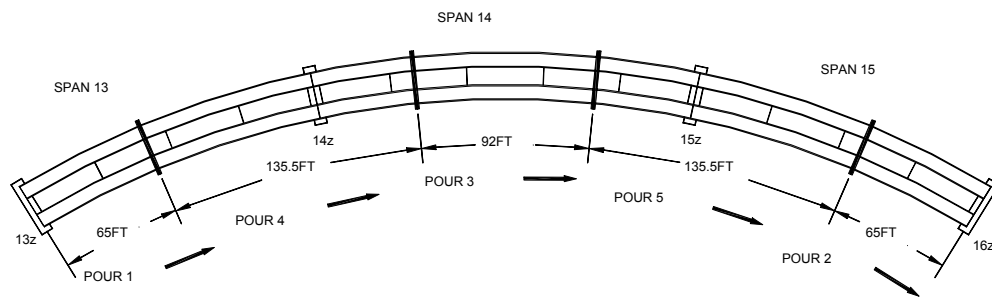


Figure 4.5: Concrete Pour Sequence and Direction of Pour

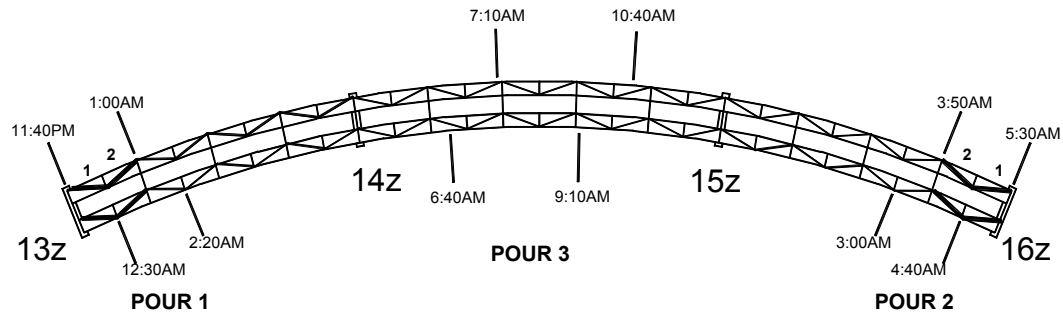


Figure 4.6: Progress of Pours 1,2, and 3

4.4 Top Lateral Results for Z-Connect

Top lateral members of the first two panels at each end of the bridge were monitored for both the inner and outer girders. Each top lateral WT had two cross sections gaged for redundancy. The majority of the force measurements for the two sections of each member were nearly identical. The two axial forces for each member were averaged for each time increment. Details on the field monitoring are given in Cheplak (2001). The following sections present the changes in force levels in the instrumented top laterals for the first three pours along with the predictions from the developed software.

4.4.1 Pour 1

Pour 1 had a length of 65 feet and took about 2 hours and 40 minutes to be completed. In the analysis, no composite action was assumed; therefore the concrete and stud stiffness were considered to be zero. The specified deck thickness was 8 inches which is measured from the top surface of the PMDF to the top of the concrete deck. Usually, the amount of concrete poured is greater than the value calculated according to the specified deck thickness. This additional concrete is needed to fill haunches and the gaps of the corrugated metal deck. In the analysis, a modified constant deck thickness that takes into account the additional concrete should be used. For this purpose, the value

of the total amount of concrete poured on the Z-connect was obtained from the contractor. From the total concrete amount, a constant deck thickness value was calculated to be 11 inches and this value was used in all the analyses related with the Z-connect. A distributed load value of 3.99 k/ft was applied to the first pour segment in order to simulate the forces resulting from the wet concrete. Changes in axial force levels for the instrumented top laterals, along with the analytical predictions, are given in Fig. 4.7. The discussion of the results will be presented in section 4.5.

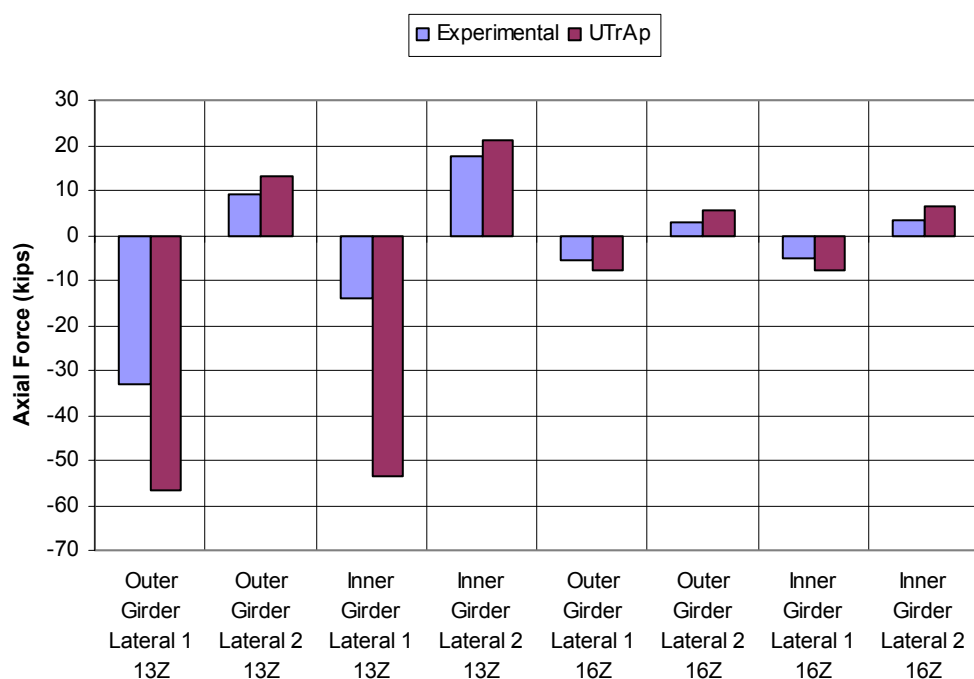


Figure 4.7: Change in Axial Force Levels Due to Pour 1

4.4.2 Pour 2

Pour 2 had a length of 65 feet and was at the opposite end (Pier 16Z) of the bridge. Two hours and 30 minutes elapsed during the completion of this pour. Previously poured concrete on portion 1 had cured nearly 4 to 6 hours when this pour had ended. Although concrete in portion 1 had gained some strength, its value was expected to be very low. ($f'_c < 300$ psi) Therefore, in the analysis of pour 2, no composite action

was assumed for deck segments 1 and 2. A stiffness value of zero was assigned to the concrete and shear studs of both deck segments, and a distributed load of 3.99 k/ft was placed on the second pour segment. Changes in axial force levels for the instrumented top laterals, along with the analytical predictions, are given in Fig. 4.8.



Figure 4.8: Change in Axial Force Levels Due to Pour 2

4.4.3 Pour 3

Pour 3 had a length of 90 feet and was placed at an equal distance from both ends. This pour was completed in 4 hours. By the time this pour was over, concrete on the first segment had cured 6 to 10 hours, and concrete on the second segment cured between 1 and 5 hours. In the analysis of this pour, concrete on segment one was assumed to cure for an average period of 8 hours. From the laboratory experiments explained in Chapter 2, the concrete stiffness for that time period was estimated to be

2800 ksi. The design connector strength at that time period was estimated to be 10.6 kips. The load-slip relationship developed in Chapter 2 (Eqn. 2.1) revealed that stud stiffness changes between $100 Q_d$ and $33.3 Q_d$. For this case, studs have an initial tangent stiffness of 1060 k/in and final secant stiffness of 353 k/in. A value of 600 k/in was selected to represent the stud stiffness in segment 1. Moreover, because a short period of time had elapsed for curing of segment 2, this segment was assumed to act non-compositely. A distributed load of 3.99 k/ft was placed on the third pour segment. Changes in axial force levels for the instrumented top laterals along with the analytical predictions are given in Fig. 4.9. For comparison purposes, the analysis results for the case where the entire bridge is assumed to act non-compositely are presented in the same figure.

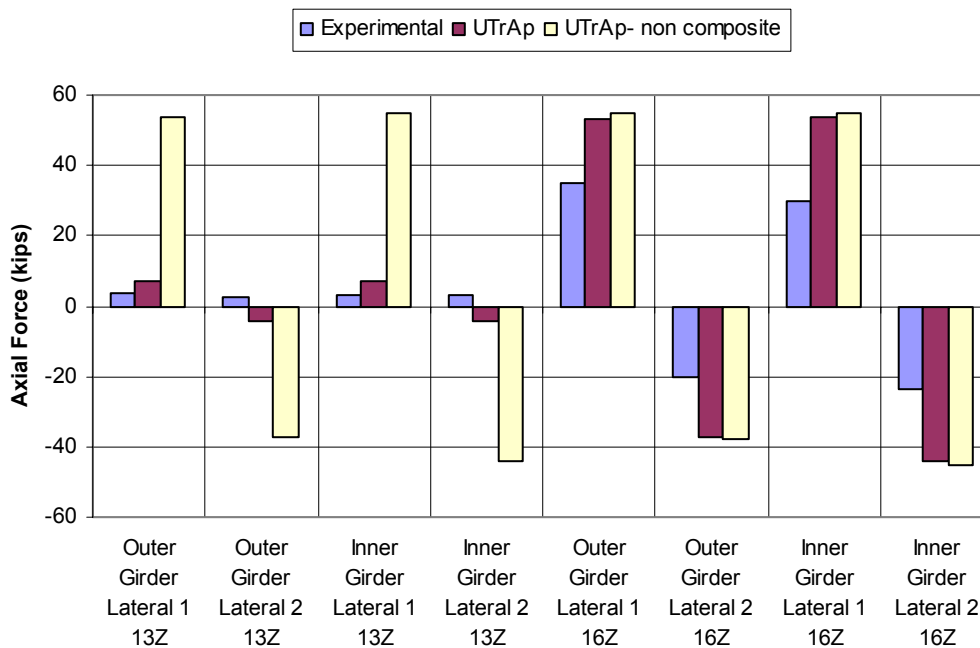


Figure 4.9: Change in Axial Force Levels Due to Pour 3

In order to investigate the validity of the assumptions made regarding the stud stiffness, several additional analyses were performed. In all these analyses, a concrete stiffness of 2800 ksi was used for the first segment, and the stud stiffness value varied between zero and 1000 k/in. Analysis results showed that varying the stud stiffness value had little effect on the axial force values of the top laterals located near pier 16Z because non-composite action was specified in the analysis. However, a change in stud stiffness had a significant effect on the axial force values of the top laterals located near pier 13Z. Figure 4.10 shows the axial force levels as a function of stud stiffness for the four top lateral members close to pier 13Z.

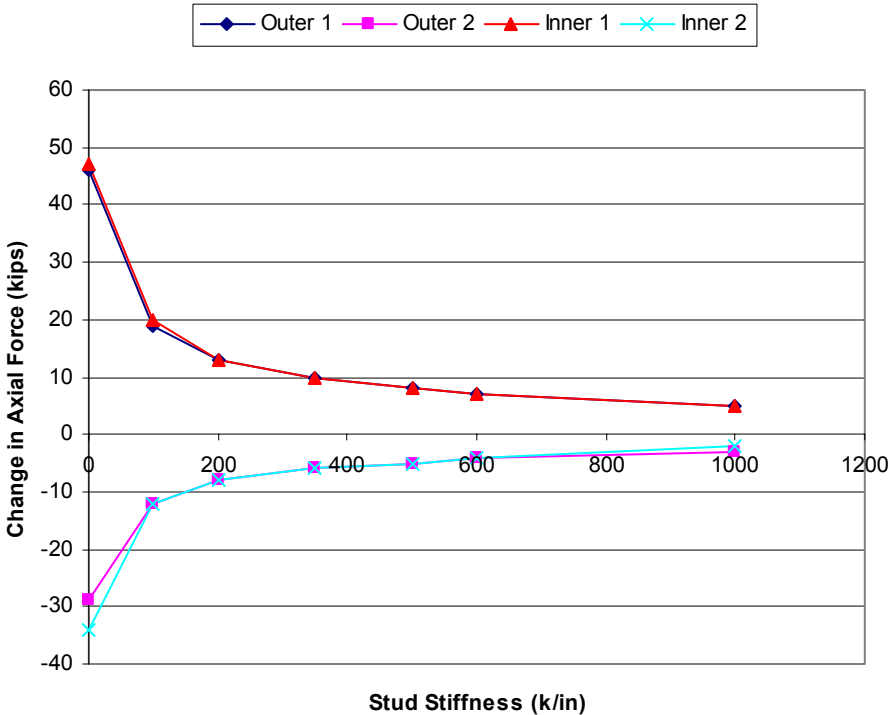


Figure 4.10: Effect of Stud Stiffness on 13Z Top Lateral Forces (Pour 3)

It could be concluded that the assumption of a 600 k/in value for stud stiffness is reasonable by comparing the measured values and the analysis results presented in

figures 4.9 and 4.10, respectively. Values of stud stiffness higher than 350 k/in produce similar results.

4.5 Discussion of Analysis Results

For all three pours, the analytical predictions are in reasonable agreement with the experimental findings. In general, the computed forces were higher than the ones observed in the field. The discrepancies could be attributable to several shortcomings of the modeling used in the developed software such as superelevation or support movements. The effects of these shortcomings on the results were investigated further. The investigation was carried out by making use of a commercially available, general-purpose finite element program, ABAQUS. In the following sections, details of the modeling with ABAQUS and a discussion of various shortcomings of UTrAp are presented.

4.5.1 Finite Element Model Used in ABAQUS

The same mesh density used in UTrAp was used for modeling the bridge in ABAQUS. Eight-node quadratic shell elements with reduced integration (S8R5) were used to model the top and bottom flanges, webs and pier diaphragms. Instead of shell elements, three-dimensional, 20-node quadratic bricks (C3D20) were used to model the concrete deck. One and twenty brick elements were used along the thickness and width of the deck, respectively. All bracing members were modeled with 2-node linear beam elements (B31). Spring elements were placed between the top flange and concrete deck to simulate the studs.

4.5.2 Shortcomings of the UTrAp Model

Superelevation

UTrAp forms the model of the bridge without accounting for the horizontal superelevation. However, in reality these bridges have moderate levels of horizontal superelevation. The Z-connect has a 6% superelevation. If there is no superelevation, then forces due to concrete weight are applied vertically to the bridge. In the case of

superelevation, concrete weight has a horizontal component that acts on the bridge. This horizontal component produces a constant torque along the length which counteracts the forces due to the vertical component. In general, including superelevation into the model reduces the level of forces calculated for top lateral members.

Deck Thickness Profile

During the design of these bridges, a constant concrete deck thickness is specified. Due to construction limitations, it is very difficult to place concrete evenly on the permanent metal deck forms. Therefore, in some cases, the deck thickness profile becomes non-uniform. This kind of non-uniformity was not included in the finite element model because it could not be predicted at the design stage. For the bridges mentioned in this study, the thickness of the deck along the width and length of the bridge were measured by TxDOT engineers during construction. The measurements revealed that the poured deck had a tapered cross section for the Z-connect. Thickness of the deck reduced gradually from the inner portion of the bridge to the outer portion. (From 12.4 inches to 9.6 inches) Placing concrete unevenly has effects on the measured forces. In this case, placing more concrete on the inner girder compared to the outer girder causes a torque along the length of the bridge that counteracts the torsional forces due to the curved geometry of the bridge.

Support Movements

In the software developed, no vertical movement is allowed at the support locations. However, in reality some vertical support movement is expected. During the construction of these bridges, elastomeric bridge bearings were used at support locations. Because bearings do not possess infinite compressive and rotational stiffness, some degree of movement should be expected at supports. The sensitivity of the measured forces to support movements will be discussed later.

Permanent Metal Deck Forms

As mentioned earlier, permanent metal deck forms (PMDF) were placed atop the girders to act as a formwork for the concrete deck. PMDF were attached to a thin angle section which was welded to the top flanges. Although this attachment detail is very weak, the PMDF stiffens the cross section to some degree. Different attachment details are under investigation (Chen, 2002). However, currently there is no information on quantifying the level of stiffness gain due to the attachment of PMDF to the top flanges. Therefore, the effects of PMDF are excluded in all finite element analyses.

Connection Details

In the Z and K connects, the top flange bracing members were bolted, not welded, to the top flanges. Bolted shear connections are more flexible compared to the rigid welded connection details. In these bridges, the bolts were specified to be fully torqued in the shop using the turn-of-the-nut tightening method (AISC, 1994). However, these bolts are frequently loosened in the field to provide some flexibility for erectors completing the girder field splices. In all the finite element analyses, welded connections were assumed. Bolted tension and shear connections were also used to connect the external diaphragms to the girders. (Cheplak, 2001) Due to the flexibility of these joints, the force distribution between the girders might be different than the calculated values.

4.5.3 Sensitivity Study

In order to investigate the effects of superelevation and deck thickness profile, two additional analyses were performed using ABAQUS. In the first analysis, pour 1 was simulated by incorporating the superelevation into the model. In the second analysis, both superelevation and the tapered deck thickness profile were included. Figure 4.11 presents the results for both of these analyses together with the experimental and analytical findings explained before. It is evident that including the superelevation and tapered deck thickness profile produces estimates that are closer to the experimental findings. Axial forces on braces tend to decrease by 9% on average by including

superelevation into the model. Forces reduced further by 17% on average by including the tapered thickness profile resulting in a total reduction of 26%.

Another issue mentioned earlier was the effect of support movements. In order to investigate this issue, a support rotation of 0.008 radians was applied to one of the end supports. This value corresponds to a 1-inch upward movement for the outer girder and 1 inch downward movement for the inner girder. Analysis results revealed that for this case the axial forces for the first and second panel top laterals changed by 21 kips. These values indicate that the support movements might have significant effects on the measured top lateral forces.

In general results from the finite element analysis with superelevation and tapered deck thickness profile were close to the field measurements. There were discrepancies that may be attributable to the lack of modeling details such as the effects of PMDF and bolted connections. In addition, there might be errors in the measured values. The large difference between measured and predicted values for inner girder 13Z top lateral 1 was inconclusive.

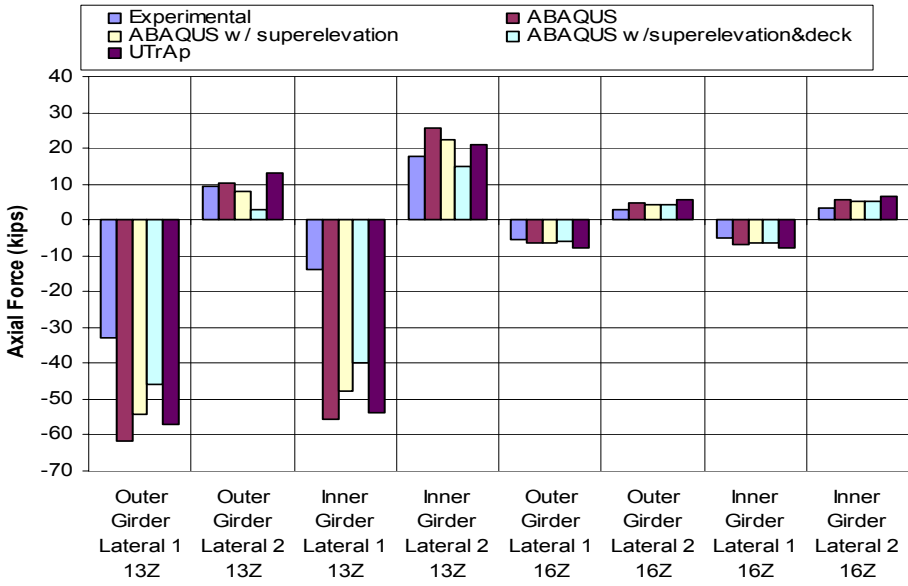


Figure 4.11: Sensitivity Study on Z-Connect

4.6 Monitoring of Connect K

Connect K provides direct access from southbound IH35 to eastbound US290. It is a three-span bridge with two side spans of 168 feet and a middle span of 242 feet. The centerline radius of the bridge is 573 feet. A plan view of the bridge is given in Fig. 4.12.

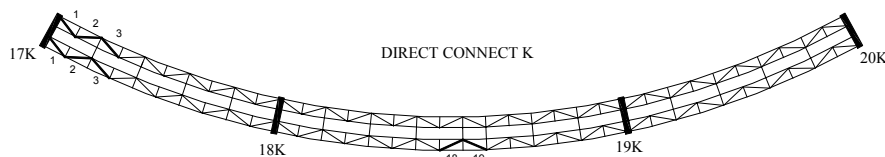


Figure 4.12: Plan View of Direct Connect K

The dimensions of the girder cross section are shown in Fig. 4.13. The plate thickness variation along the bridge and the details of internal and external braces are given in Appendix D. K-type internal diaphragms were spaced approximately every 16 feet. All top lateral brace members were WT 8x33.5 sections. Each girder centerline is offset by 94 inches from the bridge centerline. The concrete deck width and stud configuration are identical to Direct Connect Z.

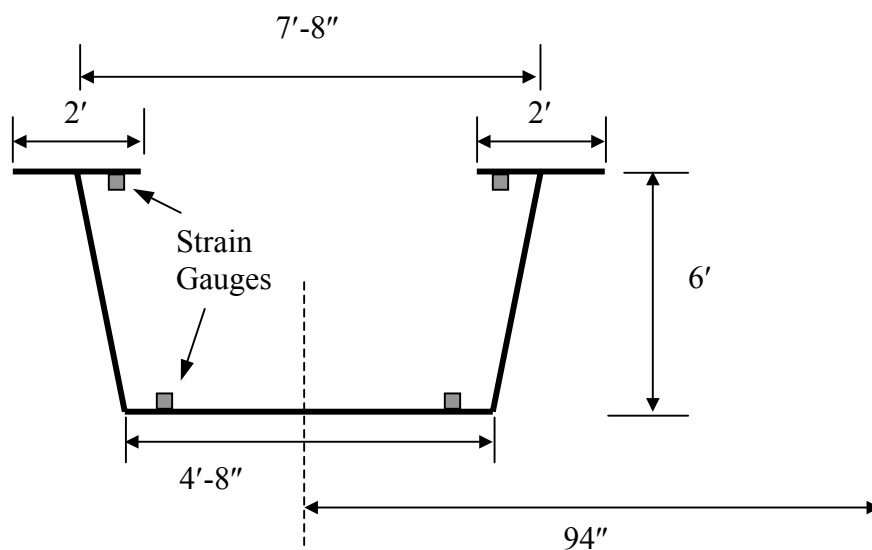


Figure 4.13: Dimensions of Girder Cross Section

4.7 Concrete Deck Pour on Direct Connect K

After the placement of the PMDF and reinforcement, the concrete deck was poured in five segments. The pour sequence and the length of the pours are given in Fig. 4.14.

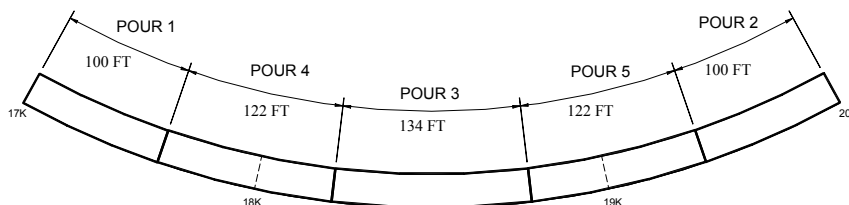


Figure 4.14: Concrete Pouring Sequence on Direct Connect K

The dates and the start and end times for the first three pours are given in Table 4.1. Eight top lateral members and four cross sections were instrumented for this bridge. Six of the instrumented top laterals were located in the first three panels at pier 17K. (Fig. 4.12) The remaining two instrumented laterals were located at panels 18 and 19 of the outer girder. (Fig. 4.12) Strain gauges were placed at the top and bottom flanges for four cross-sections. Two of the instrumented cross sections were located in the middle of panels 2 and 3. For these locations, both the inner and outer girder were monitored. The remaining two instrumented cross sections were located in the middle of panels 18 and 19. For these locations, only the outer girder was monitored. A total of four gauges were placed per girder cross section. Two of these gauges were placed at the top flanges while the others were placed at the bottom flange. (Fig. 4.13) Gauges were located at 5 inches from the edge of the plates.

Table 4.1: Start and End Times for the First Three Pours

	START		END		DURATION
POUR 1	3/13/01	8:39 AM	3/13/01	11:10 AM	2 hr 31 min
POUR 2	3/16/01	12:27 AM	3/16/01	2:05 AM	1 hr 38 min
POUR 3	3/17/01	12:00 AM	3/17/01	3:20 AM	3 hr 20 min

4.8 Top Lateral and Girder Stress Results for the K-Connect

The field monitoring procedures used for the Z-Connect were also used for this bridge. Details of the field monitoring are given in Cheplak (2002). For the cross-sectional stresses, the two strain gage values on the flange were averaged for both the top flange and the bottom flange. The following section presents the changes in force and stress levels for the first three pours along with the predictions from the developed software.

4.8.1 Pour 1

Pour 1 had a length of 100 feet and took approximately 2 hours and 30 minutes to be completed. In the analysis, no composite action was assumed; therefore the concrete and stud stiffness were considered to be zero. The specified deck thickness for this bridge was 8 inches. From the measurements taken during the concrete pour, it was found out that the deck thickness profile was fairly uniform for this bridge. A constant deck thickness value was calculated to be 10 inches to account for the extra concrete that results when using PMDF. In all the analysis related with the K-connect, a constant deck thickness of 10 inches was used. A distributed load value of 3.625 k/ft was applied to the first pour segment in order to simulate the forces arising from the wet concrete. Changes in axial force levels and cross sectional stresses are given in Figs. 4.15 and 4.16 along with the analytical predictions.

In the figures related with stresses, the following nomenclature is used: Out- Outer Girder, In- Inner Girder, T- Top Flange, and B- Bottom Flange. Therefore, Out 3B means change in stress at the bottom flange of the outer girder in the middle of panel 3.

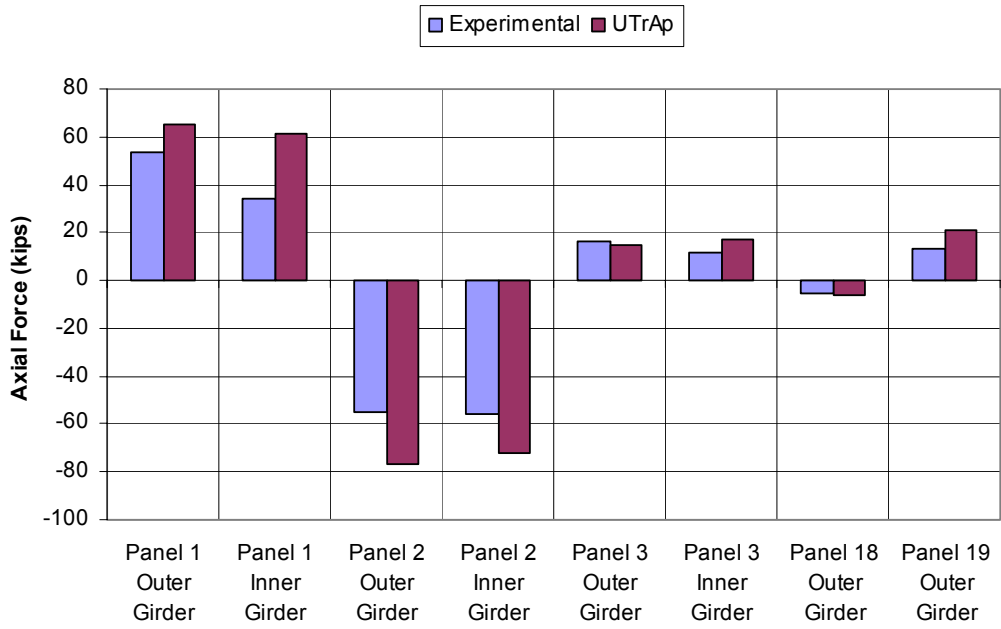


Figure 4.15: Change in Axial Force Levels Due to Pour 1

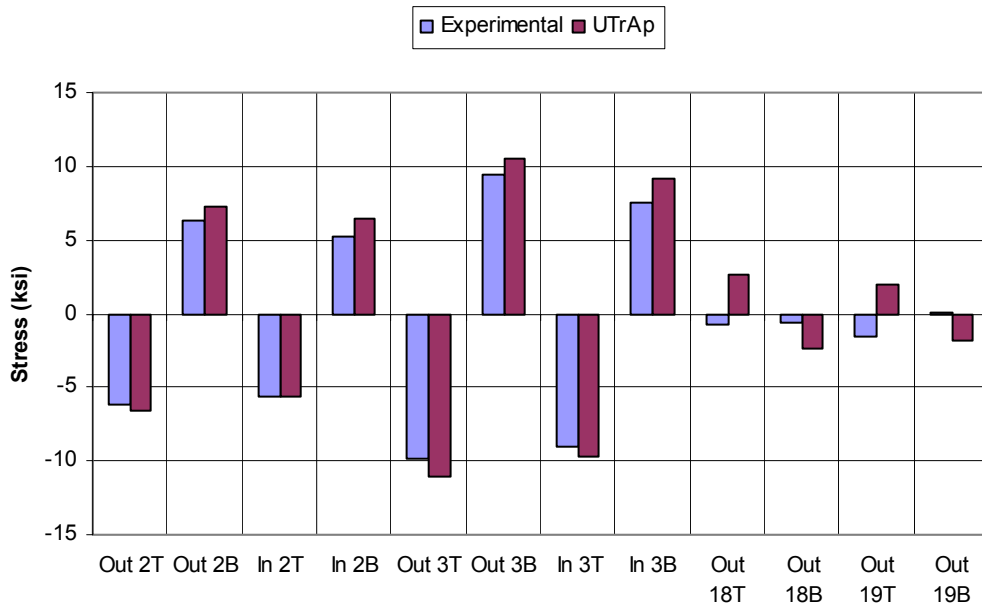


Figure 4.16: Change in Cross-Sectional Stresses Due to Pour 1

4.8.2 Pour 2

Pour 2 had a length of 100 feet and was at the opposite end (Pier 20K) of the bridge. One hour and 38 minutes elapsed during the completion of this pour. Previously poured concrete on portion 1 had cured for 3 days when this pour started. From the laboratory experiments and the developed equations, the predicted concrete and average stud stiffness were 4100 ksi and 1200 k/in, respectively for pour 1. A distributed load of 3.625 k/ft was placed on the second pour segment. Changes in axial force levels and cross sectional stresses are given in Figs. 4.17 and 4.18 along with the analytical predictions. For comparison purposes, the analysis results for the case where the entire bridge is assumed to act non-compositely are presented in the same figures.

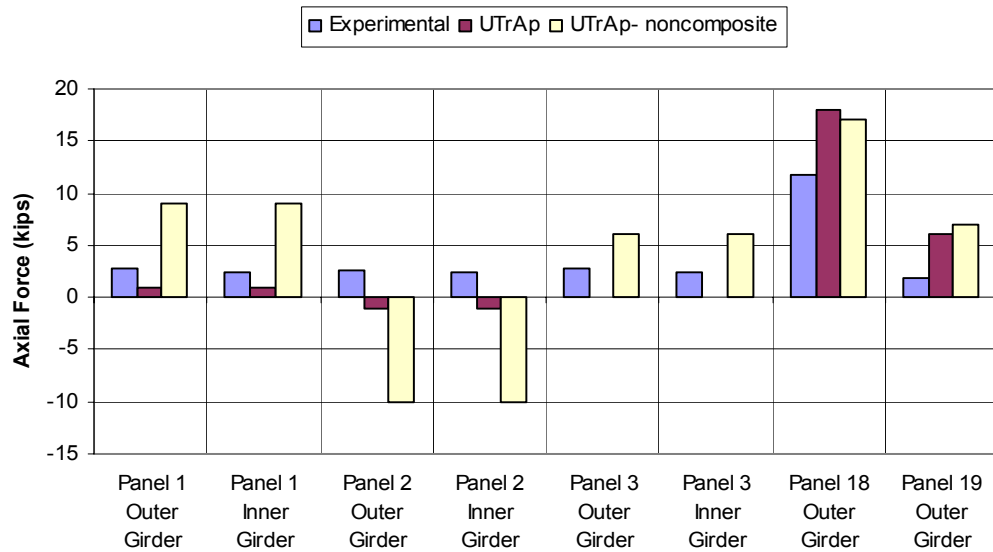


Figure 4.17: Change in Axial Force Levels Due to Pour 2

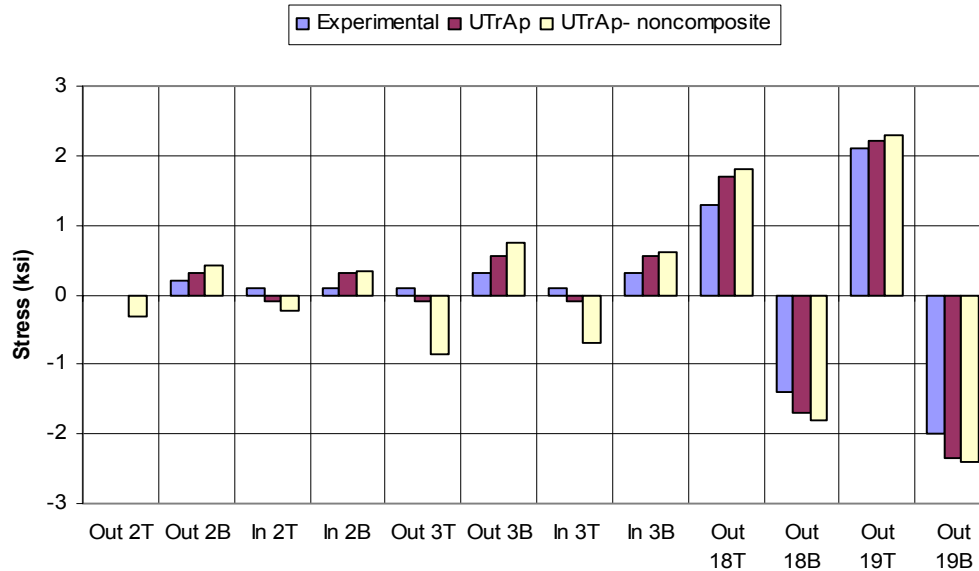


Figure 4.18: Change in Cross-Sectional Stresses Due to Pour 2

4.8.3 Pour 3

Pour 3 had a length of 134 feet and was placed at an equal distance from both ends. This pour was completed in 3 hours 20 minutes. By the time this pour was over, concrete on first segment has cured for 4 days, and the concrete on second segment has cured for one day. In the analysis, concrete and average stud stiffness were assumed to be 4100 ksi and 1200 k/in, respectively for the first segment. The corresponding values for the second segment were 3700 ksi and 1000 k/in, respectively. A distributed load of 3.625 k/ft was placed on the third pour segment. Changes in axial force levels and cross sectional stresses are given in Figs. 4.19 and 4.20 along with the analytical predictions. For comparison purposes, the analysis results for the case where the entire bridge is assumed to act non-compositely are presented in the same figures.

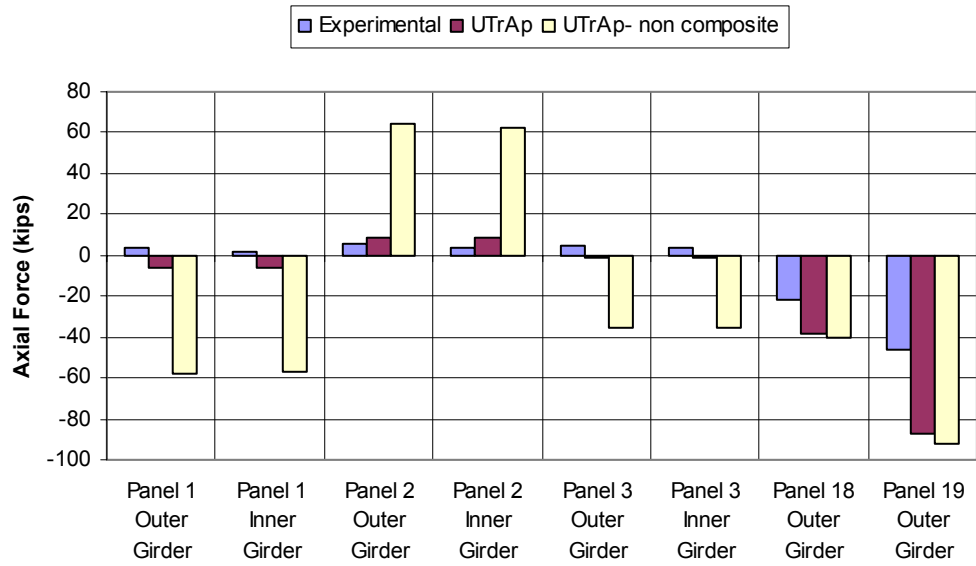


Figure 4.19: Change in Axial Force Levels Due to Pour 3

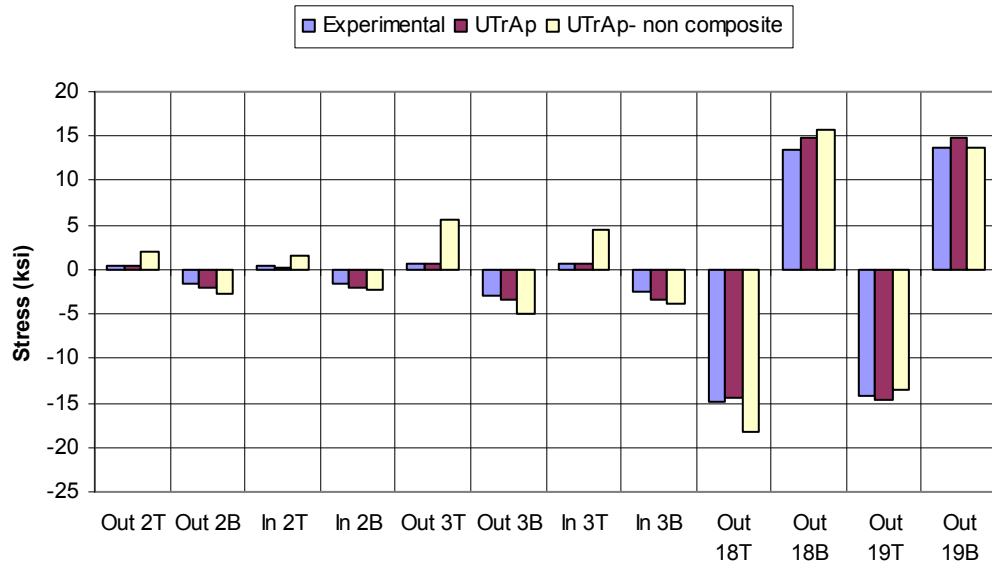


Figure 4.20: Change in Cross-Sectional Stresses Due to Pour 3

4.9 Summary of Analytical Predictions

For both of the bridges, the analytical predictions were in reasonable agreement with the experimental findings. In almost all cases, the analytical predictions were higher than the forces/stresses measured in the field. The reason for these discrepancies was the lack of knowledge on the effects of some details that were not included in the analytical model. These details were the modeling of PMDF and flexible connections as well as the support movements. In addition, it should be kept in mind that there might be errors in the measured values.

In general the program was capable of generating acceptable results for cases where there was no composite action. For the cases with early composite action, the differences in predicted and measured quantities were much higher. Based on K-connect results the predictions for girder stresses were much better than those for top lateral forces.

The experimental findings clearly reveal that composite action was occurring at very early concrete ages. For the Z-connect, the effects of composite action were observed as early as 8 hours.

CHAPTER 5

SUMMARY AND CONCLUSIONS

Recently there have been some failures of curved steel trapezoidal box girder bridges during construction. In general the failures resulted in buckling of bracing members used in these systems. The failures were attributed to the lack of knowledge of the behavior of these systems during construction and the unavailability of accurate, easy-to-use analytical tools.

The weight of wet concrete comprises the majority of the loads acting on these systems during construction. The entire deck is usually not cast in one stage because of the large volume of concrete and to control shrinkage. These systems were monitored in the past during the pouring sequence and were analyzed by making use of commercially available, sophisticated finite element programs. (Fan, 1999, and Cheplak, 2001) For later pours, significant differences were observed between the measured and predicted quantities. These differences gave an indication that the concrete poured at earlier times was acting compositely with the bridge.

An experimental program was developed to establish the behavior of the concrete deck – steel girder interface at early concrete ages. In order to investigate the behavior, load-slip curves for the connector elements (shear studs) embedded in early age concrete were obtained. This investigation could not be carried out by making use of the existing push-out test setups. A setup that enables the testing of studs at early concrete ages was developed. The study was limited to one type of concrete mix design used typically for Texas bridges. A total of 24 push-out tests were performed at eight different times varying between 4 hours and 28 days. At all time periods, cylinder tests were also conducted to determine the compressive and tensile strength and stiffness of concrete. Tests revealed that shear transfer between steel and concrete was achieved as early as 4 hours. In order to quantify the shear stud capacity at early concrete ages, a definition of design strength was proposed. This definition was based on a serviceability limit state which current code equations do not consider. Based on the test results, equations for

predicting the design and maximum stud strength were developed. The use of the current ACI equation for predicting concrete stiffness was found applicable to concrete at early ages. In order to estimate the shear stud stiffness, a load-slip relationship for studs was developed. As a last step, all specimens were retested after 28 days to find out the effects of loading early-age concrete. Test results showed that the maximum capacity decreases with the residual slip. Studs deformed up to the serviceability limit at early ages were able to develop their full strength at 28 days. Excessive deformations at early ages might also cause a decrease in initial stiffness of the studs.

To model the early composite action accurately, an easy-to-use finite element package for this specific problem was developed. The program requires no knowledge of FEM on the user's part and is capable of analyzing single and dual girder systems under construction loads. The program automatically prepares a finite element mesh based on the supplied dimensions. The developed software has post-processing capabilities for visualizing the cross-sectional stresses, moments, shear and torsion, as well as, deflections and brace forces. The results from the program were acceptable when compared to published solutions.

Two curved steel box girder bridges were monitored during construction to determine the effect of the pour sequence on girder stresses and brace member forces. The change in axial force levels in the top lateral bracing members and cross-sectional stresses were monitored during the pouring sequence. Forces and stresses obtained from field tests showed reasonable agreement with the analytical results predicted by the developed software. In general, the analytical predictions were higher than the field results. Several shortcomings related to analytical modeling were identified. Sensitivity studies were performed to investigate the effects of these shortcomings. Overall, the program produces acceptable results.

In conclusion, it was proven through laboratory experiments and field-tests that composite action develops at very early concrete ages. An easy to use tool for analyzing curved trapezoidal box girders with early composite action was developed. The study will have impacts on the fields of shear stud testing methods and bridge engineering. The setup developed for testing shear studs is much practical and reliable compared to the

conventional one. The new push-out test setup could be standardized and used for future shear stud investigations. Moreover, the concept of early composite action will lead to a better understanding of the bridge behavior. The use of this concept together with the developed software will yield more accurate and cost effective designs. Future research should extend the investigations by using different concrete mix designs and different stud geometries. Information contained herein could be used to investigate the potential benefits of early composite action in reducing the cost of these structural systems.

APPENDIX A

USER'S MANUAL AND EXAMPLE PROBLEM FOR UTrAp

UTrAp is a computer program developed for pour sequence analysis of curved, trapezoidal steel box girders. Only single and dual girder systems with constant radius of curvature can be analyzed with this program. The program consists of a Graphical User Interface (GUI) and an analysis module. The analysis module relies on the finite element method to compute the response of the three-dimensional bridge structure. Input data is supplied to the program by making use of the GUI. The program can handle multiple analysis cases and has graphics capability to visualize the output. In the following sections, details of the program are presented along with an example problem.

Example Problem Definition

The example problem presented herein is a 3-span, dual girder system with a centerline radius of curvature of 450ft. The bridge is named as “Direct Connect Z” and has a centerline arc length of 493 ft. The plan view of the bridge is given in Fig. A.1.

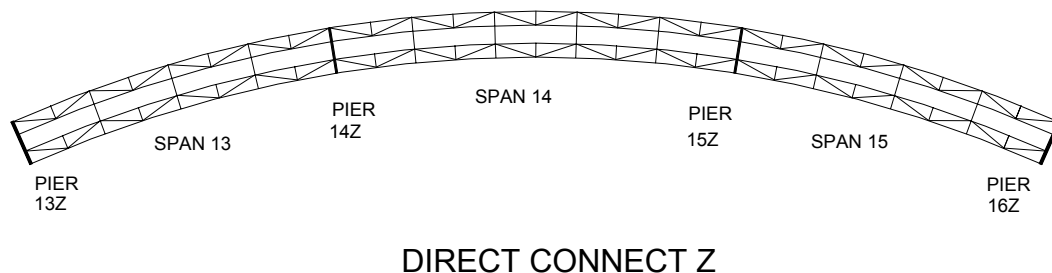


Figure A.1: Plan View of Direct Connect Z

This program accepts only positive values for the radius of curvature and the concavity layout of the structure should be similar to the one in Fig. A.1. Therefore, the left end is considered to be the start end of the bridge. In the Fig. A.1, the start end is located at PIER 13Z. Positions along the bridge are defined by the distance along the arc length relative to the start end. Cross-sectional dimensions of the Direct Connect Z are given in Fig. A.2. Web depth is measured between the centerline of top and bottom

flanges. Centerline of each girder is offset by 98 inches from the bridge centerline. The concrete deck width and thickness are 360 and 10 inches, respectively.

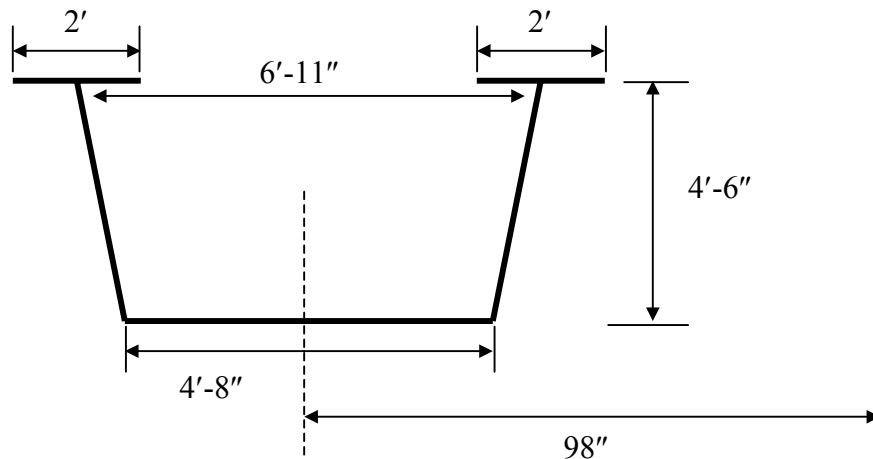


Figure A.2: Cross-sectional Dimensions

The steel plates that make up the girder have variable thickness along the length of the bridge. Table A.1 provides the details of the plate thickness. Lengths given in this table are the centerline arc lengths. Properties are listed beginning from the start end of the bridge. In this program both girders must have the same plate thickness properties.

Table A.1: Plate Properties

WEB		BOTTOM FLANGE		TOP FLANGE	
Length(ft.)	Thickness(in.)	Length(ft.)	Thickness(in.)	Length(ft.)	Thickness(in.)
100.5	0.5	100.5	0.75	127	1.25
99	0.625	26.5	1.25	10	1.75
94	0.5	10	1.5	26	2.75
99	0.625	26	2.0	10	1.75
100.5	0.5	10	1.5	147	1.25
		26.5	1.25	10	1.75
		94	0.75	26	2.75
		26.5	1.25	10	1.75
		10	1.5	127	1.25
		26	2.0		
		10	1.5		
		26.5	1.25		
		100.5	0.75		
Σ = 493 ft		Σ = 493 ft		Σ = 493 ft	

Bracing members are provided throughout the girder. Internal, external and top lateral braces are present. Locations of the braces are given in Table A.2. For internal and external braces, only one location value is required. For top lateral braces, the start and end location of each brace is needed.

Table A.2: Location of Braces

Brace Number	Internal Bracing	External Bracing	Top Lateral Bracing	
	Location (ft)	Location (ft)	Start Location (ft)	End Location (ft)
1	18.9	37.8	0	18.9
2	37.8	75.6	18.9	37.8
3	56.7	113.4	37.8	56.7
4	75.6	189.5	56.7	75.6
5	94.5	227.5	75.6	94.5
6	113.4	265.5	94.5	113.4
7	132.3	303.5	113.4	132.3
8	170.5	379.3	132.3	151.5
9	189.5	417.3	151.5	170.5
10	208.5	455.1	170.5	189.5
11	227.5		189.5	208.5
12	246.5		208.5	227.5
13	265.5		227.5	246.5
14	284.5		246.5	265.5
15	303.5		265.5	284.5
16	322.5		284.5	303.5
17	360.4		303.5	322.5
18	379.3		322.5	341.5
19	398.3		341.5	360.4
20	417.3		360.4	379.3
21	436.1		379.3	398.3
22	455.1		398.3	417.3
23	474.0		417.3	436.1
24			436.1	455.1
25			455.1	474.0
26			474.0	493.0

There are 23 internal and 26 top lateral braces per girder. In addition, there are 10 external braces between the two girders. Internal braces are in the form of K-trusses, which have members with cross-sectional area of 3.75 in². All top lateral braces have a

cross-sectional area of 6.31 in^2 , and their orientation is given in Fig. A.1. External braces are comprised of truss members with a cross-sectional area of 4.79 in^2 . Details of their configuration are provided below.

The bridge has four supports which are located 0, 151.5, 341.5, and 493 feet away from the start end. Studs are spaced every 12 inches at both ends of the bridge for a distance of ten feet from the pier. For the remainder of the bridge, studs are spaced at every 24 inches. There are 3 studs per flange over the entire length of the bridge.

The concrete deck is poured in 5 segments. The lengths and the sequence of pours are given in Fig. A.3.

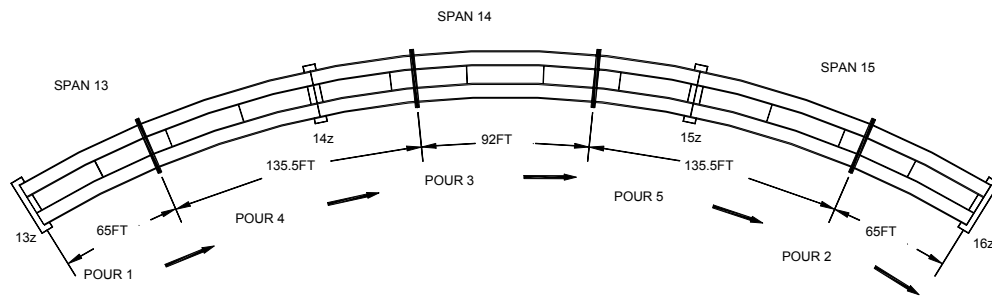


Figure A.3: Concrete Pour Sequence

This analysis example will focus on the first three pours. The program requires the lengths of the pours and number of analysis to be performed. In this example, 3 analysis cases will be considered. In the first analysis, the concrete deck is placed on the first segment, and a uniform loading of 3.625 k/ft is applied on that segment to account for the concrete self-weight. In the second analysis, it is assumed that the concrete on the first segment has cured and attained a stiffness of 1000 ksi with a corresponding stud stiffness of 250 k/in . A uniform loading of 3.625 k/ft is applied to the second segment due to the concrete weight. In the third analysis, it is assumed that for the concrete and stud stiffness have reached to 2000 ksi and 500 k/in , respectively, for the first segment. For the second segment, the concrete and stud stiffness values are assumed to attain values of 1000 ksi and 250 k/in , respectively. A uniform loading of 3.635 k/ft is applied

to the third segment to account for concrete weight. The summary of analysis parameters are given in Table A.3.

Table A.3: Pour Sequence Analysis Parameters

Deck	Length	Analysis 1			Analysis 2			Analysis 3		
		Con. Mod.	Std. Stf.	Load	Con. Mod.	Std. Stf.	Load	Con. Mod.	Std. Stf.	Load
1	65	0	0	3.625	1000	250	0	2000	500	0
2	135.5	0	0	0	0	0	0	0	0	0
3	92	0	0	0	0	0	0	0	0	3.625
4	135.5	0	0	0	0	0	0	0	0	0
5	65	0	0	0	0	0	3.625	1000	250	0
	$\Sigma=493$									

User's Guide and Solution of the Example Problem

The Graphical User Interface of UTrAp has a total of 9 menus. This section will explain each of these menus in detail. Use of these menus will be presented along with the example problem.

File Menu: This menu has four submenus and is used for data management. Files can be stored and retrieved by making use of this menu. Details of each submenu are as follows:

New Project: This submenu starts a blank project. If a new bridge model is going to be formed, this option should be selected.

Existing Project: This submenu is used to open an existing project. The UTrAp input project files have an extension of *.inp. When the existing project submenu is invoked, an open file box will appear which is used to select the existing project file.

Save Project: This submenu is used to save a project to the hard disk. It can be used to save the changes made to an existing project or the contents of a newly developed project. When the *Save Project* submenu is invoked, a save file box will appear which is used to name or rename the project file.

Exit: This submenu is used to exit the program.

Example Problem: A new project is formed by making use of the *New Project* submenu.

Geometry Menu: This menu is used to input the geometric properties of the bridge. Values should be typed in the boxes provided. A graphical representation of the cross section is displayed on the geometric properties form. After entering all the required data, the user must press the *Save Data* button. If all values are acceptable then they are stored in memory, and the form is closed. If the user does not want to save the values, the *Cancel* button should be pressed. This data saving process is valid for all subsequent forms.

Example Problem: Geometric property values are entered on the form and saved by making use of *Save Data* button. Figure A.4 shows the Geometric Properties form with the entered data.

The screenshot shows a software window titled "Geometric Properties" with a close button (X) in the top right corner. The form is divided into two main sections: "Project Information" and "Cross Section Dimensions".

Project Information:

- Project Name: Direct Connect Z 13-14-15
- Number of Girders: Radio buttons for 1 and 2, with 2 selected.
- Radius of Curvature (feet): 450
- Length of the Bridge (feet): 493
- Girder Offset (in): 98

Cross Section Dimensions:

- Depth of Web (in): 54
- Width of Bottom Flange (in): 56
- Top Width (in): 83
- Top Flange Width (in): 24
- Width of Deck (in): 360
- Thickness of Concrete Deck (in): 10

Below the input fields is a diagram of a trapezoidal girder cross-section. The diagram shows a top flange with a width of 83 inches and a depth of 24 inches. The web has a depth of 54 inches. The bottom flange has a width of 56 inches. The girder is offset from the centerline of the deck by 98 inches. The deck has a total width of 360 inches and a thickness of 10 inches.

At the bottom of the form are two buttons: "Save Data" and "Cancel".

Figure A.4: Geometric Properties Form

Plate Properties Menu: This menu is used to input the plate properties related with the bridge. The plate properties form has three folders. Each folder is reserved for either the web, the bottom flange or the top flange properties. Properties are input in a tabular form. The length of the plate and its thickness should be entered from the start to the end of the bridge. There are two buttons used to add and remove properties. Their function is explained below.

Add: This button is used to add properties. A change in plate thickness requires the user to specify a new property. The user should enter the number of properties that will be needed to characterize the bridge. After, the number of rows in the table is increased by the total number of properties specified by the user.

Remove: This button is used to remove properties. The property number that is going to be removed should be specified in the box next to the *Remove* button.

Example Problem: In each folder, the number of properties are increased by the *Add* button. All plate properties are entered in a tabular format. A representative input for bottom flange plate properties are given in Fig. A.5.

The screenshot shows a software window titled "Plate Properties" with three tabs: "Web Thickness", "Bottom Flange Thickness" (which is selected), and "Top Flange Thickness". Inside the "Bottom Flange Thickness" tab, there is a table with 13 rows and 3 columns. The columns are labeled "Length (ft)" and "Thickness (in)". The table contains the following data:

	Length (ft)	Thickness (in)
1	100.5	0.75
2	26.5	1.25
3	10	1.5
4	26	2
5	10	1.5
6	26.5	1.25
7	94	0.75
8	26.5	1.25
9	10	1.5
10	26	2
11	10	1.5
12	26.5	1.25
13	100.5	0.75

Below the table, there is a large green rectangular area. To the right of the table, there are two buttons: "Add" and "Remove". Next to the "Add" button is a text input field labeled "properties". Next to the "Remove" button is a text input field labeled "property number". At the bottom of the dialog, there are two buttons: "Save Data" and "Cancel".

Figure A.5: Plate Properties Form

Bracing Menu: This menu is used to input bracing information related with the bridge. The brace properties form has three folders. Each folder is reserved for either the internal, external, or the top lateral brace properties. Properties are input in a tabular form. Depending on the version of the program, different geometrical types of braces could be specified for internal and external braces. Location, type and member cross-sectional area information are required for the internal and external braces. The type, start location, end location, and cross-sectional area are required for the top lateral braces. There are buttons provided to add and remove braces. Functions of the buttons are explained below.

Add: This button is used to add braces. The user should enter the number of braces that will be added to the box next to the *Add* button. The number of rows in the table is increased by the corresponding number entered by the user.

Equally Space: This button is used to add braces at equally spaced intervals. The number of braces to be added is specified in the box next to the button. For this button to function properly, two more location values must be entered. Braces are placed at equal intervals between these values. The location value in the first box must be smaller than the location value in the second box.

Remove: This button is used to remove braces. The brace number that is going to be removed should be specified in the box next to the *Remove* button.

Remove All Braces: This button is used to remove all the braces specified previously in a certain folder.

Type: This button is displayed in the internal and external braces folder. It is used to assign the same type to all braces. The type of the brace should be entered into the box next to this button. The available bracing types and their configurations are displayed in a separate form using *Show Internal/External Brace Types* buttons.

Area: This button is used to assign the same cross-sectional area value to all brace members. The cross-sectional area value should be entered in to the box next to this button.

Show Internal/External/Top Lateral Brace Types: These buttons are used to display the types of braces that a user can specify in the program. When this button is pressed, a

form that shows the geometry and types of braces are displayed on the screen. Figure A.6 shows the types of internal and external braces supported by the current version of the program.

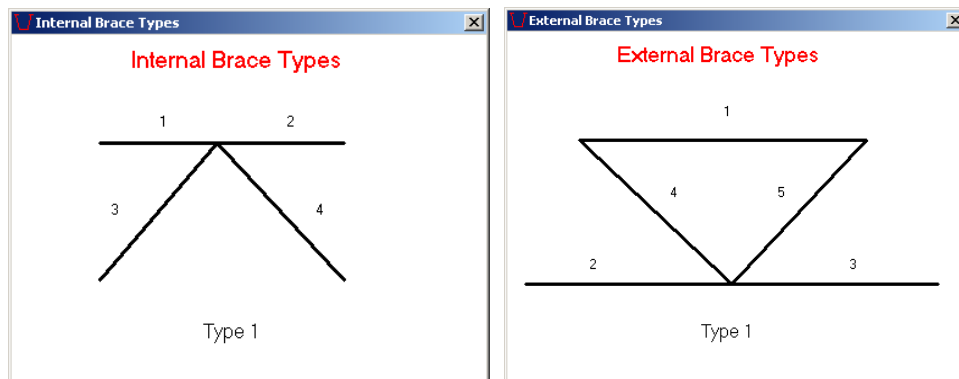


Figure A.6: Internal and External Brace Types

All Type 1: This button is displayed only in the top lateral braces folder. It is used to assign type 1 to all top lateral braces. Top lateral braces can have only two orientations. Therefore, there are two types of top lateral braces which are shown in Fig. A.7.

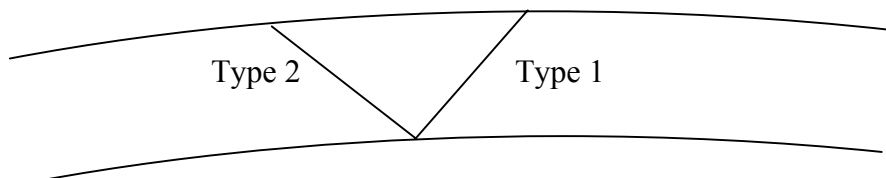


Figure A.7: Top Lateral Brace Types

All Type 2: This button is displayed only in the top lateral braces folder. It is used to assign type 2 to all top lateral braces.

Alternating Starting with Type 1: This button is displayed only in the top lateral braces folder. It is used to assign alternating types to consecutive braces. The first brace will be of type 1 and the second brace will be of type 2, etc.

Alternating Starting with Type 2: This button is displayed only in the top lateral braces folder. It is used to assign alternating types to consecutive braces. The first brace will be of type 2 and the second brace will be of type 1, etc.

Example Problem: Twenty-three internal braces, 10 external braces and 26 top lateral braces are added to the folders by making use of the *Add* button. Brace locations, types and cross sectional areas are entered into the folders according to the information given in Table A.2. All internal and external braces are type 1. Top lateral braces have alternating types starting with type 2. Figures A.8 and A.9. show the two folders of the bracing properties form.

	Location (ft)	Type	Area (sq.in.)
1	18.9	1	3.75
2	37.8	1	3.75
3	56.7	1	3.75
4	75.6	1	3.75
5	94.5	1	3.75
6	113.4	1	3.75
7	132.3	1	3.75
8	170.5	1	3.75
9	189.5	1	3.75
10	208.5	1	3.75
11	227.5	1	3.75
12	246.5	1	3.75
13	265.5	1	3.75
14	284.5	1	3.75
15	303.5	1	3.75
16	322.5	1	3.75
17	360.4	1	3.75
18	379.3	1	3.75
19	398.3	1	3.75
20	417.3	1	3.75

internal braces
 braces
 between ft. and ft.
 brace number

 Identical Brace Properties

Figure A.8: Bracing Properties Form - Internal Braces Folder

	Type	Location1 ft.	Location2 ft.	Area (sq.in.)
1	2	0	18.9	6.31
2	1	18.9	37.8	6.31
3	2	37.8	56.7	6.31
4	1	56.7	75.6	6.31
5	2	75.6	94.5	6.31
6	1	94.5	113.4	6.31
7	2	113.4	132.3	6.31
8	1	132.3	151.5	6.31
9	2	151.5	170.5	6.31
10	1	170.5	189.5	6.31
11	2	189.5	208.5	6.31
12	1	208.5	227.5	6.31
13	2	227.5	246.5	6.31
14	1	246.5	265.5	6.31
15	2	265.5	284.5	6.31
16	1	284.5	303.5	6.31
17	2	303.5	322.5	6.31
18	1	322.5	341.5	6.31
19	2	341.5	360.4	6.31
20	1	360.4	379.3	6.31

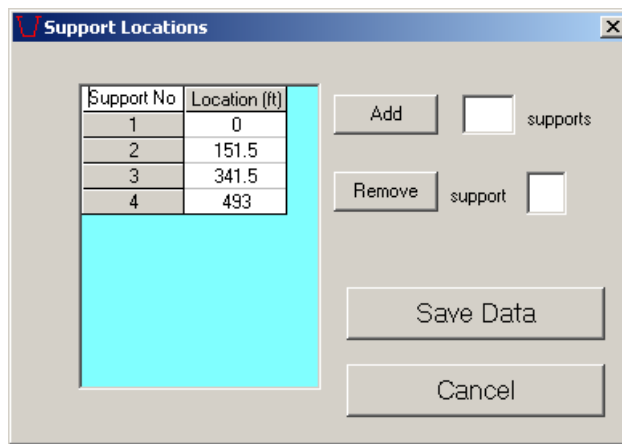
Figure A.9: Bracing Properties Form – Top Lateral Braces Folder

Support Menu: This menu is used to input support locations. Locations are input in a tabular form. The program assumes that only one of the supports is pinned and the rest are rollers. The first support specified is considered to be the pinned one. Number of rows of the tabular input form is controlled by the *Add* and *Remove* buttons. Functions of the buttons are explained below.

Add: This button is used to add supports. The user should enter the number of supports that will be added to the box next to the *Add* button. The number of rows in the table is increased by that specific amount.

Remove: This button is used to remove supports. The support number that is going to be removed should be specified in the box next to the *Remove* button.

Example Problem: Four supports are added to the table by making use of the *Add* button. Support locations given in the description of the bridge are entered on the table. Figure A.10 shows the support locations form along with the entered data.



The screenshot shows a window titled "Support Locations" with a table and several buttons. The table has two columns: "Support No" and "Location (ft)". The data in the table is as follows:

Support No	Location (ft)
1	0
2	151.5
3	341.5
4	493

Below the table, there are two buttons: "Add" and "Remove". To the right of the "Add" button is a text input box with the label "supports". To the right of the "Remove" button is a text input box with the label "support". Below these buttons are two larger buttons: "Save Data" and "Cancel".

Figure A.10: Support Locations Form

Stud Menu: This menu is used to input stud properties. Properties are input in tabular form. Spacing of the studs and the number of studs per flange should be supplied to the program along the bridge length. The number of rows of the tabular input form is controlled by the *Add* and *Remove* buttons. Functions of these buttons are explained below.

Add: This button is used to add properties. The user should enter the number of properties that will be added to the box next to the *Add* button. Number of rows in the table is increased by that specific amount.

Remove: This button is used to remove properties. The property number that is going to be removed should be specified in the box next to the *Remove* button.

Example Problem: For this problem, stud properties change three times along the bridge length. Therefore, three rows are added to the table by making use of the *Add* button.

Cells of the table are filled according to the geometry information given in the bridge description. Figure A.11 shows the stud properties form along with the entered data.

	Length (ft)	Spacing (in)	No per Flange
1	10	12	3
2	473	24	3
3	10	12	3

Figure A.11: Stud Properties Form

Pour Sequence Menu: This menu is used to input pour sequence analysis parameters. Parameters are input in tabular form. The concrete deck can be divided into segments corresponding to each pour, and there can be multiple analyses that are independent from each other. For each analysis, properties of deck segments and loading on the segments should be provided as input. Properties for a deck segment include the stiffness of concrete and the stiffness of studs. Lengths of the deck segments are the same for all analyses and their values should be given as input. The tabular form is controlled by four buttons. These buttons are used to add and remove columns and rows to the table. Functions of the buttons are explained below.

Add Analysis Case: This button is used to add a new analysis case to the table. Three columns for analysis parameters are added to the right of the table each time a new analysis is added.

Remove Analysis Case: This button is used to remove a specific analysis case. The analysis number that is going to be removed should be entered into the box next to this

button. Three columns related with the analysis number specified are removed from the table.

Add Deck Property After: As mentioned before, the concrete deck can be divided into segments. At least one deck property must be specified. This button is used to add a new deck property row to the table. The new deck property is added after the deck number specified in the box next to this button. If no deck has been defined in the table previously, a value of zero should be used. Specifying a value of zero adds blank cells to the first row.

Remove Deck Property: This button is used to remove a deck property row. The number of the deck property to be removed should be entered into the box next to this button. The specified row is deleted from the table.

Example Problem: In this problem, the concrete deck is divided into five segments. These deck segments are added to the table by making use of the *Add Deck Property After* button. There are a total of three analyses to be performed. These analysis cases are added to the table by using the *Add Analysis Case* button. The table is filled with parameters specified in Table A.3. Figure A.12 shows the pour sequence form together with the input data.

The screenshot shows a software window titled "Pour Sequence" with a table and several control buttons. The table has 8 columns: an empty header cell, "Length (ft)", "Conc. Mod.(ksi)", "Analysis 1" (with sub-columns "Stud Stiff.(k/in)" and "Loading (k/ft)"), "Analysis 2" (with sub-columns "Conc. Mod.(ksi)", "Stud Stiff.(k/in)", and "Loading I"). The data rows are as follows:

	Length (ft)	Conc. Mod.(ksi)	Analysis 1	Analysis 2
			Stud Stiff.(k/in)	Conc. Mod.(ksi)
Deck1	65	0	0	1000
Deck2	135.5	0	0	0
Deck3	92	0	0	0
Deck4	135.5	0	0	0
Deck5	65	0	0	0

Below the table, there are four buttons: "Add Analysis Case", "Remove Analysis Case" (with an adjacent input box), "Add Deck Property After" (with an adjacent input box), and "Remove Deck Property" (with an adjacent input box). At the bottom are "Save Data" and "Cancel" buttons.

Figure A.12: Pour Sequence Form

Analysis Menu: This menu is used to perform the finite element analysis using the data entered previously on each of the forms. As the user inputs data using the forms, a graphical representation of the overall bridge properties is displayed in the main form of the program. There are three figures displayed. On the very top figure, the plate thickness along the length is shown in elevation view. The middle figure shows the deck numbers and their relative lengths. The bottom figure is a plan view of the bridge showing all the supports and braces. Figure A.13 shows the main form after all the data are provided.

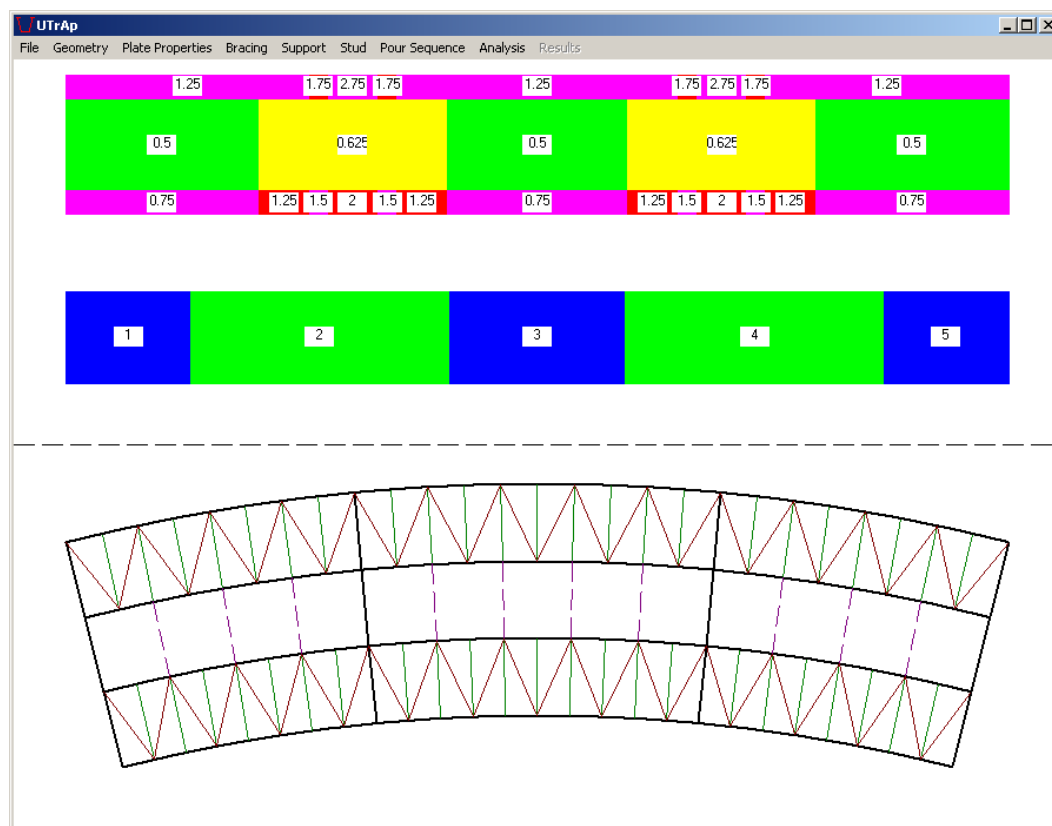
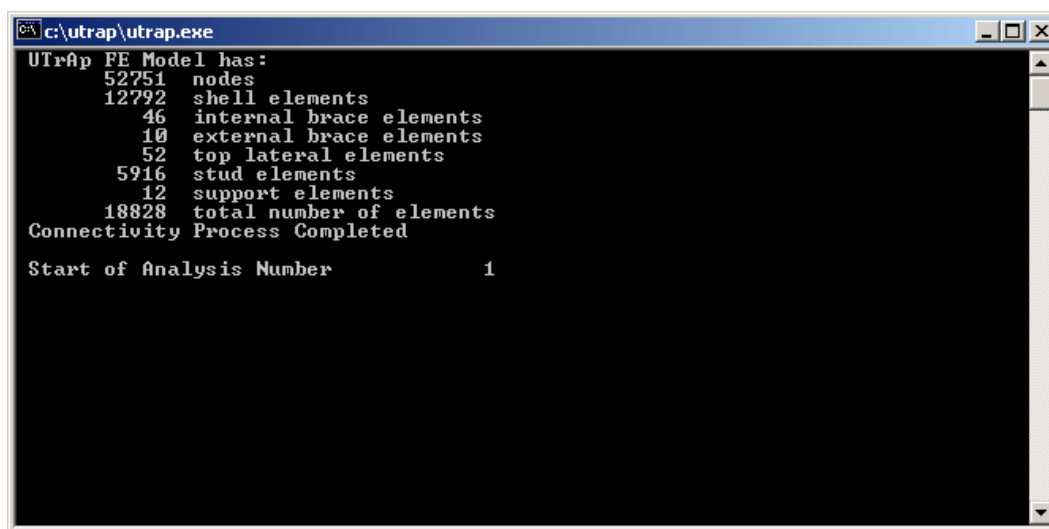


Figure A.13: Main form of UTrAp

When the user invokes the Analysis menu, the program checks if all the entries provided by the user are legal. Length of plates and decks should add up to the bridge length. Brace and support locations should be admissible. If any of the entries are missing or

violate the geometric constraints, the program will give an error message. If all entries are permissible, then the Analysis menu calls the Analysis Module to perform the finite element analysis. The analysis module runs under the DOS environment. A user can trace the progress of the analysis by observing the messages displayed in the DOS screen. Figure A.14 shows a representative analysis screen. The DOS screen automatically disappears when the analysis is completed.



```
c:\utrap\utrap.exe
UTrap FE Model has:
  52751 nodes
  12792 shell elements
    46 internal brace elements
    10 external brace elements
    52 top lateral elements
  5916 stud elements
    12 support elements
  18828 total number of elements
Connectivity Process Completed

Start of Analysis Number      1
```

Figure A.14: DOS Screen for an Analysis

Results Menu: This menu consists of 8 submenus and is used to visualize the output. Details of the submenus will be given in the following sections with figures obtained by the solution of the example program.

Deflections/Cross Sectional Rotations Submenus: These submenus are used to visualize the vertical deflections and cross sectional rotations of the bridge. Since they have identical properties, both menus will be explained in this section together. Deflection values are the vertical deflection of the center of the bottom flange. Rotation values are the rotation of the bottom flange. For twin girder systems only the deflection/rotation of the outer girder is reported. Both tabulated and graphical output can be displayed. Tabulated output is in the form of deflection/rotation values at every

two feet along the length of the bridge. The user can request deflection/rotation values for each analysis or the summed deflection/rotation values after each case. Deflections/Cross Sectional Rotations forms have four buttons to control the display of results. Functions of the buttons are explained below.

Tabulate Incremental Deflections/Rotations: This button is used to display the tabulated results of incremental deflection/rotation at every two feet along the bridge length. Values are presented for all analysis cases and are not summed. Figure A.15 shows the deflections form with the results.

Tabulate Total Deflections: This button is used to display the tabulated results of total deflection/rotation at every two feet along the bridge length. Deflection/rotation values after each analysis are presented. Total deflection values include the summation of all previous analyses. For example, values in column 3 are the summation of deflections/rotations due to analysis 1, 2, and 3.

Plot Incremental Deflections: This button displays the incremental deflection/rotation diagram. Incremental deflections/rotations due to all analyses are displayed on the same graph. Figure A.16 shows a typical deflection diagram.

Plot Total Deflections: This button displays the total deflection/rotation diagram. Total deflections/rotations due to all analyses are displayed on the same graph.

The screenshot shows a window titled 'Deflections' with the subtitle 'Incremental Deflections (in)'. It contains a table with 4 columns: 'Location (ft)', 'Analysis 1', 'Analysis 2', and 'Analysis 3'. The table lists values for locations from 0 to 44 feet in increments of 2. Below the table are four buttons: 'Tabulate Incremental Deflections', 'Plot Incremental Deflections', 'Tabulate Total Deflections', and 'Plot Total Deflections', along with a 'Cancel' button.

Location (ft)	Analysis 1	Analysis 2	Analysis 3
0	0	0	0
2	-0.17	-0.02	0.1
4	-0.33	-0.03	0.2
6	-0.49	-0.05	0.3
8	-0.66	-0.06	0.4
10	-0.82	-0.08	0.5
12	-0.97	-0.09	0.6
14	-1.13	-0.11	0.69
16	-1.28	-0.12	0.79
18	-1.42	-0.14	0.89
20	-1.57	-0.15	0.99
22	-1.71	-0.16	1.08
24	-1.84	-0.18	1.18
26	-1.97	-0.19	1.27
28	-2.09	-0.21	1.37
30	-2.2	-0.22	1.46
32	-2.31	-0.24	1.55
34	-2.42	-0.25	1.64
36	-2.51	-0.26	1.73
38	-2.6	-0.28	1.82
40	-2.68	-0.29	1.9
42	-2.76	-0.3	1.99
44	-2.82	-0.31	2.07

Figure A.15: Deflections Form

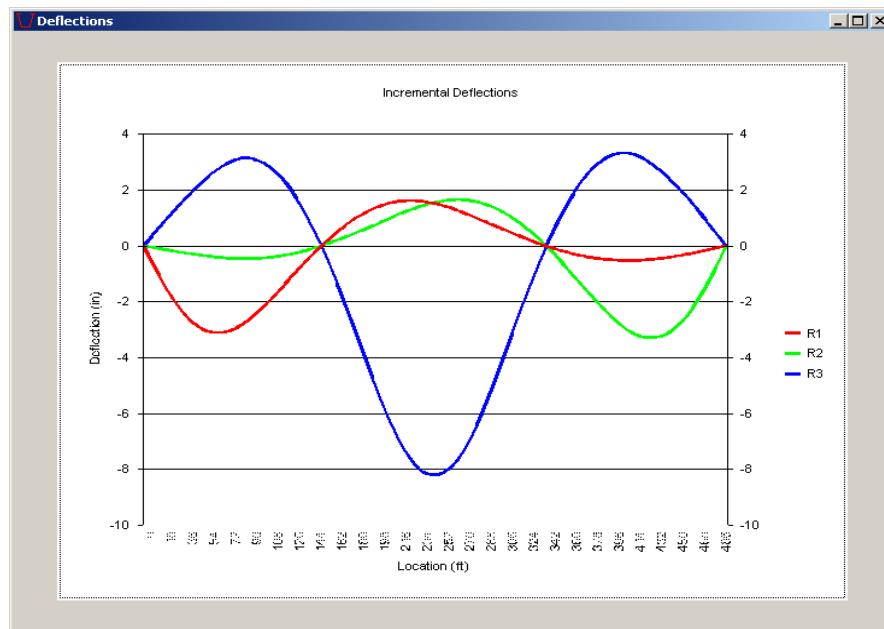


Figure A.16: Deflection Diagram

Cross Sectional Forces Submenu: This submenu is used to visualize the cross-sectional forces. Information on shear, moment and torsion are available. For twin girder systems quantities are summed for the two girders. Both tabulated and graphical output can be displayed. Tabulated output is in the form of shear, moment and torsion values for every two feet along the length of the bridge. In addition, shear, moment and torsion diagrams can be displayed graphically. Cross-Sectional Forces form has six buttons to control the display of results. Functions of the buttons are explained below.

Tabulate Shear: This button is used to display the tabulated results of shear at every two feet along the bridge length. Incremental values are presented for all analysis cases. Figure A.17 shows the Cross Sectional Forces form with the results.

Tabulate Moment: This button is used to display the tabulated results of internal bending moment at every two feet along the bridge length. Incremental values are presented for all analysis cases.

Tabulate Torque: This button is used to display the tabulated results of torque at every two feet along the bridge length. Incremental values are presented for all analysis cases.

Plot Shear Diagram: This button displays the shear diagram. Shear values for all analyses are displayed on the same graph. Figure A.18 shows a typical shear diagram.

Plot Moment Diagram: This button displays the moment diagram. Moment values for all analyses are displayed on the same graph.

Plot Torque Diagram: This button displays the torque diagram. Torque values for all analyses are displayed on the same graph.

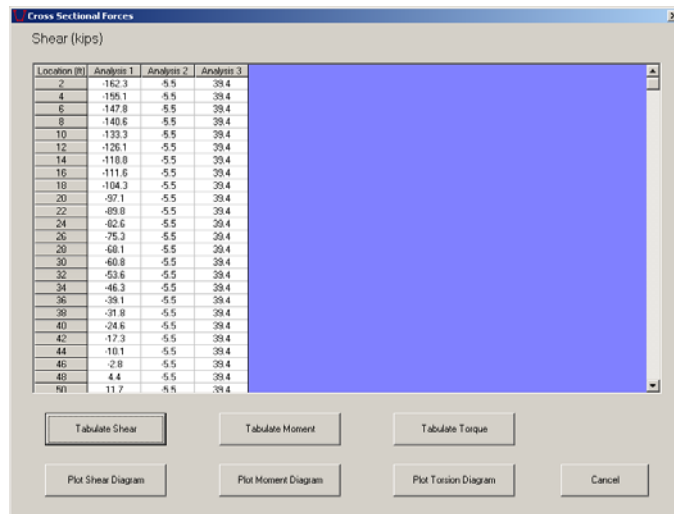


Figure A.17: Cross Sectional Forces Form

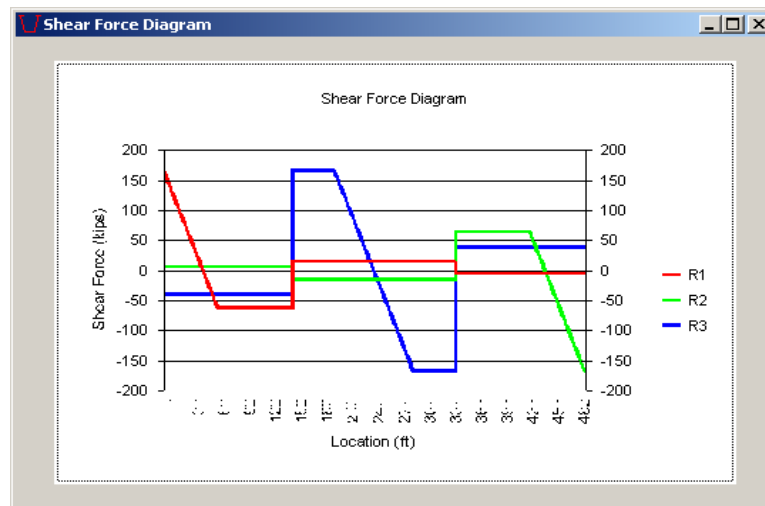


Figure A.18: Shear Force Diagram

Stresses Submenu: This submenu is used to visualize the cross-sectional stresses. The analysis module calculates normal and shear stresses at certain locations of the cross section at every two feet along the bridge length. These calculations are performed for all analysis cases. The locations on the cross section where stresses are calculated are named as section points. There are 26 and 52 section points on the cross section for the single and dual girder systems, respectively. The stresses form is used to tabulate the stress values along the length of the bridge for all section points. Both shear and normal stress can be tabulated in incremental or total format. In incremental format, results of all analyses are independent of each other. In total format, results after an analysis include the summation of all previous analyses. Radio buttons are placed on the form to select between shear and normal stress as well as between incremental and normal values. This form is also used to display the stress diagram. Variation of normal or shear stress along the bridge length can be plotted for a specified section point. Furthermore, this form could be used to display stresses at all section points on a certain cross section along the bridge length. The stresses form has three buttons that interact with three scroll-down boxes. Functions of the buttons are explained below.

Tabulate Stresses: This button is used to tabulate the stress values along the bridge length for all section points. Normal or shear stress can be tabulated depending on the user's selection. An analysis case must be selected using the scroll-down boxes. In addition, total or incremental values can be displayed. Figure A.19 shows a tabulated stress output in the stresses menu.

Plot Stress Diagram: This button is used to display the variation of normal or shear stress along the bridge length for a certain section point. An analysis case and section point must be selected using the scroll-down boxes. Figure A.20 shows a plot of normal stress along the bridge length for analysis number 1 and section point 52.

Visualize Cross Sectional Stresses: This button is used to display the stresses at all section points for a certain cross section. An analysis case and a location must be selected using the scroll-down boxes. Figure A.21 shows the normal stress distribution due to analysis 1 in a cross section 101 feet away from the start end. Section points and

stress values are given on the cross section diagram. The arrow in the figure shows the center of the arc that defines the curvature of the bridge.

Stresses

Incremental Normal Stresses due to Analysis Number 1

Normal Shear Incremental Total

Loc/S Pt	20	21	22	23	24	25	26	27	28	29	30
29	0	-6.07	-7.95	-5.16	-1.22	2.81	6.66	8.44	8.35	8.26	8.2
31	0	-6.53	-8.28	-5.43	-1.23	3.05	7.13	8.96	8.73	8.51	8.33
33	0	-7.14	-8.43	-5.67	-1.2	3.33	7.64	9.48	9.08	8.7	8.39
35	0	-7.9	-8.43	-5.93	-1.13	3.63	8.18	10.05	9.42	8.83	8.28
37	0	-7.75	-7.63	-5.52	-0.93	3.78	8.7	10.44	9.64	9.05	8.16
39	0	-6.9	-7.35	-5.06	-0.72	3.86	8.34	10.25	9.7	9.17	8.67
41	0	-6.65	-7.84	-5.17	-0.75	3.76	8.05	9.96	9.67	9.38	9.16
43	0	-6.49	-8.11	-5.25	-0.87	3.58	7.82	9.79	9.66	9.54	9.46
45	0	-6.46	-8.21	-5.3	-0.97	3.43	7.62	9.63	9.63	9.64	9.68
47	0	-6.57	-8.13	-5.33	-1.05	3.3	7.46	9.5	9.59	9.69	9.82
49	0	-6.81	-7.87	-5.34	-1.1	3.21	7.33	9.38	9.53	9.69	9.89
51	0	-7.19	-7.44	-5.32	-1.12	3.15	7.23	9.27	9.45	9.64	9.87
53	0	-7.71	-6.84	-5.28	-1.12	3.12	7.16	9.18	9.36	9.55	9.76
55	0	-8.33	-6.06	-5.21	-1.12	3.07	7.12	9.11	9.25	9.42	9.6
57	0	-8.26	-5.91	-5.13	-1.11	3.01	6.99	8.95	9.09	9.27	9.46
59	0	-7.5	-6.38	-5.05	-1.09	2.94	6.78	8.71	8.9	9.09	9.33
61	0	-6.85	-6.7	-4.93	-1.07	2.86	6.6	8.48	8.68	8.88	9.12
63	0	-6.35	-6.88	-4.79	-1.03	2.79	6.44	8.27	8.44	8.62	8.81
65	0	-5.98	-6.92	-4.62	-0.98	2.76	6.32	8.09	8.21	8.32	8.45
67	0	-5.69	-6.85	-4.45	-0.88	2.77	6.25	7.94	7.97	8	8.03
69	0	-5.48	-6.67	-4.29	-0.77	2.81	6.23	7.83	7.75	7.66	7.57
71	0	-5.36	-6.4	-4.13	-0.66	2.89	6.26	7.76	7.53	7.29	7.08
73	0	-5.32	-6.03	-3.96	-0.59	2.93	6.34	7.8	7.35	6.91	6.47
75	0	-5.54	-5.98	-4.05	-0.65	2.84	6.48	7.76	7.13	6.63	5.89
77	0	-5.43	-6.14	-4.09	-0.7	2.71	5.98	7.31	6.8	6.3	5.81

Buttons: Tabulate Stresses, Plot Stress Diagram, Visualize Cross Sectional Stresses

Analysis Number: 1
Section Point: 1
Location (ft): 1

Cancel

Figure A.19: Tabulated Cross Sectional Stresses

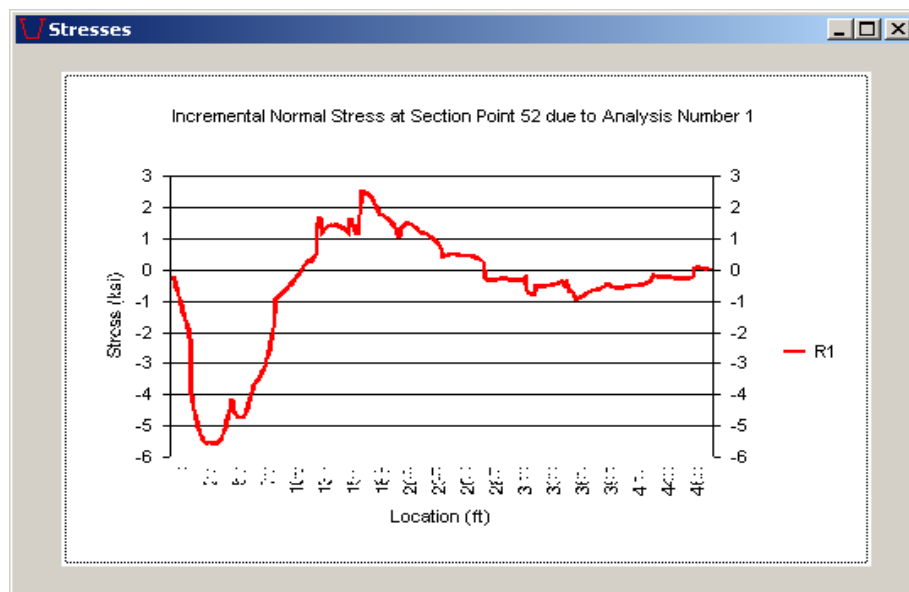


Figure A.20: Stress Diagram For Section Point 52

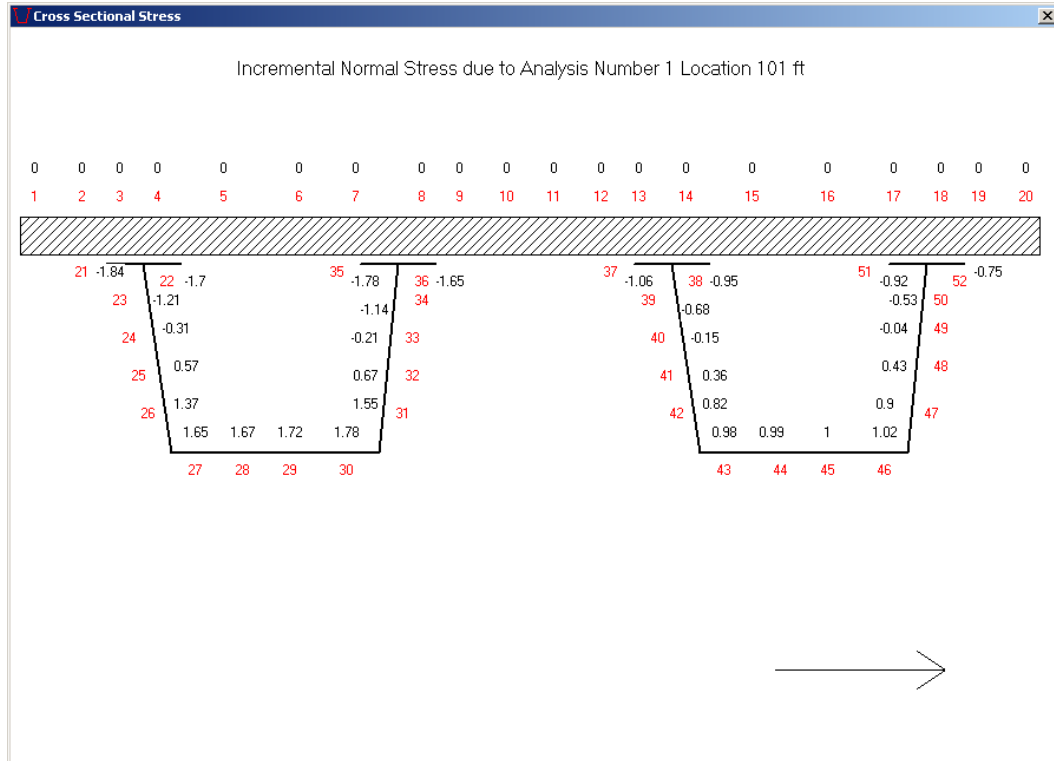


Figure A.21: Cross-Sectional Stresses

Top Lateral Forces Submenu: This submenu is used to display the forces in the top lateral braces. Force values can be tabulated or visualized as a bar graph. Forces due to each analysis or total forces after each analysis case could be displayed. Four buttons are used to control the output in this form. Functions of these buttons are explained below.

Tabulate Incremental Forces: This button is used to tabulate the forces in top lateral members due to each analysis case. Positive values correspond to tension forces in the brace members. This convention is used throughout the program. *Top Lateral Forces* form along with the tabulated results are shown in Fig. A.22 .

Tabulate Total Forces: This button is used to tabulate the forces in top lateral members after each analysis case. Values of all previous analyses are summed.

Plot Incremental Forces: This button is used to display the bar chart of top lateral brace forces. Incremental force values due to each analysis case are displayed. Figure A.23 shows a typical bar chart of brace forces.

Plot Total Forces: This button is used to display a bar chart of top lateral brace forces. Total force values after each analysis case are displayed.

Incremental Forces (kips)

Brace #	Type	Loc1 (ft)	Loc2 (ft)	Analysis 1	Analysis 2	Analysis 3
1	2	0	18.9	-51.58	-2.07	8.2
2	1	18.9	37.8	12.01	1.07	-4.17
3	2	37.8	56.7	-42.62	-2.74	11.87
4	1	56.7	75.6	-23.58	0.99	-4.62
5	2	75.6	94.5	0.14	-5.21	37.13
6	1	94.5	113.4	-30.68	-5.26	33.86
7	2	113.4	132.3	28.65	-0.38	7.6
8	1	132.3	151.5	-20.21	-11.38	71.02
9	2	151.5	170.5	34.26	5.67	-32.06
10	1	170.5	189.5	-6.15	-13.85	66.72
11	2	189.5	208.5	19.59	11.61	-71.5
12	1	208.5	227.5	5.12	-9.38	7.42
13	2	227.5	246.5	2.19	12.4	-54.85
14	1	246.5	265.5	11.89	2.54	-55.89
15	2	265.5	284.5	-9.28	5.32	9.44
16	1	284.5	303.5	11.48	20.8	-70.81
17	2	303.5	322.5	-13.83	-6.74	67.49
18	1	322.5	341.5	7.07	35.32	-33.64
19	2	341.5	360.4	-12.91	-21.16	73.99
20	1	360.4	379.3	2.07	29.71	5.21
21	2	379.3	398.3	-7.15	-32.14	35.69
22	1	398.3	417.3	-2.94	-0.61	34.92
23	2	417.3	436.1	-0.09	-24.03	-4.51
24	1	436.1	455.1	-6.41	-44.7	18.63
25	2	455.1	474	4.99	13.58	-7.98
26	1	474	493	-6.99	-53.47	14.82
27	2	0	18.9	-48.79	-2.19	8.44
28	1	18.9	37.8	19.22	0.99	-3.54
29	2	37.8	56.7	-35.1	-2.94	13.68

Buttons: Tabulate Incremental Forces, Tabulate Total Forces, Plot Incremental Forces, Plot Total Forces, Cancel

Figure A.22: Tabulated Top Lateral Brace Forces

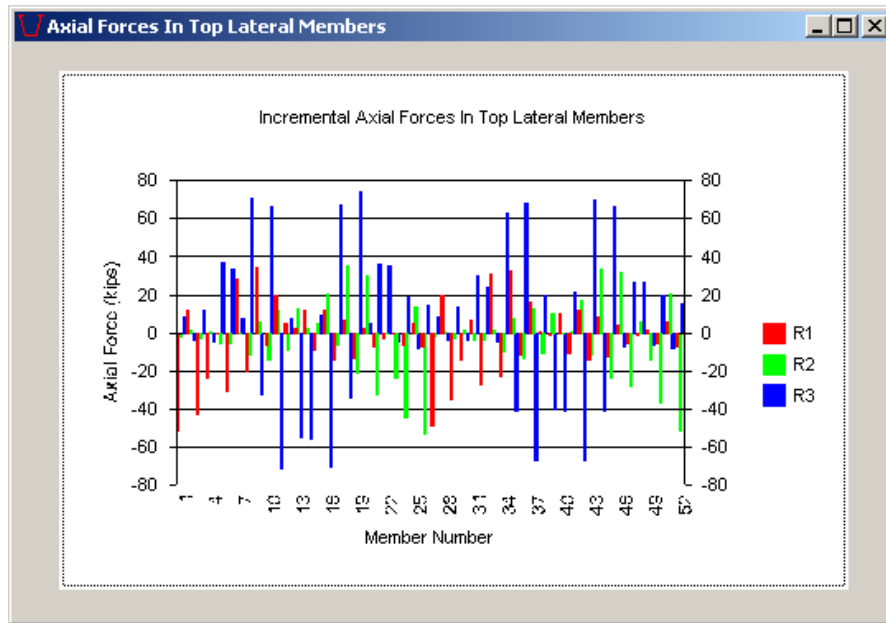


Figure A.23: Bar Chart of Top Lateral Forces

Internal Brace Forces and External Brace Forces Submenus: These submenus are used to display the member axial forces for internal and external braces. Since they have identical properties, both menus will be explained in this section together. Axial force values can be tabulated or visualized as a bar graph. Axial forces due to each analysis or total forces after each analysis case can be displayed. Four buttons that act together with a scroll-down box are used to control the output in these forms. Functions of these buttons are explained below.

Tabulate Incremental Forces: This button is used to tabulate the forces in bracing members due to each analysis case. Because internal and external braces are made up of several members, only results for a certain member can be displayed. Therefore, the member number must be selected using the scroll-down box. The configuration of internal and external braces, and the corresponding member numbers were presented previously (Fig. A.6). Figure A.24 shows the *Internal Brace Forces* form together with the table of axial force values for member 2 of all internal braces.

Tabulate Total Forces: This button is similar to the *Tabulate Incremental Forces* button. It is used to tabulate the total forces after each analysis.

Plot Incremental Forces: This button is used to display a bar chart of axial force values for a certain member number. The member number must be selected using the scroll-down box. Figure A.25 shows a bar chart of axial force values for member 2 of all internal braces.

Plot Total Forces: This button is similar to the *Plot Total Forces* button. It is used to display the total forces after each analysis.

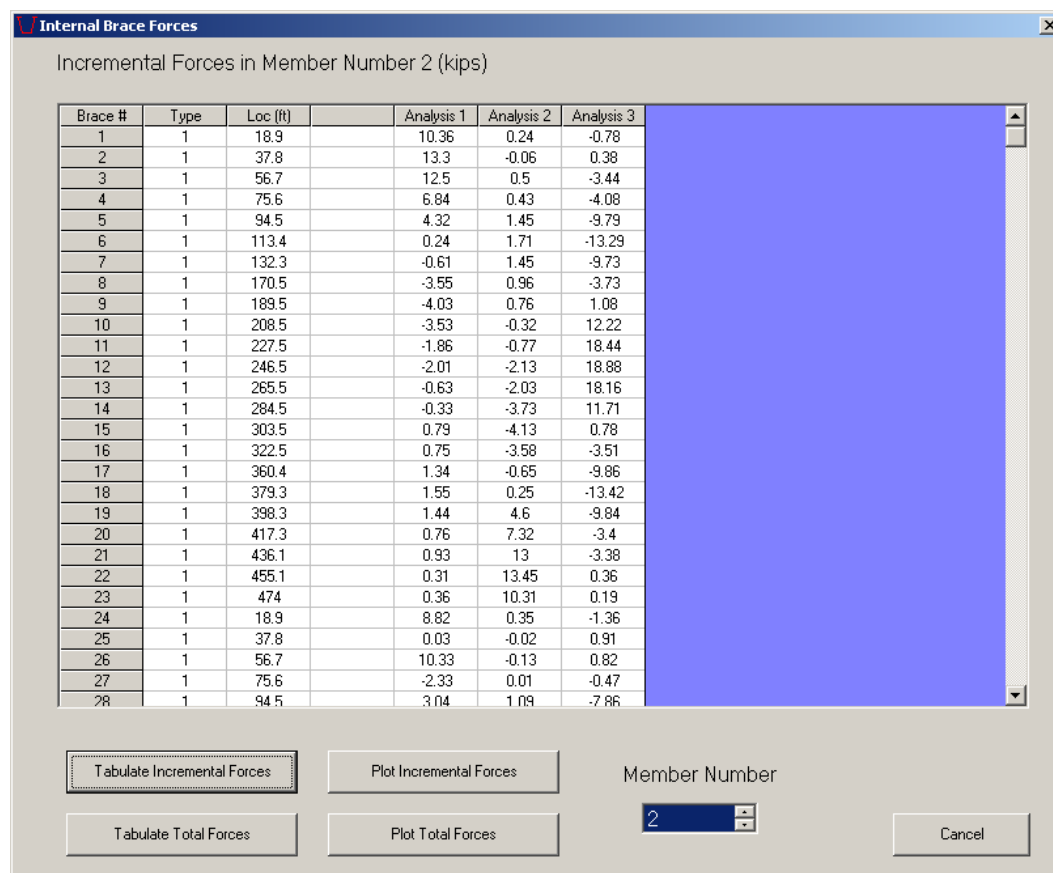


Figure A.24: Internal Brace Forces Form

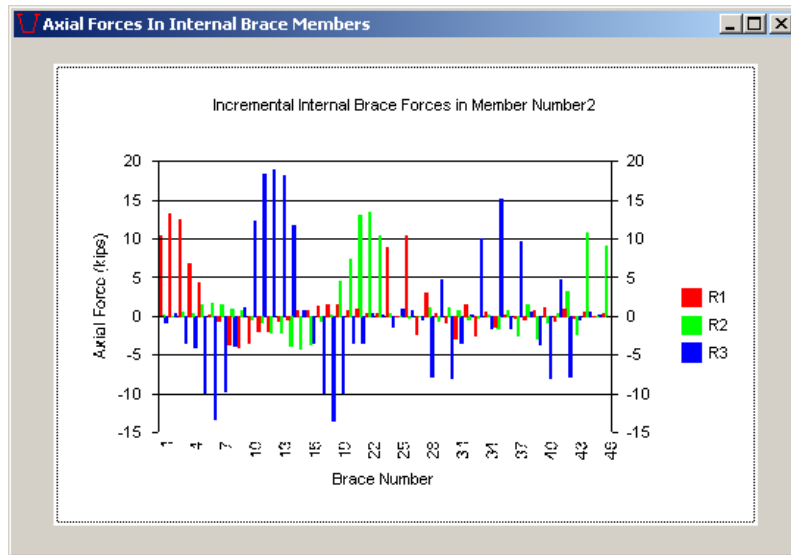


Figure A.25: Bar Chart of Internal Brace Forces

Analysis Summary Submenu: This submenu is used to visualize the maximums of useful quantities for each analysis. Maximum deflection, shear force, axial stress etc. are tabulated in this form. The Analysis Summary form is shown in Fig. A.26.

Summary of Maximum Quantities					
Quantity	Value	Analysis 1		Analysis 2	
		Value	Location (ft)	Value	Location (ft)
Incremental Upward Deflection (in)	1.61	222		1.65	264
Incremental Downward Deflection (in)	-3.11	60		-3.29	426
Total Upward Deflection (in)	1.61	222		3.06	244
Total Downward Deflection (in)	-3.11	60		-3.79	424
Incremental Rotation (rad)	0.005244	74		0.005571	418
Total Rotation (rad)	0.005244	74		0.00668	418
Incremental Shear (kips)	162.3	1		168.3	491
Incremental Positive Moment (kip-ft)	3911.9	149		4020.9	339
Incremental Negative Moment (kip-ft)	-2055.8	149		-2144.4	339
Incremental Torque(kip-ft)	384.9	1		400.6	491
Incremental Positive Normal Stress (ksi)	10.44	37		10.7	455
Incremental Negative Normal Stress (ksi)	-8.43	33		-8.69	457
Incremental Shear Stress (ksi)	2.08	3		2.12	489
Total Positive Normal Stress (ksi)	10.44	37		11.31	455
Total Negative Normal Stress (ksi)	-8.43	33		-9.33	437
Total Shear Stress (ksi)	2.08	3		2.24	489
Incremental Positive Top Lateral Axial Force (kips)	34.26	9		35.32	18
Incremental Negative Top Lateral Axial Force (kips)	-51.58	1		-53.47	26
Total Positive Top Lateral Axial Force (kips)	34.26	9		42.39	18
Total Negative Top Lateral Axial Force (kips)	-51.58	1		-60.46	26
Incremental Positive Top Lateral Axial Stress (ksi)	5.429477	9		5.597465	18
Incremental Negative Top Lateral Axial Stress (ksi)	-8.174327	1		-8.473851	26
Total Positive Top Lateral Axial Stress (ksi)	5.429477	9		6.717908	18

Figure A.26: Analysis Summary Form

Final Comments

After an analysis was performed, the user can reanalyze the system by making modifications to the geometry or the pouring sequence.

The program works under Windows 98 and Windows 2000 operating systems. A physical memory of 1 GB is recommended for problems involving twin girders. In cases where the physical memory is not enough, the program uses the virtual memory to solve the problem. However, using virtual memory significantly increases the time for solution.

APPENDIX B

Two-Node Three Dimensional Truss Stiffness Matrix



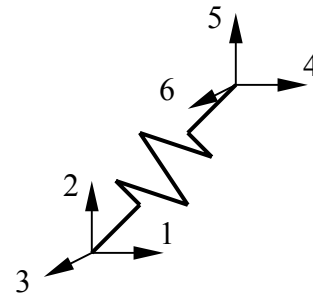
$$\begin{bmatrix} \frac{EA}{L} & 0 & 0 & -\frac{EA}{L} & 0 & 0 \\ 0 & 0 & 0 & 0 & 0 & 0 \\ 0 & 0 & 0 & 0 & 0 & 0 \\ -\frac{EA}{L} & 0 & 0 & \frac{EA}{L} & 0 & 0 \\ 0 & 0 & 0 & 0 & 0 & 0 \\ 0 & 0 & 0 & 0 & 0 & 0 \end{bmatrix}$$

Where;

E : Modulus of Elasticity, A : Area of Truss Member, and L : Length of Truss Member.

Two-Node Three Dimensional Spring Stiffness Matrix

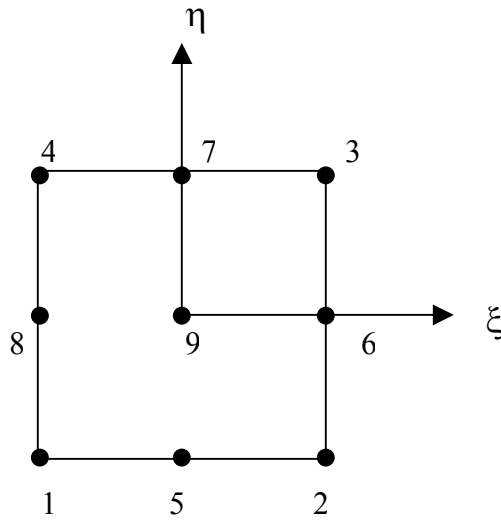
$$\begin{bmatrix} \mathbf{K}_1 & 0 & 0 & -\mathbf{K}_1 & 0 & 0 \\ 0 & \mathbf{K}_2 & 0 & 0 & -\mathbf{K}_2 & 0 \\ 0 & 0 & \mathbf{K}_3 & 0 & 0 & -\mathbf{K}_3 \\ -\mathbf{K}_1 & 0 & 0 & \mathbf{K}_1 & 0 & 0 \\ 0 & -\mathbf{K}_2 & 0 & 0 & \mathbf{K}_2 & 0 \\ 0 & 0 & -\mathbf{K}_3 & 0 & 0 & \mathbf{K}_3 \end{bmatrix}$$



Where; K_1, K_2, K_3 are stiffness values in three global directions

APPENDIX C

Nine-Node Element Shape Functions



$$N_1 = \frac{1}{4}(\xi^2 - \xi)(\eta^2 - \eta)$$

$$N_2 = \frac{1}{4}(\xi^2 + \xi)(\eta^2 - \eta)$$

$$N_3 = \frac{1}{4}(\xi^2 + \xi)(\eta^2 + \eta)$$

$$N_4 = \frac{1}{4}(\xi^2 - \xi)(\eta^2 + \eta)$$

$$N_5 = \frac{1}{2}(1 - \xi^2)(\eta^2 - \eta)$$

$$N_6 = \frac{1}{2}(\xi^2 + \xi)(1 - \eta^2)$$

$$N_7 = \frac{1}{2}(1 - \xi^2)(\eta^2 + \eta)$$

$$N_8 = \frac{1}{2}(\xi^2 - \xi)(1 - \eta^2)$$

$$N_9 = (1 - \xi^2)(1 - \eta^2)$$

APPENDIX D

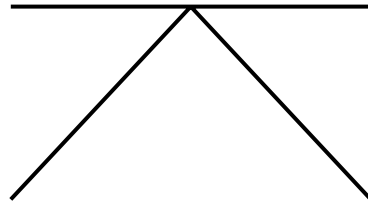
Z-Connect Plate Properties

WEB		BOTTOM FLANGE		TOP FLANGE	
Length(ft.)	Thickness(in.)	Length(ft.)	Thickness(in.)	Length(ft.)	Thickness(in.)
100.5	0.5	100.5	0.75	127	1.25
99	0.625	26.5	1.25	10	1.75
94	0.5	10	1.5	26	2.75
99	0.625	26	2.0	10	1.75
100.5	0.5	10	1.5	147	1.25
		26.5	1.25	10	1.75
		94	0.75	26	2.75
		26.5	1.25	10	1.75
		10	1.5	127	1.25
		26	2.0		
		10	1.5		
		26.5	1.25		
		100.5	0.75		
Σ = 493 ft		Σ = 493 ft		Σ = 493 ft	

K-Connect Plate Properties

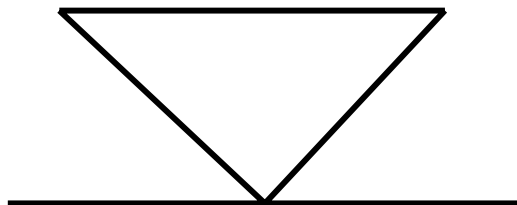
WEB		BOTTOM FLANGE		TOP FLANGE	
Length(ft.)	Thickness(in.)	Length(ft.)	Thickness(in.)	Length(ft.)	Thickness(in.)
134	0.625	96	0.75	96	1.0
113	0.75	60	1.5	47	1.5
84	0.625	23	2.0	13	2.0
113	0.75	47	1.5	23	3.0
134	0.625	126	0.75	46	2.0
		47	1.5	128	1.0
		23	2.0	46	2.0
		60	1.5	23	3.0
		96	0.75	13	2.0
				47	1.5
				96	1.0
Σ = 578 ft		Σ = 578 ft		Σ = 578 ft	

Typical Internal Brace Used in Z and K Connects



All
Members
L 4x4x1/2

Typical External Diaphragm Used in Z and K Connects



All
Members
L 5x5x1/2

BIBLIOGRAPHY

Ahmad, S., Irons, B. M., and Zienkiewicz, O. C. (1970). "Analysis of Thick and Thin Shell Structures by Curved Finite Elements." *International Journal for Numerical Methods in Engineering*, Vol. 2, pp.419-451.

ABAQUS (1997). "Standard User's Manual." Hibbitt, Karlsson, and Sorensen, Inc., USA.

ACI (1999). "Building Code Requirements for Structural Concrete and Commentary." ACI 318R-99, Farmington Hills, Michigan.

AISC (1994). "Manual of Steel Construction – Load and Resistance Factor Design." 2nd Ed., Chicago.

ASTM C 39/C 39M-99 (1999). "Standard Test Method for Compressive Strength of Cylindrical Concrete Specimens." West Conshohocken, PA.

ASTM C496-96 (1996). "Standard Test Method for Splitting Tensile Strength of Cylindrical Concrete Specimens." West Conshohocken, PA.

ASTM C469-94 (1994). "Standard Test Method for Static Modulus of Elasticity and Poisson's Ratio of Concrete in Compression." West Conshohocken, PA.

Bathe, K. J. (1982). "Finite Element Procedures in Engineering Analysis." Prentice-Hall, Inc., Englewood Cliffs, New Jersey.

Bathe, K. J., Ho, L. W. (1981). "Some Results in the Analysis of Thin Shell Structures." Nonlinear Finite Element Analysis in Structural Mechanics, W. Wunderlich, E. Stein, K. J. Bathe (eds), Springer-Verlag, Berlin.

Brockenbrough, R. L. (1986). "Distribution Factors for Curved I-Girder Bridges." ASCE Journal of Structural Engineering, Vol. 112, No. 10, pp. 2200-2215.

Bull, J. W. (1990). "Finite Element Applications to Thin-Walled Structures." Elsevier Applied Science, England.

Chen, B. S. (2002). "Top-Lateral Bracing Systems for Trapezoidal Steel Box-Girder Bridges" Dissertation, University of Texas at Austin.

Cheplak, B. A. (2001). "Field Measurements of Intermediate External Diaphragms on a Trapezoidal Steel Box Girder Bridge." Thesis, University of Texas at Austin.

Cheplak, B. A., Memberg, M., Frank, K. H., Yura, J. A., Williamson, E. B., Chen, B. S., and Topkaya, C. (2002) "Field Studies of Steel Trapezoidal Box Bridges." Research Report, University of Texas at Austin.

Cornell, G. (1998). "Visual Basic 6 from the Ground Up." McGraw-Hill.

Fan, Z. (1999). "Field and Computational Studies of Steel Trapezoidal Box Girder Bridges." Dissertation, University of Houston.

Fan, Z., and Helwig, T. A. (1999). "Behavior of Steel Box Girders with Top Flange Bracing." ASCE Journal of Structural Engineering, Vol. 125, No. 8, pp.829-837

Gullerud, A. S., Koppenhoefer, K. C., Roy, A., RoyChowdhury, S., and Dodds, R.H. (2001). "WARP3D-Release 13.12, 3-D Dynamic Nonlinear Fracture Analysis of Solids

Using Parallel Computers and Workstations.” Research Report, Structural Research Series No. 607, University of Illinois at Urbana-Champaign

Holt, J. (2001) TxDot Design Engineer, Personal Contacts.

Hughes, T. J. R. (2000), “The Finite Element Method- Linear Static and Dynamic Finite Element Analysis.” Dover Publications, Mineola, New York.

Khan, A. A., Cook, W. D., and Mitchell D. (1995). “Early Age Compressive Stress-Strain Properties of Low-, Medium-, and High-Strength Concretes.” ACI Materials Journal, Vol. 92, No. 6, pp. 617-624.

Kollbrunner, C. F., Basler, K. (1969). “Torsion in Structures – An Engineering Approach.” Springer-Verlag, New York.

Lew, H. S., Reichard, T. W. (1978). “Mechanical Properties of Concrete at Early Ages.” ACI Journal, Vol. 75, No. 10, pp.533-542.

MacGregor, J. G. (1997). “Reinforced Concrete: mechanics and design.” 3rd Edition, Prentice Hall, Inc., Upper Saddle River, New Jersey.

Mo, Y. L., Chang, W. L., and Lee, Y. C. (1998). “Early Form Removal of Reinforced Concrete Slabs.” ASCE Practice Periodical on Structural Design and Construction, Vol. 3, No. 2, pp. 51-55.

Ollgaard, J. G., Slutter, R. G., and Fisher, J. W. (1971). “Shear Strength of Stud Connectors in Lightweight and Normal-Weight Concrete.” AISC Engineering Journal, 8(2), pp. 55-64.

Oluokun, F. A., Burdette, E. G., and Deatherage, J. H. (1991). "Elastic Modulus, Poisson's Ratio, and Compressive Strength Relationship at Early Ages." *ACI Materials Journal*, Vol. 88, No. 1, pp. 3-10.

Razaqpur, A. G., Nofal, M. (1989). "A Finite Element for Modeling the Nonlinear Behavior of Shear Connectors in Composite Structures." *Computers and Structures*, Vol. 32, No. 1, pp. 169-174.

Tabsh, S. W., Sahajwani, K. (1997). "Approximate Analysis of Irregular Slab-on-Girder Bridges." *ASCE Journal of Bridge Engineering*, Vol. 2, No. 1, pp.11-17.

Tarhini, K. M., Frederick, G. R. (1992). "Wheel Load Distribution in I-Girder Highway Bridges." *ASCE Journal of Structural Engineering*, Vol. 118, No. 5, pp. 1285-1294.

Texas Department of Transportation (TxDot) (1993). "Standard Specification Book." Austin, Texas.

Sennah, K. M., Kennedy, J. B. (2001). "State-of-the-art in Design of Curved Box Girder Bridges." *ASCE Journal of Bridge Engineering*, Vol. 6, No. 3, pp. 159-167.

Viest, I. M., Colaco, J. P., Furlong, R. W., Griffis, L. G., Leon, R. T., and Wyllie, L. A. (1997). "Composite Construction Design for Buildings." McGraw-Hill, New York.

Wang, Y. C. (1998). "Deflection of Steel-Concrete Composite Beams with Partial Shear Interaction." *ASCE Journal of Structural Engineering*, Vol. 124, No. 10, pp. 1159-1165.

Zienkiewicz, O. C. (1977). "The Finite Element Method." 3rd Edition, McGraw-Hill, UK.

VITA

Cem Topkaya was born in Ankara, Turkey on February 16, 1976, the son of Ilhan Topkaya and Yavuz Topkaya. After graduating from high school in 1993, he entered the Middle East Technical University in Ankara, Turkey. He received the degree of Bachelor of Science in Civil Engineering from M.E.T.U. in July 1997. In September 1997, he entered the Graduate School of the University of Texas at Austin. He received his Master of Science degree in Civil Engineering in May 1999 and continued for his doctoral studies. During his graduate education, he worked as a research assistant at the Phil M. Ferguson Structural Engineering Laboratory.

Permanent Address: Cem Topkaya
Bilkent Camlik Sitesi
Kugu Cikmazi Sokak B 26/1
Bilkent – Ankara – Turkey

This dissertation was typed by the author.